Computational Analysis of Multi-Fuel Micro Gas Turbine Annular Combustion Chamber

By

Anis Ahmad Sher

Reg. No 00000206036

Session 2017-2019

Supervised by

Dr. Adeel Javed

A Thesis Submitted to the US-Pakistan Center for Advanced Studies in Energy in partial fulfillment of the requirements for the degree of MASTERS of SCIENCE in Thermal Energy Engineering

US-Pakistan Center for Advanced Studies in Energy (USPCAS-E)

National University of Sciences and Technology (NUST)

H-12, Islamabad 44000, Pakistan

February 11, 2020

THESIS ACCEPTANCE CERTIFICATE

Certified that final copy of MS/MPhil thesis written by Mr. **Anis Ahmad Sher**, (Registration No**. 00000206036**) of **MS student** (USPCAS-E) has been vetted by undersigned, found complete in all respects as per NUST Statues/Regulations, is within the similarity indices limit and is accepted as partial fulfillment for the award of MS/MPhil degree. It is further certified that necessary amendments as pointed out by GEC members of the scholar have also been incorporated in the said thesis.

Signature: _____

Name of Supervisor <u>Dr. Adeel Javed</u>

Date: _____

Signature (HoD): _____

Date: _____

Signature (Dean/Principal): _____

Date: _____

Certificate

This is to certify that work in this thesis has been carried out by **Mr. Anis Ahmad Sher** and completed under my supervision in High performance computer laboratory, US-Pakistan Center for Advanced Studies in Energy (USPCAS-E), National University of Sciences and Technology, H-12, Islamabad, Pakistan.

Supervisor: _____

Dr. Adeel Javed
USPCAS-E
NUST, Islamabad

GEC member # 1: **_____**

Dr. Muhammad Bilal Sajid
USPCAS-E
NUST, Islamabad

GEC member # 2: **_____**

Dr. Majid Ali
USPCAS-E
NUST, Islamabad

GEC member # 3: **_____**

Dr. Rabia Liaquat
USPCAS-E
NUST, Islamabad

HoD- (TEE) _____

Dr. Adeel Javed

A Principal/ Dean **_____**

Dr. Adeel Waqas
USPCAS-E
NUST, Islamabad

Acknowledgment

I am thankful to almighty Allah to create me as a human and give me health and helped me in every step of this work. I have no words to thanks almighty Allah for introducing new ideas in my whole life. Indeed, I am nothing and can't do work for a single zeptosecond without Your priceless help and guidance.

I am thankful to my beloved parents who lead me in every moment of life and raised me to such a position. Of course, without their moral, financial and every type of supports and pray I am nothing.

I am thankful to my supervisor Dr. Adeel Javed for helping me. Through his remarkable guidance, I have always come out of problems.

I am thankful to Dr. Patrick Phelan for his valuable guidance. I will remember him forever for his inspirational suggestion and help.

I am grateful for USAID for their financial support.

I would like to aknowledge the support of my thesis GEC members Dr. Muhammad Bilal Sajid, Dr. Majid Ali and Dr. Rabia Liaquat.

I am grateful for the National University of Sciences and Technology, Pakistan and Arizona State University, USA for providing easy excess facilities in my research work.

Finally, I would like to express my gratitude to all those who help me in any movement of my research.

Dedicated to my beloved parents and all educated community who lead me to such tremendous and wonderful accomplishment and success.

Abstract

In this research, the annular combustion chamber with swirlers is introduced in the micro gas turbine engine for power production. Impact of the dilution holes position and blade angles of swirler on the combustion performance of the combustion chamber is investigated. In addition, the combustor is optimized for multifuel comprising of pure methane, natural gas, and ethanol. In order to investigate suitable fuel, the review has been done based on their combustible properties, energy density, price, pollutant emissions, and availability. The combustor is designed in SolidWorks, and simulations are performed in Ansys Fluent for two positions of dilution holes in the liner and angles of the swirler blade. The model used is non-premixed with a compressible k-ε turbulent flow model and an equilibrium probability density function for the chemical reaction. In order to measure the performance of the combustion chamber, pollutant emissions, combustion efficiency, and temperature at the outlet are examined. Pollutant emissions as carbon monoxides (CO) and unburned fuels exist in a small amount, however nitric oxides (NO) are negligible. The combustion efficiency found is above 98% for methane and natural gas, while almost 100% for ethanol. Furthermore, simulation results are compared to theoretical data in terms of temperatures for all fuels. Finally, simulation findings reveal that the swirler vane angle of 45º widely improved combustor performance.

Table of Contents

List of Figures

List of Tables

List of Publications

Introduce Straight-Through Annular Combustor in Micro Gas Turbine Engine

Anis Ahmad Sher, Adeel Javed

International Conference on Mechanical Engineering (ICME-2020)

Computational Analysis of a Multi-Fuel Annular Combustion Chamber for Micro Gas Turbine Application with Focus on Swirler and Dilution Hole Design

Anis Ahmad Sher, Adeel Javed, Patrick Phelan

Journal: Combustion Theory and Modeling (Taylor & Francis)

Nomenclature

Latin Symbols

A	Area of diffuser, Area of combustor
A/F	Air fuel ratio
C_d	Discharge coefficient
$C_{d\infty}$	Asymptotic of discharge coefficient
C_p	Specific heat at constant pressure
D	Diameter
E	Rate of deformation
J	Momentum flux ratio
K	hole to annulus mass flow rate
k	Ratio of liner and casing cross-section area
L	Wall length of diffuser
M	Mach number
$\dot{m}$	Mass flow rate
n	Number
p	Static pressure
P	Total Pressure
q	Dynamic pressure
R	Half of the height of diffuser opening
S	Swirl
T	Temperature
t_v	Thickness
U	Velocity
u	Mean velocity
W	Height of diffuser opening
w	Thickness
y	Jet penetration

Greek symbols

α	Kinetic energy coefficient
β	Vane angle
Δ	Change
λ	Loss coefficient
η_c	Combustion efficiency
η	Overall effectiveness
θ	Divergence angle, jet angle
τ	Stress
μ	Eddy viscosity

Subscripts

1	Diffuser inlet
2	Diffuser outlet
3	Combustor inlet
4	Combustor outlet
d	diffuser
h	Hole
h,geo	Hole geometric
h,eff	Hole effective
j	Jet
l	Liner
N	Number
opt	Optimum
ref	Reference
sw	Swirler
v	Swirler vane

Abbreviations

AR	Area ratio
CFD	Computational Fluid Dynamics

CO	Carbon Monoxides
GT	Gas turbines
LGT	Large Gas Turbines
MGT	Micro gas turbines
MGTC	Micro Gas Turbine Combustor
NO	Nitric oxides
OPL	Overall pressure loss
PLF	Pressure loss factor
ppm	Particles per million
RPM	Revolution per minute
UHC	Unburned Hydro Carbon

Chapter 1
Introduction

1.1 Background

In the last 10 years, Micro gas turbines (MGT) has gained a lot of interest in the field of industry market and electricity generation. They are advantageous in terms of line losses and can easily installed with a low initial cost. In general, MGT has a low weight per unit power and has the capability of adaptation to a variety of fuels which is the main reason for the attraction of researcher interest. However, the combustor in a micro gas turbine is usually a simple geometry with low combustion efficiency and requires improvement. As the use of Gas Turbines (GT) have been dominant both in power production and propulsion since many decades while using natural hydrocarbon fuel. However, today's world facing the issue of natural hydrocarbon fuel depletion and pollutant emissions which needs switch to alternative fuel with less pollutant emissions. Renewable fuel such as ethanol produced from bio matters have net-zero carbon emission and can easily be produced. In this research, the author introduces an annular combustion chamber in a micro gas turbine applying multi-fuel.

1.2 Micro Gas Turbine

GT are type of engine operating on Brayton or Joule or Gas turbine cycle. It may be micro, small or large depends on its power capacity. While their cycle may be open-cycle or closed cycle. A large gas turbines (LGT) usually produces power more than 5 MW, while Small gas turbines (SGT) have a power capacity of less than 5 MW [1]. MGT power are in the range of 1 kW – 300 kW [2] or maybe up to 500 kW [3]. In this research, we are focusing on the micro gas turbine engine of power 30 kW.

MGT are a typical gas turbine operating on a Brayton cycle with power in the range of 1 kW to 500 kW. It is the same as the original gas turbine engine but due to scaling down both turbine and combustion efficiency decreases [4]. And its shaft speed is very high as

compared to normal gas turbine and rotational speed is over 40000 RPM. MGT may consist of a single shaft with a radial turbine and centrifugal compressor rotating in the speed range of 50000 to 120000 RPM. While some have a split shaft with approximately 3000 RPM of power turbine and compressor speed depends on output load and varies with it and gives better part-load efficiency [3]. In general, MGT have a low weight per unit power and has the capability of adaptation to a variety of fuels which is the main reason for researcher interest in it [3]. It is light in weight and simple and their maintenance can be possible easily. MGT are usually used for power generation in combination heating. Its electrical efficiency is approximately 15% – 25%. Its thermal efficiency may touch 70% for combined heat and power by MGT, While its overall efficiency is in the range of 75% - 85% [4]. It has the following advantages

- Low emissions
- Compact in size
- Light in weight
- It can be installed in a small space
- It can be easily adjusted due to flexibility
- Its overall efficiency is high
- Its maintenance is easy and of low cost
- Less vibrations and noise
- Noise is acceptable

This type of engine may have some disadvantages

- Its combustion efficiency is lower
- Its electrical efficiency is less than the large gas turbine
- Higher cost

The main components of the MGT are

- Compressor
- Combustor
- Turbine
- Generator
- Recuperator in some engines

The compressor used to pressurize air to the required pressure from atmospheric pressure. It is usually a centrifugal type compressor. The turbine is used to extract power from high temperature and pressure combustion products and then convert to rotational kinetic energy. This energy is transferred to electrical energy by the generator. The generator and compressor are connected to the turbine by shaft. Recuperator is a heat exchanger used to extract the waste heat from the exhaust gases at the turbine outlet and used for preheating or heating water in combined heat and power (CHP). Combustor is a chamber in which combustion takes place and increase temperature up to certain limits.

1.2.1. Micro Gas Turbine Combustor

In combustor, the process of combustion happened due to which fuel burnt and referred is the combustion chamber. Combustion may be diffusion combustion or dry low NOx or dry low emission combustion[5]. In diffusion combustors usually, has single injector used while in dry low NOx combustors have multiple fuel injectors. In diffusion type combustor steam or water may be injected for limiting and control of NOx production.

The combustor used in MGT are micro gas turbine combustor. Combustors are of various types such as Annular, Can or Tubular and Canular Combustor. In this research, we use the annular type combustion chamber. An annular combustor may be reverse flow or straight-through flow combustor. We have modeled and simulated a straight-through flow combustor. An annular combustor is of various components. Liner, Casing, Fuel injector while some combustor also contains swirler for swirling air. Liner has different zone, the primary zone where air and fuel initially mixed and combust, secondary zone in which more air introduce through-hole for completing combustion. The last zone is an intermediate or dilution zone in which extra air is introduce for diluting and lowering the temperature of hot combustion gases so that makes it compatible with turbine blades material. These zones are usually in every type of combustor, but in some combustor may have no secondary zone. The annular combustor consists of multiple injectors and swirlers, which are in single liner and casing. And its size is usually compact. Numbers of experimental and computational research on gas turbine combustors have already performed which include the sustainability of flame over the range of air-fuel ratio with low weight to unit power [6]. Computational Fluid Dynamics (CFD) study is used by the

number of researchers for the design and emissions and performance analysis of the combustor [7], [8], [9], [10].

1.3 Basic design considerations

The basic design considerations of conventional Gas Turbine Combustors are instructive for defining the essential components.

Figure 1-1 shows types of combustor in which the straight wall duct connects the compressor to the turbine. But this simple arrangement is not practical because of excessive pressure loss. As the pressure loss due to combustion is proportional to the air velocity. For the compressor, outlet velocity is 170 m/s and the loss in it is almost one-third of pressure rise in the compressor. This pressure loss is reduce by using diffuser, which lower velocity by factor of 5 and flow reversal must be used so that flame is anchored in low-velocity region and this reversal may be accomplished by plain baffle as shown in Figure 1-1. The only defect is to produce the required temperature and in the combustion chamber the overall Air/fuel ratio may be in the range of 30-40. Ideally, the ratio in the primary zone is 18 but sometimes higher value is preferred as 24 for low NOx. The air downstream of combustion is added to lower the temperature to the desired value. The gas turbine combustion chamber logical development in Figure 1-1 illustrates its wide features. In which the components are diffuser, air casing, liner, and fuel injector.

The choice of particular is made on the basis of the specification of gas turbine engine specifications. And which the most desirable is the space availability. In large aircraft engines, invariably large straight through combustor while in small aircraft engine reverse flow annular combustor is most appropriate. The fuel injectors may be of different type, in some combustor fuel is atomized in the form of drop under pressure through the nozzle and in some liner, wall is used under pressure differential to produce a high-velocity stream of air that shatter fuel into droplet and transport it into the combustion zone.
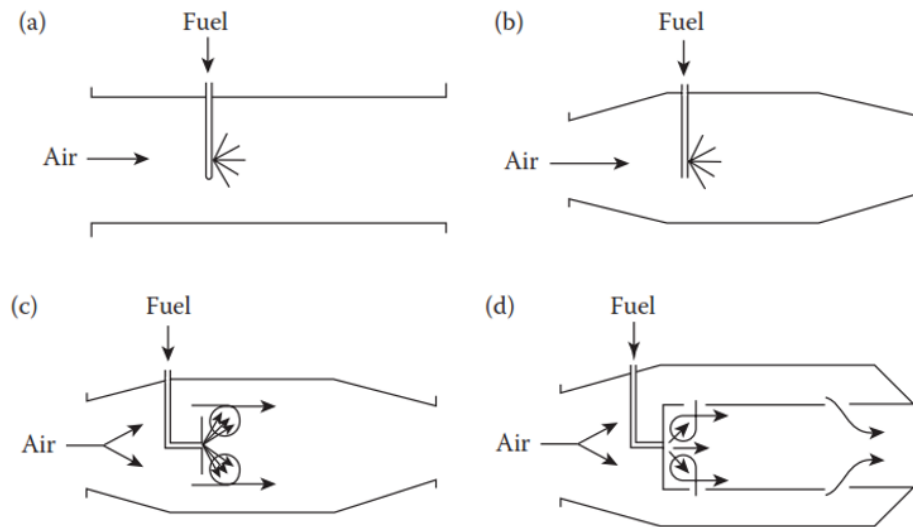
Figure 1-1. Derivation of conventional combustor configuration

1.3.1. Combustor Requirements

The following are basic requirements for combustor

➢ High combustion efficiency so that fuel is completely burned and all chemical energy is converted into heat
➢ Reliable, continuous and smooth ignition
➢ The flame should be stable in a wide range of pressure and air/fuel ratios
➢ The pressure loss in the combustor should be lowest
➢ The pattern factor that optimizes the life of turbine blades and nozzle guide vanes
➢ Low pollutant emissions
➢ Low smoke emissions
➢ Freedom from that manifestation which produces instability in the combustions (i.e pressure pulsations)
➢ Size is related to the space available
➢ Shape that is compatible with the engine
➢ Design in such a way so that easily manufactured and low manufacturing cost
➢ Maintenance should be easily possible
➢ Durable
➢ Multi-fuel using capability

➢ Low fuel consumption

➢ Low weight for aircraft

➢ Long operating life

1.4 Problem statement

Gas turbines used both in propulsion and power generation while using fossil fuels. Power turbines can also run on the number of other fuels which include both renewable and non-renewable. For power applications, various gas turbines such as large, small and microturbines can be installed. Usually, microturbines used the simple tube as combustor and their combustion efficiency is in the range of 90 – 96% and its size are large. To improve its performance, we need a combustor of high combustion efficiency and compact and small size. To achieve such a milestone the author introducing annular gas turbine combustor which is straight through flow combustor. To check its viability, need some experimental and simulation for introducing such a combustion chamber. Due to a lack of resources, the author performed only a simulation study in ANSYS fluent while skipping experimental study.

1.5 Objectives

In this paper, the author has simulated an annular micro combustor. As the annular combustor size is small and compact, that's why we are introducing it in MGT. Here we have used a non-premixed model and analyzed outlet temperature, NOx, CH_4 and CO at the outlet. On the basis of emissions, combustion efficiency is determined and compared. The objective of this research is to investigate alternative fuel (bio-fuel) having low emissions and better performance by reviewing different fuels. Moreover, modeling of an efficient gas turbine combustor for the fuel is part of this research. And to optimize the performance of the micro gas turbine combustion chamber, while using two different parameters such as dilution holes positioning and swirler blade angle.

1.6 Thesis outlines

1.6.1. Chapter 2

This chapter is about the litreture which I have review for the research. It includes the descrition of gas tubine combustion chamber history, and its types. It also determine the fuels properites and their selection criteria. The previous works which has already done on gas turbine combustor are discussed.

1.6.2. Chapter 3

This chapter is about the methematical modelling of combustion chamber for gas turbine. All the equations which are used for chamber modelling are identified and presented.

1.6.3. Chapter 4

In this chapter the solidworks model is presented. The setup for numerical simulation which include mesh generation along with its statistics and model, boundary condition are presented.

1.6.4. Chapter 5

This chapter is presenting all the results. The results including nitric oxides, temperature, unburned fuel and carbon monoxides are presented along with their distribution inside and outlet of combustion chamber. Furthermore, combustion performance is also investigated.

1.6.5. Chapter 6

This chapter is concluding all the research results and also presented problems along with recommnedations.

1.7 Summary

This chapter is about the general introduction of GT, MGT, swirler and Combustion chamber. This chapter also covers the need of MGT in the current power system and why the conventional fuel should be replaced? In the end, the motivation, objective and background of this research are slightly discussed.

References

[1]   M. P. Boyce, "An Overview of Gas Turbines Gas Turbine Cycle in the Combined Cycle or Cogeneration Mode," *Gas Turbine Eng. Handb.*, pp. 3–88, Jan. 2012.

[2]   E. I. Gutirrez Velsques *et al.*, "Micro Gas Turbine Engine: A Review," *Prog. Gas Turbine Perform.*, 2013.

[3]   I. I. Enagi, K. A. Al-attab, and Z. A. Zainal, "Combustion chamber design and performance for micro gas turbine application," *Fuel Process. Technol.*, vol. 166, pp. 258–268, Nov. 2017.

[4]   R. Boukhanouf, "Small combined heat and power (CHP) systems for commercial buildings and institutions," *Small Micro Comb. Heat Power Syst.*, pp. 365–394, Jan. 2011.

[5]   M. P. Boyce, "Advanced industrial gas turbines for power generation," *Comb. Cycle Syst. Near-Zero Emiss. Power Gener.*, pp. 44–102, 2012.

[6]   A. A. Ayon, I. A. Waitz, M. A. Schmidt, Xin Zhang, C. M. Spadaccini, and A. Mehra, "A six-wafer combustion system for a silicon micro gas turbine engine," *J. Microelectromechanical Syst.*, vol. 9, pp. 517–527, 2002.

[7]   B. Asgari and E. Amani, "A multi-objective CFD optimization of liquid fuel spray injection in dry-low-emission gas-turbine combustors," *Appl. Energy*, vol. 203, pp. 696–710, 2017.

[8]   A. Farokhipour, E. Hamidpour, and E. Amani, "A numerical study of NOx reduction by water spray injection in gas turbine combustion chambers," *Fuel*, vol. 212, no. August 2017, pp. 173–186, 2018.

[9]   C. Abagnale, M. C. Cameretti, R. De Robbio, and R. Tuccillo, "CFD Study of a MGT Combustor Supplied with Syngas," in *Energy Procedia*, 2016, vol. 101, pp. 933–940.

[10]   H. Y. Shih and C. R. Liu, "A computational study on the combustion of hydrogen/methane blended fuels for a micro gas turbines," *Int. J. Hydrogen Energy*, vol. 39, pp. 15103–15115, 2014.

Chapter 2
Literature Review

2.1 Gas Turbine Combustor

2.1.1. Introduction

This study concentrates on the the requirements of Gas Turbine Combustor. It describe different types employed in propulsion and power systems. The common features of Gas Turbine Combustor used in both systems reviewed. The basic features of conventional Gas Turbine Combustor basics features were established by around 1950. The basic geometry of Gas Turbine Combustor is dictated by the needs of the diffuser, though which the pressure loss can be minimized and liner for providing stable operation over a wide range of Air/Fuel ratios and by the needs of size and frontal area limit by other engine components. In the mid 20th century, Combustor pressure rises from 5 to 50 bar and inlet temperature from 450 to 950K while outlet temperature from 1100 to 1850K. Today Combustor efficiency may reach 100% while operating conditions are normal including idling and reduction in emissions pollutants substantially. The life expectancy of liner rises from a few hundred to tens of thousands.

However, many problems remain in design, multi-fuel capability of the gas turbine engine and to reduce pollutant emissions required new concepts and technology. Today's depletion of fossil fuels and rising cost promote research on alternative fuels and designing combustor for it. Another problem is acoustic resonance, resulted when instabilities of combustion are coupled with combustor noise and in lean premixed combustion it will be critical for future development.

2.1.2. Types of Combustor

There are 2 basic types of combustor annular and tubular while compromise between these is tub-annular or can-annular. The choice of combustor out of these combustors defend the need, type of engine and available space.

2.1.2.1. Tubular

It is also called can combustor and comprised of cylindrical liner within concentric casing. These Can are arranged along the circle with different numbers varying from 6-16 per engine shown in Figure 2-1. The main advantage is that little amount of money and time is required for its development. However, its use is prohibited in aviation application due to its weight and length and mostly installed in the stationary system (Gas turbine power plant).
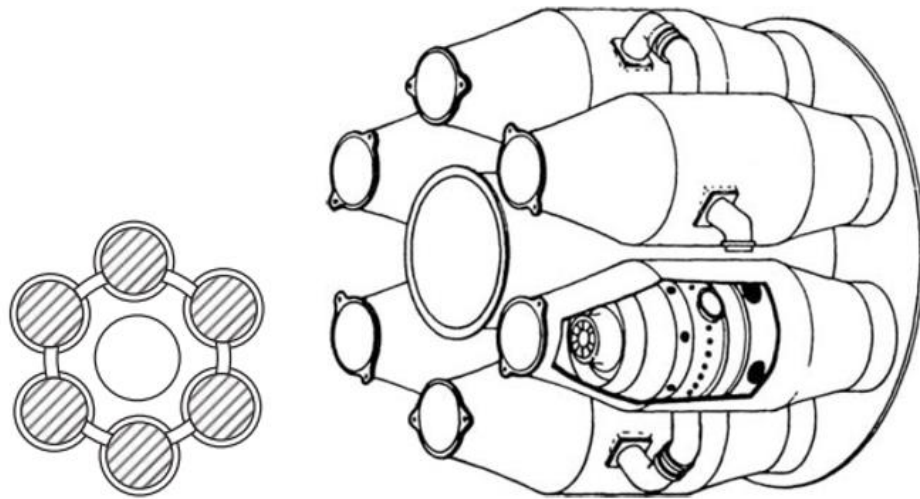
Figure 2-1. Multi-Can combustor arrangement (Courtesy of Northern Research and Engineering Corporation Report No. 1344-1)

2.1.2.2. Annular

The liner is located inside concentrically in the casing shown in Figure 2-2, with number of holes arranged in various zones. It may be an ideal combustor because of its layout, which make it compact and result less loss of pressure. However its cost is very high.

2.1.2.3. Tubu-annular

An engine pressure ratio started increasing in 1940 and scientists realize that combustors are required that can handle both high-pressure ratio and compactness. For this purpose, they propose combustor which has both Can and Annular combustor properties and developed Can-annular combustor, in which the liners in the single casing shown in

Figure 2-3. This combustor has both compactness of Annular and mechanical strength of Can combustors. Its drawback is it requires interconnectors.
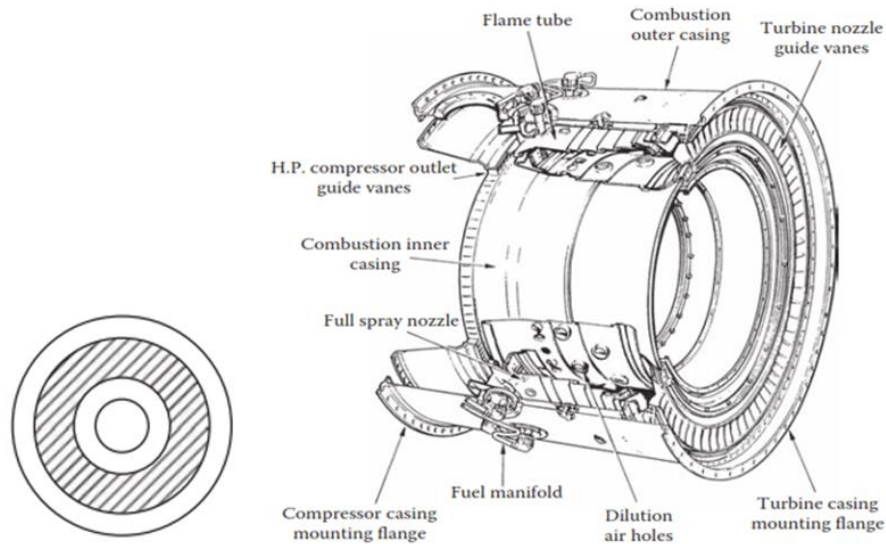
Figure 2-2. Annular combustor (Courtesy of Rolls Royce plc)
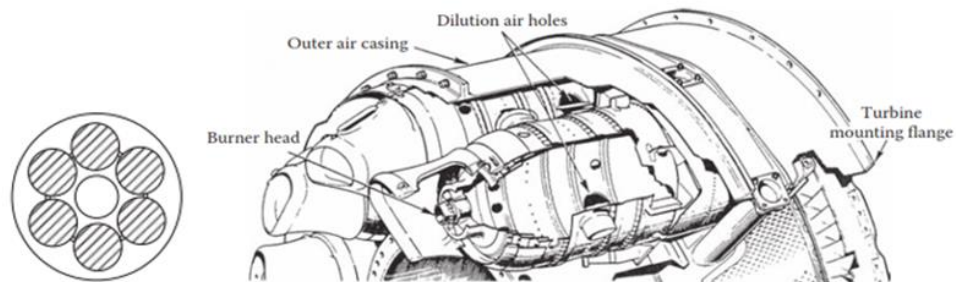
Figure 2-3. Tubu-annular combustor arrangement (Courtesy of Rolls Royce plc)

2.1.3. Diffuser

Designing combustor for minimizing the pressure drop across it. The stream of air across combustor is pushed through the pressure drop part (cold pressure). While heat addition to the high-velocity stream causes the remaining pressure drop (hot pressure) which is

$$\Delta P = \Delta P_{cold} + \Delta P_{hot} \qquad (2.1)$$

The cold pressure loss is the sum of pressure losses in the diffuser and combustor liner. The cold pressure loss is not considered in overall engine performance, but for combustor, it is valuable because diffuser pressure loss is wasted, while the pressure loss in the liner is beneficial to combustion and mixing because of liner wall manifested as turbulence. So the ideal combustor will be in which the entire cold pressure loss is in the liner. Typical value of cold pressure loss is about 2.5 to 5% of the combustor inlet pressure. The expression for hot pressure loss is

$$\Delta P_{hot} = 0.5U^2\rho\left[\frac{T_4}{T_3} - 1\right] \qquad (2.1)$$

Where T_3 is the inlet temperature while T_4 is the outlet temperature, ρ is the density of stream and U is the velocity of the stream.

The diffuser is used for reducing the velocity so that pressure loss is tolerable. The diffuser is not only this function but also to recover dynamic pressure loss as much as possible and to present smooth and stable flow to the liner. Two types of diffuser first is aerodynamic or faired diffuser shown in Figure 2-4 (a) and long to achieve maximum dynamic recovery pressure it is of two types of section in the first section almost 35% reduction is achieved in the velocity before snout and then it divides into 3 separate diffuser. One of them conveys air into the dome for dome cooling and atomization while the other two covey air into inner and outer annuli. The other diffuser is called dump or step diffuser shown in Figure 2-4 (b) it is shorter in length and reduces velocity up to half of the inlet. At the exit, the air is dumped by itself into the dome, inner and outer annuli.

Both diffusers are used, but due to higher variations in tolerance of profile of inlet velocity Dump diffuser and dimensions of hardware.
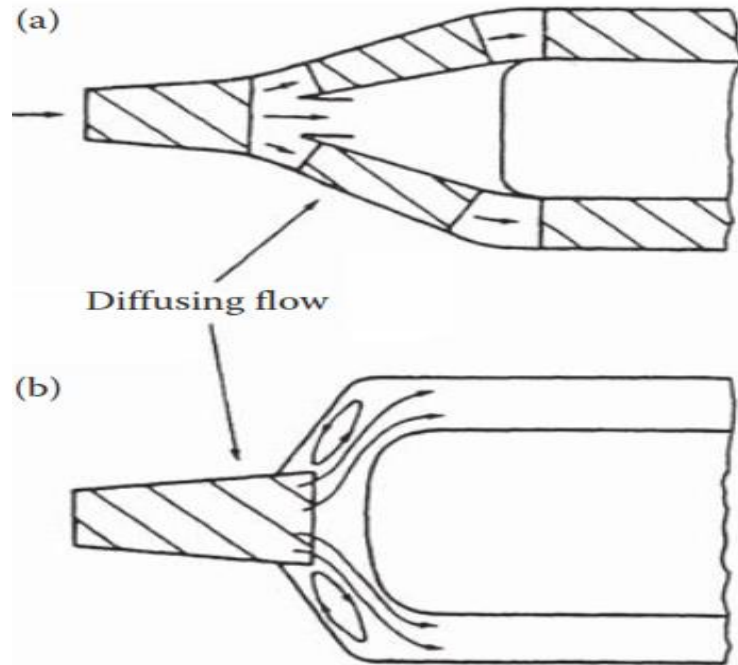
Figure 2-4. annular diffusers: (a) aerodynamic, (b) dump

2.1.4. Combustor zones

Combustor is the following zones

2.1.4.1. Primary Zone

The primary zone main function is flame anchoring by giving enough time, turbulence, temperature and place to the air/fuel mixture. Flow patterns of different types are employed but especially toroidal patterns with reversal of a portion of hot gases for continuing the ignition of incoming air and fuel shown in Figure 2-5. Some combustor uses swirler while others use the drill holes in the liner for reversal in the primary zone. If proper choice of swirler angle, size, number and axial location of primary holes, number and size is made then the flow recirculation generated by each will strengthen each other and the result will be strong and stable flow in the primary zone that will provide good performance combustion and provide freedom from instabilities in the flow that produce pulsation and noise in the combustion.
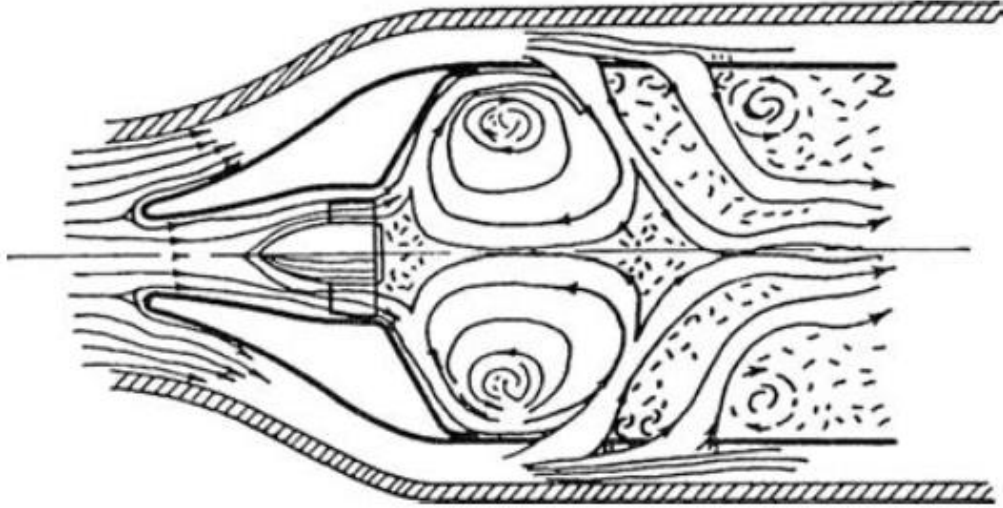
Figure 2-5. primary-zone airflow pattern

2.1.4.2. Intermediate (Secondary) Zone

The combustion temperature of the primary zone outlet products may exceeds 2000 K and dissociation reaction will result significant concentration of CO and H_2. If these gases are directly passed to the dilution zone then it will be frozen due to a massive amount of air entry through the dilution zone and CO will exhaust unburned which is both the source of pollution and inefficient combustion. The addition of small air results complete combustion of CO and unburned hydrocarbons, with smaal drop in temperature.

2.1.4.3. Dilution Zone

The remaining air (after combustion and wall cooling) is admit in the dilution zone. The result is to provide the hot gases temperature distribution from the intermediate zone so that acceptable for the turbine. This temperature distribution is called temperature transverse quality or pattern factor. The air available to the dilution zone is 20 – 40%. The entry of these air to the zone is through holes in the liner which are of different shapes, sizes and numbers depends on the optimization required for mixing. As the mixed-ness improved by increasing the length of mixing length and slower the rate. That's why the the ratio of dilution zone length to the diameter of the combustor is kept narrow in the range of 1.5 – 1.8.

15

If the temperature at the blade root is minimum, where stresses is usually high, it will be an ideal pattern factor where stresses are high and the turbine blade tip to protect seal materials. The attainment of such a pattern factor is paramount and a large portion of the total combustor development is devoted to achieving it. The location of various zones described with the holes and other combustor components is shown in Figure 2-6.
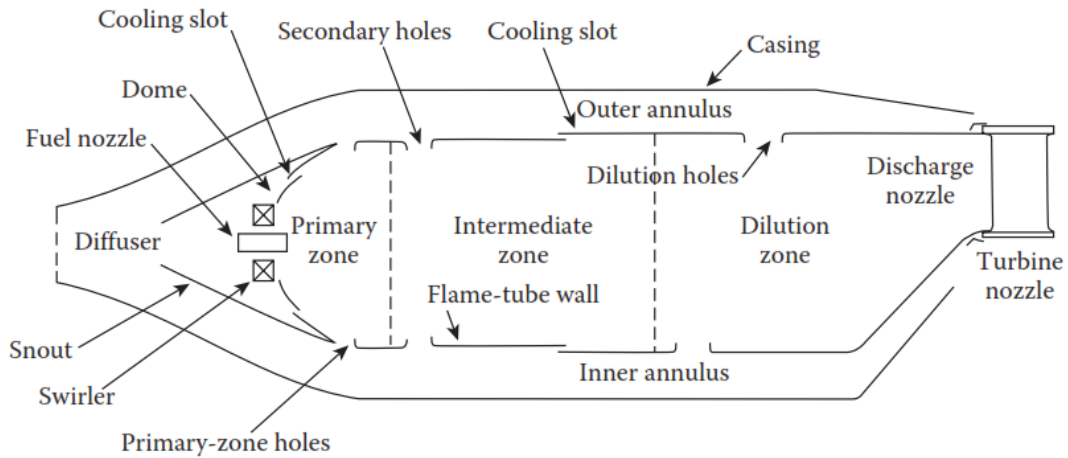
Figure 2-6. Schematic of annular combustor

2.1.5. Fuel Review

Energy exists in-universe, in various forms such as chemical, potential, kinetic, solar and can be changed to other forms such as mechanical, electrical, thermal. Energy in chemical forms exists in fuels which on burning in the presence of oxygen can be converted into thermal energy and then into shaft energy. In the ancient age burning of woods was used as a fuel for fulfilling needs, after which coal was introduced in the field of thermal energy, which was regularly used in vehicles, ships, heating and is still using in the field of power generation and lots of industries. But the issue related to the combustion of coal was climate change due to pollutant emissions. With time and advancement in technology petroleum after coal was explored, due to their comforts and benefits, most activities shifted to petroleum. Petroleum or Oil is one of fossil fuel while other most common fossil fuels are Coal, Natural gas and Orimulsion. Fossil fuels are non-renewable [1], [2] obtained directly from natural sources which are usually part of underground sources, and with little refining and modification, it is made useful for various applications. These fuels

can be converted into refined fuels through various chemical and physical processes for further applications. Fuels derived from fossil fuels are liquified natural gas (LNG), liquid petroleum gas (LPG), compressed natural gas (CNG), petrol, diesel, kerosene, methane, ethane, propane. And after processing raw materials valuable fuels such as producer gas, syngas [3] and blends of fuel are synthesized. As fossil fuels creates environmental issues due to emissions of particulate matter, greenhouse gas emissions, and other toxic emissions as well as facing depletion problem. To address these issues scientist community continues their research and have the derived, synthesized and distillate number of various fuels obtained from renewable and sustainable sources that have compatible energy density to petroleum, and can burn easily and used for various application. In the modern world of the 21st century, most of the energy is obtained from various other sources also which include renewable, sustainable and energy from other advanced fossils fuel such as blend fuels. As solar, hydro and wind energy are sustainable energy, but majority of our applications are still based on thermal energy obtained from burning of different fuels. Now a day's various types of fuel can be applied in internal and external fired engines and heating, which include both fossil fuels and renewable fuels. To address problems related to fuels burning number of fuels have been explored which have derived from different sources such as bio matters and other renewable sources and are using in various conditions. These fuels overcome emissions to some extent, but the issue is their production, due to which their prices are high.

2.1.5.1. Basic Properties of fuel

As there are the number of fuels in this universe, some are very common and available to everyone, while some are remaining hidden or out of eyes and it needs research and exploration. For determination of these fuels required some characteristic properties. In this paper, the presenter determined various combustible fuels based on basic combustible properties. Some of these combustible properties are presented in Figure 2-7 and disused briefly in Table 2-1.

17
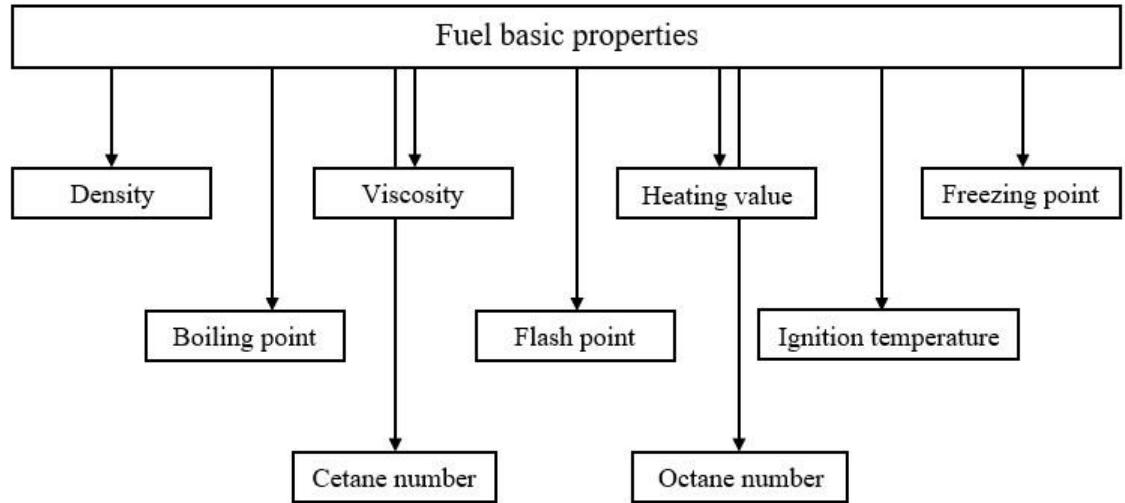
Figure 2-7. Basic fuel properties

Table 2-1. Basic properties of fuel

Fuel Property	Impact
Viscosity	It is the property of fluid due to which it results in internal resistance against its flow. If the viscosity is lower, then more fuel will pour to the combustion chamber due to which combustion will not be completed and soot will be produced. The carbon monoxides and unburned hydrocarbon will be increased in emissions. But if the fuel is reduced then no proper pressure will be generated in the burner and use energy will be lost. This will require the exchange of the nozzle. If the viscosity is higher it will pour the low amount of fuels and the excess air will be more, which will result in more chimney loss and result in poor combustion efficiency. So it is very important in combustion that viscosity of light fuels should be $0.5 – 0.8$ cSt and for medium fuels $1 – 1.5$ cSt [4]. Its effects can be seen in combustion and wear [5], [6]. It also affects the atomization quality [7].
Density	Density is defined as the mass of any substance contained in unit volume. If the density of the fuel is higher as for heavy fuel it will result in more energy and if fuel has lower density such as light fuel it will result in lower energy. For example, if the density of light fuel is 0.8 kg/liter and heavy fuel is 0.9 kg/liter, while the heating value

	for both is 40 MJ/kg. On supply of 200 liters of light and heavy fuel will result in energy of 6400 MJ and 7200 MJ. So, for getting the same energy will require more light fuel and less heavy fuel. Cetane numbers also related to density [7].
Ignition temperature	Ignition temperature is the property of fuel above which the fuel combustion is self-sustaining. The ignition temperature is lower for higher volatile fuel due to which biomass has lower ignition value compared to coal [8], while the gas is more volatile than both liquid and solid fuels and its ignition temperature is lower than both types fuel. Before flammable mixture burns, it needs that its temperature should be higher than the flash point.
Boiling point	The boiling point affects the combustion and vaporization. A low boiling point evaporates quickly and cause shorter penetration of fuel. It results in wetting of liquid wall and dilution problem of fuel-in-oil avoided [9], [10]. Low boiling point also reduce particulate matter production but NOx emission increases [11].
Freezing point	Fuels are usually a mixture of different compounds and structures due to which freezing point is not unique and solid crystals of some structure developed by reaching its temperature to its freezing points. The freezing point is very critical in the case of aviation and areas in which ambient temperature is very low. If the temperature is lower than fuel freezing points solid crystals of hydrocarbon will be developed. Aromatic hydrocarbon effects the freezing temperature of fuels [12].
Flash point	The flash point is the lowest point or temperature above which air-fuel mixture ignited and is important for the characterization of the flammability of the solvent [13]. It is also used as a fire safety characteristic. However, it does not affect combustion directly but makes it safer for storage and transportation [7].
Cetane number	Cetane number is the property of fuels related to their ignition delay. It measures the ignition of fuel under compression. Ignition delay

	will be short if the cetane number is high as for n-hexadecane the ignition delay is the shortest of any diesel and the cetane number is 100. Conversely lower the cetane number longer will be ignition delay and α-methyl naphthalene cetane number is 0 and its ignition delay is the longest of any diesel. It also affects fuel consumption, higher the cetane number lower fuel consumption due to the higher temperature of the combustion process [14]. Lower cetane number also reduces emissions of particulate matter due to reduction of cracking reaction and enhance unburned hydrocarbon production, while high cetane number increase particulate matter emissions [15] and reduce unburned hydrocarbon due to increased oxidation of fuels [14]. The sulfur also affects PM emissions and increase it slightly [16].
Octane number	Octane number tells how much the compression ratio for air-fuel mixture ignitions. And it prevents ignition before the spark plug does and thus measure resistance of knock of gasoline. So, whatever the octane number is compression ratio changes accordingly [17]. It may be a research octane number (RON) and motor octane number (MON). RON is usually more than MON. RON describes the behavior of fuel at lower speed and temperature, while MON describes fuel behavior at high speed and temperature.
Heating value	It is also referred to as calorific value or heat of combustion which is the amount of heat released by burning of fuels completely. It may be a higher heating value (HHV) or gross calorific value and lower heating value (LHV) or net calorific value. Fuel energy density determined from its calorific or heating value [18]. It is an important consideration for selecting a gas turbine engine or a combined heat power plant. Carbon monoxide concentration in exhaust is also effected by heating value [19].

2.1.5.2. Overview of Fuels and their characteristics

Any things or materials that contain energy in chemical forms that on reaction with oxygen converted into heat and liberated is called fuel. They are either primary or secondary type. Natural or primary fuels are those fuels that exist naturally and little modification can be used such as wood, peat, coal, natural gas, petroleum, etc. While artificial or secondary fuels are those that can be synthesized or produced such as charcoal, coke, biofuel, etc. These primary and secondary fuels have different states such as gaseous, liquid and solid. Which may be renewable or non-renewable. Renewable fuels are those which can't deplete due to their existence in the cycle, while non- renewable fuels are not in cycle and its reservoir will go to depletion. The overall classification of fuels is shown in Figure 2-8.

Fuels may be in gaseous, liquid and solid forms and they have various characteristics [20] as shown in Figure 2-9. Solid fuels cannot be used in internal combustion engines, but they should be externally fired and then use for various applications. Liquid fuels have high calorific value and its combustion is clean and can be used in both internal combustion engines. While gaseous fuel has high calorific value and can be used in both internal and external combustion engines.

2.1.5.3. Fuel selection criteria

Fuel for combustion engines and heating can be selected based on some important properties. Which is volatility, combustion products, energy density, lubricating properties, and availability. For the selection of proper fuel, the following factors or parameters should be meet [21] which are shown in Figure 2-10. The expert should focus on the following properties such as its burning should be steadily and easily and produce enough amount of heat, and after burning there should be no ash or less ash and pollutant emissions. It should easily and cheaply available in the market and should not affect other application like biofuel derived from seeds may have competition with foods. And the performance of gas turbine engines and other combustion engines can be measured by the following properties, Such as air ratio, pressure ratio, work ratio, compressor efficiency, engine efficiency, combustion efficiency, machine efficiency, and thermal efficiency. While combustion efficiency effected by fuel factors and properties.
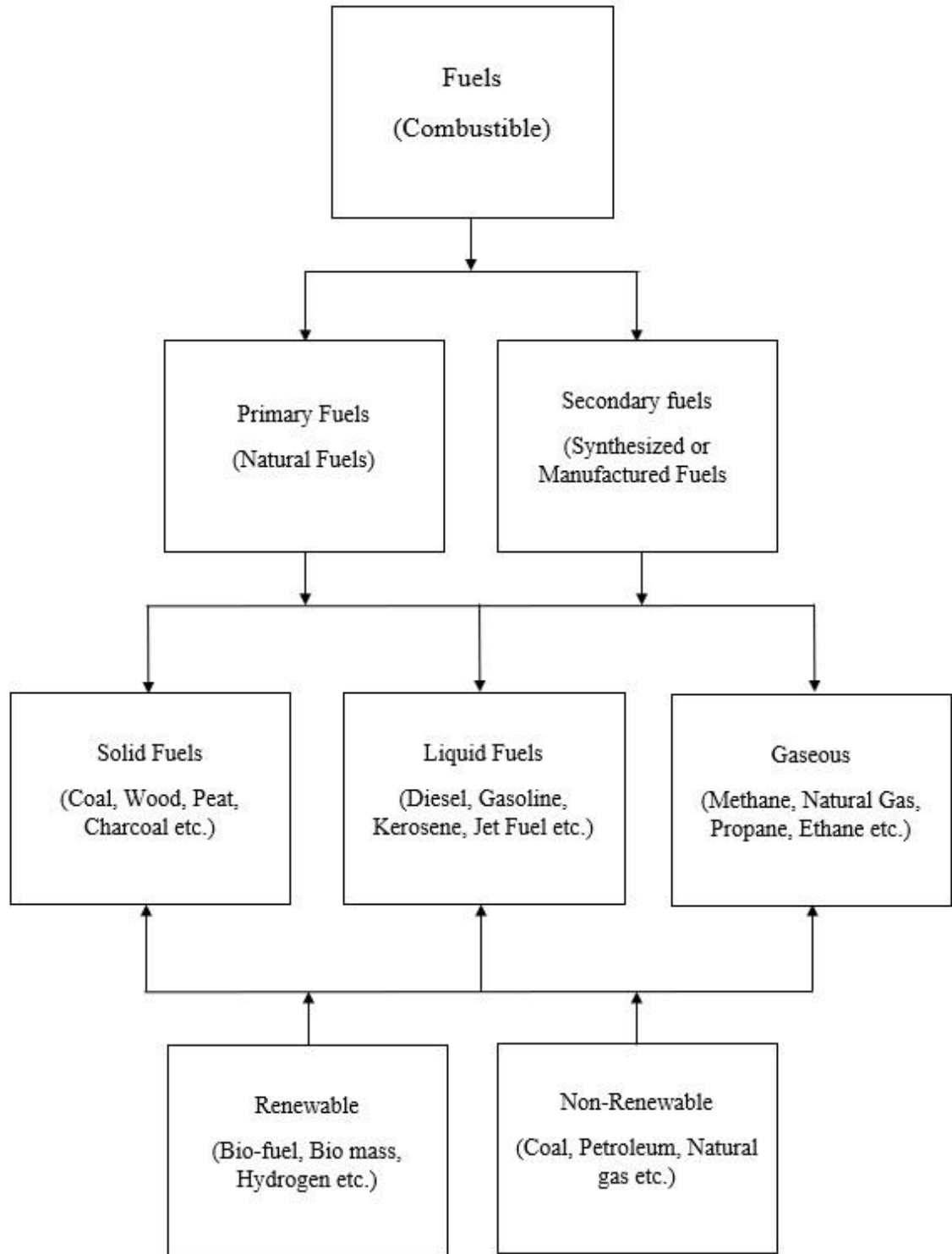
Figure 2-8. Schematic of Combustible Fuel classification

Fuel characteristics		
Solid fuels	**Liquid fuels**	**Gaseous fuels**
• In room condition or during time of using they are in solid form • Cannot be used in IC engine and externally fired • Combustion residue or ash is high • Thermal efficiency is low • Form clinker when burnt • Calorific value is low • Large excess air is required for combustion • It can handle not easily and require high cost	• They are burn in liquid or melted form. • Calorific value is high • It is clean fuel • No ash • Less excess air is required • It can be fired both internally and externally • Combustion system required less space • Less space required for storage	• During their application these fuels are in gaseous form • High heat content • Large storage space required • No ash

Figure 2-9. Characteristic of Fuels

And besides these factors fuel should possess some other characteristic properties [22][20]. Such as, fuel should have the highest possible calorific value, while its combustion should be controlled, and its combustion rate should be of moderate value. Moreover, the ignition temperature should be specific and proper, neither critically low nor high for controlling pollutant emissions such as carbo monoxides and NOx which is

produced at low temperatures and high temperatures respectively. Besides these, the moisture contents of fuel should be the lowest possible.

Parameters for proper fuel selection	
• Burn easily • Burn steadily • Burn efficiently • No spontaneous combustion • Good amount of energy • No or low pollutant emissions • Combustion products not toxic and easily dispose • Easily available	• Cheap • Large reservoirs • Low storage cost • Safely store, handle and transport • Easily store, handle and transport • Not effects its other application beside combustion • Compatible in existing infrastructure

Figure 2-10. Parameters for proper fuel selection

2.1.6. Previous Work

2.1.6.1. Combustor fueled with hydrogen

The gas turbine combustor which is fueled with hydrogen is tested and examine the performance by comparing it with the performance of natural gas fed combustor. The study main objectives are to evaluate the capacity of basic CFD methods so that to predict the inside temperature of the combustion chamber [23]. During the experiment, the temperature of the inlet and liner is measured. A similar analysis is also done in [24], [25]. From the comparison, it is clear to an acceptable pairing between the CFD results and the temperature which are measure on the inner side of the wall. The thermal field which is calculated is important for explaining the non-uniform distribution of temperature at the entry of the turbine. But however, the differences exist in the axial coordinate of those temperatures which is on the peak, but for the numerical modeling, the results are satisfactory. At the discharge of combustor in terms of non-dimensional a close match between experimental and CFD is found, According to the results CFD results can be considered to evaluate the selection of new combustion chamber configuration[23]. Moreover, many researchers have performed on hydrogen and its mixture with other fuels [26]–[30]. [31] Performed experiments to investigate pollutant emissions and control by

adding hydrogen. Furthermore, research on gas turbine combustor has been done by [32]–[36]for investigating hydrogen as an alternative fuel.

2.1.6.2. Comparison of Hydrogen fueled combustor with Jet A fuel

In this study, hydrogen fuel operating combustor is compared with jet-A, as aircraft are no more economic and now then hydrogen fuel was found superior in many aspects. This numerical analysis of the gas combustor for fuel Jet A and hydrogen compares the emission of pollutants. All analysis is in the range of excess air ratio "EAR" for engine speed at different values of rpm [37]. The percentage of unburned hydrocarbon and carbon dioxide emissions for Jet A decreases by increasing the values of EAR. The engine speed does not affect the emission of unburned hydrocarbon and carbon dioxide. Hydrogen burning was found to be advantageous in terms of pressure drop, the temperature at the outlet of the combustor, carbon monoxide, and unburned hydrocarbon emission values. It was seen as advantageous in terms of NO emission values at low excess air ratio values but found that at higher excess air ratio values as disadvantageous[37]. In [38] studied concentration of species and temperature by large-eddy simulating of can type combustor and combustion is non-premixed. The turbulent heat exchange of the combustion chamber is modeled numerically by [39]. Also studied hydrogen added with Jet A-1 or kerosene fuel-fed combustor with kerosene fuel on the basis of flame stability and pollutant emissions (carbon monoxides and NOx) [40]. A number of research have been done by researchers for combustion efficiency and emissions following National Combustion Code and compare with experimental data [41]–[43].

2.1.6.3. Syngas fed combustor performance

Combustor of different configuration has been investigated on a 3-D geometry, by giving rotation motion to the inlet air and a different number of holes with a detail injector. From this study it is found and clear the most important method is that one in which the numbers of holes near the primary zone, so when there is less amount of air added, then NO formation reduces with fruitful percentage. This configuration was further examined and studied by different fuels. On the other hand, the opposite behavior of the syngas derived from anaerobic digestion NO emission will be low while CO emission will be high [44]. The emission of pollutants is reduced dramatically due to heat transfer. The expected

25

trends resulted from computational analysis which is relevant to the heat transfer model must be introduced. The flame temperature will be of good results if hydrogen is present in the fuel. The results show that there will be no reduction in pollution by varying fuels, the two different syngas derived from different processes (gasification and pyrolysis of biomass will increase pollution but the reactant will combust well[44]. This paper is about to produce new micro annular combustor geometry using low calorific value gases [45]. From this paper, the internal temperature is reduced but the primary zone flame is close to the injector with the implication of emissions. In this case, syngas derived from biomass by pyrolysis. Similar research has been done in [46]–[48]. In [49] study of 2.D, turbulent, steady and swirling flow have done. In [50] rich-quench lean-burn combustion of the annular combustor with 2 different configuration 1st for natural gas which is original while 2nd is modified for syngas and identify its advantages. It used RANS while for the NOx non-adiabatic PDF model. From [51], [52] temperature decrease with syngas increase and nitric oxides NOx also decreases, But for the same amount of syngas with a greater amount of hydrogen gas NOx emissions increase. [53] Studied and compared the impact of alternative fuel on gas turbine combustor performance.

2.1.6.4. Hydrogen Methane blended for Micro Gas Turbine Combustor (MGT)

Numbers of tests are performed on combustor for investigating the combustion performance, where the fuel is a mixture of hydrogen and methane fuel in which hydrogen volumetric ratio changes in the range of 0% - 90%. Results are compared while focusing on the structure of flame and performance of combustion include average temperature of the flame in the entry zone, combustion chamber outlet temperature, while Pattern factor and emissions have been investigated. The study shows that the exit temperature of flame increase with increasing the proportion of hydrogen range, so flame temperature decreases, but the function of the engine may affect badly [54]. Similar work has been done in which up to 40% of hydrogen is blended with other fuels for improving the performance of the combustor [55], [56]. Hydrogen in blend is used commercially in which hydrogen proportion is 10% [57]. Hydrogen methane mixture is used as a fuel while laminar burning velocity is investigated by experimentation [58]. The evaluated results present the effect of hydrogen addition on the gas turbine combustor performance and as the hydrogen/CH_4 mixture fuels used at constant injection velocity[54]. To make

of good comparison equal amount of flow rate of hydrogen and methane blended fuel was used and the combustion chamber performance was investigated. So, at the same flow rate the flame temperature and outlet combustor chamber temperature increase which is beneficial for the turbine but produces some issues because cooling of the blade will be required, and NO emission will be increase which are the main focus. But NOx production can be reduced by using blends of hydrogen natural gas [59]. The temperature which is delivered at the exit is enough for maintaining the gas turbine performance, but emission of CO shows a decrease in efficiency of combustion. However emissions can be reduced by improving fuel injectors performance and mixing of air fuel [60], [61]. Changes in combustor design is required especially in entry and tertiary zone. By maintaining hydrogen percentage optimum good combustion performance can get. However, for analysis of mixed fuel for MGT further experimental testing and measurement of performance is needed so that understand combustion properties and optimum design of the combustor by adding hydrogen for which the simulation of model is very much important[54]. Besides hydrogen can be supply as additional fuel without blending to improve flammability and ignitibility in case of lean premixed flames [62], [63].

In paper [64]also the author introduces hydrogen methane blende with hydrogen amount changes from 0% – 80% by volume. PDF and k-ε model used for chemical reaction and studies the flame structure, along with flow field, flame temperature, major species, and emissions.

2.1.6.5. Gas turbine combustor fed with biodiesel

The burning of biodiesel fuel and its blends in a combustor chamber with preheated air and give it a larger spiral pattern. Along with minimum vaporization and combustion rate, the biodiesel has so much running challenges. Some of these properties can be very much improved as a result of mixing these biofuels with conventional fossil fuels. Elaborated examination of emissions and combustion properties for different fuels and air in preheat conditions. The carbon monoxide, hydrocarbon and NOx emissions for only biodiesel running engine are in orders of concentration. Carbon monoxide emissions of pure biodiesel are reduced significantly by reducing the speed of blades when the air preheating temperature is increased. Mixing of these fuels also helps in reducing emissions of NOx and unburned hydrocarbons after the combustion. Soot formation at all equal ratios is

found to be higher than for mixed biodiesel, kerosene. The air which is preheated and temperature shows less effect on soot formation[65] and overall biofuel give good results, but the emission problem still exists.

Also, the authors in papers [66]–[68] investigated biofuel and simulated their combustion in micro gas turbine combustor while the biofuels are both liquid and gaseous. These review papers describe in details that how to extend the use of biofuels in transportation and power plants [69]–[71].

2.1.6.6. Bioethanol fueled gas turbine combustor

Diesel, natural gas and bioethanol can be used for comparing the performance of gas turbine combustor, but NO emission problems arise in the case of natural gas and diesel because of temperature in the combustor to be high. In order to same specific work output for all fuel, the turbine inlet temperature (TIT) and thermal performance should be considered, by changing the ratio of diesel and bioethanol leads to the second condition, by the same amount of energy low NOx has achieved but hot slash problem raise. By these results, some optimization processes can be used to the analysis so that there is equality between turbine inlet temperature, work output, and performance and hot slash and NO emissions [72]. These fuel modeled with an equal amount of energy can satisfy the turbine inlet temperature and the specific work output, but there is variance in the emission of CO. the CO_2 produced due to the combustion of bioethanol and diesel are similar which is almost normal but lower than natural gas[72]. However, the main difference is due to the origin of biofuel, diesel and natural gas such that from where the biofuel is obtained. The main benefits of using biofuel giving less NO, because of the lower temperature produced by ethanol in the combustion chamber as compared to natural gas and diesel. There is a reduction in NOx emission using bioethanol as compared with conventional fuels. Further, in this sense of movement of slash to the gas turbine combustor, issue of non-irregularity at the TIT decrease and it will have less effect on the thermo-mechanical which damage in the first stage of the blades of turbine[72]. Works in [73]–[75] involves bioethanol and focusing on life cycle assessment for measuring greenhouse gas emissions. Bioethanol is widely used in automotive in the form of blend with gasoline for increasing octane number and gives advantages in terms of emissions [76]–[78].

2.1.6.7. Stability maps of gas turbine combustor

Under oxygen-rich air combustion conditions define the stability limits of the methane flames of gas turbine combustor chamber in which air has rotated pattern. One experiment composition is oxygen and carbon dioxide mixture and the second one is the mixture of nitrogen and oxygen, but oxygen concentration is large. The experiment is performed on various fraction of oxygen, equivalence ratio, fuel flow rate and Reynolds number of oxidizer component. Over the ranges of the operating parameter, the study of visualization of flame in terms of appearance, length, and color is carried out and gives the following information. Increasing the oxygen proportion increasing the flame stability. The momentum of oxygen and carbon dioxide mixture proportional to oxygen ratio increase, which prevents the oxygen-fuel flames of higher oxygen ratios from stabilizing at larger oxidizer turbulence. At smaller flames of oxygen ratio, the oxygen fuel flame lifts and blows out at higher equivalence ratios (fuel momentum) because of the less oxygen. For the same oxygen fractions and Reynolds number, the oxygen fuel flames can stabilize at higher equivalence ratios and fuel flow rates when compared to the air-fuel flames which are oxygen-rich. Then this is concluded in two ways, in the first type consider then oxygen and carbon dioxide mixture has a smaller momentum than the oxygen and nitrogen mixture for the same Reynolds number and oxygen ratio [79]. Flame stability and emissions like CO_2 and NO are investigated experimentally while using FGR (flue gas recirculation) [80]. NO emissions reduced approximately by 93%, while the flame length is noticeably reduced due to an increase in turbulent intensity. The combustor stability map was determined by quantifying blowout and flash back limits within the specific range of oxygen fraction and equivalence ration [81].

2.1.6.8. Air-swirl design criteria for gas turbine combustors through CFD optimization

In gas turbine combustors the simulation of swirl stabilized combustion has been studied by choosing a better model right for the design optimization consideration process which involves a large number of simulations and optimization. For this purpose, the four equation transition model for high Reynolds number system has used in relation with the steady model for turbulence interaction and an appropriate choice for the reaction mechanism in the next stage, the model was used to find the effects of air motion spiraling

pattern on the number of different goals in a multi-purpose, i.e. combustion efficiency, emission and pattern factor, entropy production minimization. So gives different result by changing these [82]. Numbers of researchers have carried research on swirler stabilized combustion most of which are reviewed in [83], [84]. [85] investigate the effect of outlet conditions through CFD analysis. The author determined that NOx and temperature are highly affected by the swirl number[86]. In this [87] non-premixed combustion with strong local extinction was validated with swirler. The finding of [88] is improving combustion efficiency and flame stabilization. [89] Studied combustion with strong swirl natural gas air reaction and its objective is the prediction of chemical concentration and temperature using PDF model and Reynold stress model. These papers [32], [33]are related about swirler stabilized combustion.

2.1.6.9. Gas turbine emissions

There is a problem with Green House gas and NOx, unburned hydrocarbon which affects combustion efficiency. The main purpose of designing a geometry and its dimensions is to focus on the need of the flame combustion mode. Air of which high inlet velocity is required to achieve higher Reynolds number and that's why it promotes mixing. A higher velocity function is to reduce the combustion, which reduces NOx and that's why it is an important parameter for emission. Higher temperature input would reduce the recirculated flow and the emission will have a bad impact. It is excellent to insert fuel through different holes located at a different location so that to ensure combustion inside the combustor is uniform. Air injection through the number of points can be considered for measure of scaleup the combustor. A large flow of air can be inserted for maintaining conditional pressure. Stoichiometric equivalence ratio would achieve the highest flame temperature, which is desirable for better performance. But high temperature produces more NOx, this produces more NOx and less CO, and It can be realized before the entry of combustor. Different fuels have different compositions and different calorific values and produce different emissions. The fuel-air mix before combustor entry produces good combustion performance and thus lower emissions. Recirculation ratio is significant for combustion which is flameless [90]. The author has studied traditional gas turbine combustor wall temperature and emissions and converted it to lean premixed pre-vaporized [91]. In [92] author study the NOx problem in the industrial boiler by using the model furnace and the

fuel used is methane. Environmental protection agencies regulate emissions and direct NOx emissions limit up to 15 ppm at 15% oxygen [93] and carbon monoxides (CO) by 150 ppm at 3% oxygen [94]. While for aircraft to cut down NOx productions by 90% by 2050 [95]. It looks the researcher is interested in swirler design and introduces different designs of swirler [96]–[100] and 2 different geometries of swirler created and tested and getting results [99], [100]. For reduction of NOx using the FGR method is used and experimental results are presented [80].

2.2 Summary

In this chapter, I present the history of Gas Turbine Combustor, Types of combustor use both in power and propulsion. This chapter also presents various fuels and their combustion properties. Most importantly I discussed the previous work done on combustion, emissions, fuels and their modeling with detail, so to show the importance of this research and to prove the techniques implied in this research is already implemented, with different parameter.

References

[1]   P. Gautam, S. Kumar, and S. Lokhandwala, "Energy-Aware Intelligence in Megacities," in *Current Developments in Biotechnology and Bioengineering*, Elsevier, 2019, pp. 211–238.

[2]   A. H. Lefebvre, And, and D. R. Ballal, *GAS Turbine Combustion Alternative Fuels and Emissions*, 3rd ed. Boca Raton: CRC Press, LLC, 2010.

[3]   *Americas Energy Future: Technology and Transformation*. Washington, DC: The National Academies Press, 2009.

[4]   Grupa Warter, "The effect of viscosity on the fuel combustion process," *Zakłady Chemiczne*. 2011.

[5]   M. S. Graboski and R. L. McCormick, "Combustion of fat and vegetable oil derived fuels in diesel engines," *Progress in Energy and Combustion Science*, vol. 24, no. 2. Pergamon, pp. 125–164, 01-Jan-1998.

[6] R. E. Tate, K. C. Watts, C. A. W. Allen, and K. I. Wilkie, "The densities of three biodiesel fuels at temperatures up to 300 °C," *Fuel*, vol. 85, pp. 1004–1009, 2006.

[7] E. Alptekin and M. Canakci, "Determination of the density and the viscosities of biodiesel-diesel fuel blends," *Renew. Energy*, vol. 33, no. 12, pp. 2623–2630, Dec. 2008.

[8] C. Dust, N. Dakota, B. Col-, and B. Illi-, "Learn more about Ignition Temperature Gas and Dust Explosions Biomass Characteristics," 2019.

[9] K. Kitano, I. Sakata, and R. Clark, "Effects of GTL fuel properties on di diesel combustion," in *SAE Technical Papers*, 2005.

[10] R. Nishiumi, A. Yasuda, Y. Tsukasaki, and T. Tanaka, "Effects of Cetane Number and Distillation Characteristics of Paraffinic Diesel Fuels on PM Emission from a DI Diesel Engine," *SAE Technical Paper Series*, vol. 1. 2010.

[11] S. Kook and L. M. Pickett, "Effect of Fuel Volatility and Ignition Quality on Combustion and Soot Formation at Fixed Premixing Conditions," *SAE Int. J. Engines*, vol. 2, pp. 11–23, 2009.

[12] "FREEZING POINT DETERMINATION OF AVGAS AND JET FUEL Per the Federal Aviation Administration ' s (FAA) website , Aviation Gasoline , Avgas , is the last remaining lead- containing transportation fuel . Lead , a toxic , heavy metal , is used as an anti-kno," p. 77064.

[13] E. Stauffer, R. Newman, and D. Analysis, "Learn more about Flash Point Flammable and Combustible Liquids Other Possible Examinations Conduct- ed on Fire Debris," 2016.

[14] R. Cataluña and R. Da Silva, "Effect of cetane number on specific fuel consumption and particulate matter and unburned hydrocarbon emissions from diesel engines," *Journal of Combustion*. 2012.

[15] W. F. Northrop, P. V. Madathil, S. V. Bohac, and D. N. Assanis, "Condensational growth of particulate matter from partially premixed low temperature combustion of biodiesel in a compression ignition engine," *Aerosol Sci. Technol.*, vol. 45, pp. 26–36, 2011.

[16] M. Deqing, Q. Junnan, S. Ping, M. Yan, Z. Shuang, and C. Yongjun, "Study on the Combustion Process and Emissions of a Turbocharged Diesel Engine with EGR," *Journal of Combustion*. pp. 1–9, 2012.

[17]   "What Does Octane Do In Gasoline_ Octane Ratings." .

[18]   Rena, P. Gautam, and S. Kumar, "Landfill Gas as an Energy Source," *Curr. Dev. Biotechnol. Bioeng.*, pp. 93–117, 2019.

[19]   Y. Bin Yang, C. Ryu, A. Khor, N. E. Yates, V. N. Sharifi, and J. Swithenbank, "Effect of fuel properties on biomass combustion. Part II. Modelling approach - Identification of the controlling factors," *Fuel*, vol. 84, no. 16, pp. 2116–2130, Nov. 2005.

[20]   V. reddy Chennu, "Characteristics and properties of fuels," 2017.

[21]   Balbir, "10 essential criteria's for selecting proper fuel," *PreserveArticles*. .

[22]   Bishm khanna, "The characteristics of an ideal fuel," *Preservearticles*, 2019. .

[23]   P. Gobbato, M. Masi, A. Toffolo, and A. Lazzaretto, "Numerical simulation of a hydrogen fuelled gas turbine combustor," *Int. J. Hydrogen Energy*, vol. 36, no. 13, pp. 7993–8002, 2011.

[24]   B. C. Ruud LGM, Eggels R, "Comparison of numerical and experimental results of a premixed DLE gas turbine combustor," *P. ASME Turbo Expo GT-0065*, 2001.

[25]   V. S. Sivaramakrishna G, Muthuveerappan N and S. TK., "CFD modelling of the aero gas turbine combustor," *P. ASME Turbo Expo GT-0063*, 2001.

[26]   L. W. Wan J, Fan A, Maruta K, Yao H, "Experimental and numerical investigation on combustion characteristics of premixed hydrogen/air flame in a micro-combustor with a bluff body," *Int J Hydrog. Energy*, vol. 37, pp. 19190–7, 2012.

[27]   U. J. Tuncer O, Acharya S, "Dynamics, NOx and flashback characteristics of confined premixed hydrogen-enriched methane flames.," *Int J Hydrog. Energy*, vol. 34, pp. 496–506, 2009.

[28]   G. A. Kim HS, Arghode VK, Linck MB, "Hydrogen addition effects in a confined swirl-stabilized methane-air flame.," *Int J Hydrog. Energy*, vol. 34, pp. 1054–62, 2009.

[29]   O. J. Strakey P, Sidwell T, "Investigation of the effects of hydrogen addition on lean extinction in a swirl stabilized combustor. 2007;," *Proc Combust Inst*, vol. 31, pp. 3173–80, 2007.

[30]   G. I. Tabet F, Sarh B, "Hydrogen–hydrocarbon turbulent non-premixed flame structure.," *Int J Hydrog. Energy*, 2009.

[31]   G. L. Juste, "Hydrogen injection as additional fuel in gas turbine combustor. Evaluation of effects," *Int. J. Hydrogen Energy*, vol. 31, pp. 2112–2121, 2006.

[32]   G. A. Kim HS, Arghode VK, Linck MB, "Hydrogen addition effects in a confined swirl-stabilized methane-air flame," *Int. J. Hydrog. energy 2009*, vol. 34, pp. 1054–62, 2009.

[33]   O. J. Strakey P, Sidwell T, "Investigation of the effects of hydrogen addition on lean extinction in a swirl stabilized combustor," *Proc. Combust. Inst. 2007*, vol. 31, pp. 3173–80, 2007.

[34]   L. W. Wan J, Fan A, Maruta K, Yao H, "Experimental and numerical investigation on combustion characteristics of premixed hydrogen/air flame in a micro-combustor with a bluff body," *Int. J. Hydrog. energy 2012*, vol. 37, pp. 19190–97, 2012.

[35]   U. J. Tuncer O, Acharya S, "Dynamics, NOx and flashback characteristics of confined premixed hydrogen-enriched methane flames," *Int. J. Hydrog. Energy 2009*, vol. 34, pp. 496–506, 2009.

[36]   G. I. Tabet F, Sarh B, "Hydrogen–hydrocarbon turbulent non-premixed flame structure," *Int. J. Hydrogen Energy*, vol. 34, pp. 5040–47, 2009.

[37]   N. Kahraman, S. Tangöz, and S. O. Akansu, "Numerical analysis of a gas turbine combustor fueled by hydrogen in comparison with jet-A fuel," *Fuel*, vol. 217, no. August 2017, pp. 66–77, 2018.

[38]   F. Di Mare, W. P. Jones, and K. R. Menzies, "Large eddy simulation of a model gas turbine combustor," *Combust. Flame*, vol. 137, pp. 278–294, 2004.

[39]   S. A. Lysenko DA, "Numerical modeling of turbulent heat exchange in the combustion chambers of gas-turbine plants with the use of the fluent package," *J. Eng. Phys. Thermophys. 2003*, vol. 76, pp. 888–91, 2003.

[40]   J. P. Frenillot, G. Cabot, M. Cazalens, B. Renou, and M. A. Boukhalfa, "Impact of H 2 addition on flame stability and pollutant emissions for an atmospheric kerosene/air swirled flame of laboratory scaled gas turbine," *Int. J. Hydrogen Energy*, vol. 34, no. 9, pp. 3930–3944, 2009.

[41]   M. A. Aydın H, Turan Ö, Karakoç TH, "Exergo-sustainability indicators of a turboprop aircraft for the phases of a flight," *Energy 2013*, pp. 550–60, 2013.

[42]   N. S. Seilbert M, "Simulation of dual firing of hydrogen-rich reformate and JP-8 surrogate in a swirling combustor," *Int. J. Hydrog. energy 2013*, vol. 38, pp. 5911–17, 2013.

[43]   E. Benini, S. Pandolfo, and S. Zoppellari, "Reduction of NO emissions in a turbojet combustor by direct water/steam injection: Numerical and experimental assessment," *Appl. Therm. Eng.*, vol. 29, no. 17–18, pp. 3506–3510, 2009.

[44]   C. Abagnale, M. C. Cameretti, R. De Robbio, and R. Tuccillo, "CFD Study of a MGT Combustor Supplied with Syngas," in *Energy Procedia*, 2016, vol. 101, pp. 933–940.

[45]   M. Fantozzi, F., Bianchi, M., Pinelli, M., Laranci, P., De Pascale, A., Cadorin, "CFD Simulation of a Microturbine Annular Combustion Chamber Fuelled With Methane and Biomass Pyrolysis Syngas: Preliminary Results," *ASME Pap. GT2009-60030*, 2009.

[46]   U. Herzler, J., Herbst, J., Kick, T., Naumann, C., Braun-Unkhoff, M., Riedel, "Alternative Fuels Based on Biomass: an Investigation of Combustion Properties of Product Gases," *ASME Pap. GT2012-69282*, 2012.

[47]   F. Laranci, P., Bursi, E., Fantozzi, "Numerical Analysis of Biomass-Derived Gaseous Fuels Fired in a RQL Micro Gas Turbine Combustion Chamber: Preliminary Results," *ASME Pap. GT2011-45807*, 2011.

[48]   D. Camporeale, S.M., Pantaleo, A.M., Fortunato, B., Sciacovelli, "Biomass Utilization in Dual Combustion Gas Turbines for Distributed Power Generation in Mediterranean Countries," *ASME Pap. GT2011-45727*, 2011.

[49]   M. El Salmawy, H.A., Shaalan, M.R., Anwar Ismail, "Prediction of Flow and Combustion Characteristic for a Gas Turbine Combustor Burning Low Heating Value Fuel," *ASME Turbo Expo, Glas. UK. Pap. GT2010-22156*, 2010.

[50]   F. Laranci, P., Bursi, E., Fantozzi, "Numerical Analysis of Microturbine Combustion Chamber Modified for Biomass Derived Syngas," *GT2011-45551., ASME Pap.*, 2011.

[51]   C.-R. L. Hsin-Yi Shih, "Model Analysis of Syngas Combustion and Emission for a Micro Gas Turbinex," *ASME Pap. Pap. GT2014-25589*, 2014.

[52]   C.-R. L. Hsin-Yi Shih, "A Computational Investigation of Syngas Substitution Effects on the Combustion Characteristic for a Micro Gas Turbine," *ASME Pap. GT2012-68950*, 2012.

[53]   W. C. Rye L, "The influence of alternative fuel composition on gas turbine ignition performance," *Fuel 2012*, vol. 96, pp. 277–83, 2012.

[54]   H. Y. Shih and C. R. Liu, "A computational study on the combustion of hydrogen/methane blended fuels for a micro gas turbines," *Int. J. Hydrogen Energy*, vol. 39, no. 27, pp. 15103–15115, 2014.

[55]   Y. W. Bannister RL, Newby RA, "Development of a hydrogen-fueled combustion turbine cycle for power generation.," *J. Eng. Gas Turbines Power*, vol. 120(2), pp. 267–83, 1998.

[56]   R. R. Phillips JN, "Hydrogen-enriched natural gas offers economic NOx reduction alternative," *Power Eng.*, vol. 105 (5), 2000.

[57]   B. A. Morris JD, Symonds RA, Ballard FL, "Combustion aspects of application of hydrogen and natural gas fuel mixtures to MS9001E DLN-1 gas turbines at elsta plant. Terneuzen, The Netherlands 1998.," *ASME Pap. 98-GT-359*, 1998.

[58]   M. Ilbas, A. P. Crayford, I. Yilmaz, P. J. Bowen, and N. Syred, "Laminar-burning velocities of hydrogen-air and hydrogen-methane-air mixtures: An experimental study," *Int. J. Hydrogen Energy*, vol. 31, pp. 1768–1779, 2006.

[59]   K. Y. Ilbas M, Yilmaz I, "Investigations of hydrogen and hydrogen-hydrocarbon composite fuel combustion and NOx emission characteristics in a model combustor," *Int. J. Hydrog. Energy 2005*, vol. 30, pp. 1139–47, 2005.

[60]   S. S. Therkelsen P, Werts T, McDonell V, "Analysis of NOx formation in a hydrogen-fueled gas turbine engine," *J. Eng. Gas Turbines Power 2009*, vol. 131(3), 2009.

[61]   M. A. Hernandez SR, Wang Q, Mcdonell V and H. B. Steinthorsson E, "Micromixing fuel injectors for low emissions hydrogen combustion," *Pap. GT2008-50854. Berlin, Ger. Turbo Expo,* 2008.

[62]   G. O. Guo H, Smallwood GJ, Liu F, Ju Y, "The effect of hydrogen addition on flammability limit and NOx emission in ultra-lean counterflow CH4/air premixed flames," *Proc. Combust. Inst. 2005*, vol. 30, pp. 303–11, 2005.

[63]   K. J. Wicksall DA, Agrawal AK, Schefer RW, "The interaction of flame and flow field in a lean premixed swirlstabilized combustor operated on H2/CH4/air," *Proc. Combust. Inst. 2005*, vol. 30, pp. 2875–83, 2005.

[64]   C.-R. L. Hsin-Yi Shih, "Combustion Characteristic and Hydrogen Addition Effects on the Performance of a Can Combustor for a Micro Gas Turbine," *ASME Pap. GT2010-22231*, 2010.

[65]   V. M. Reddy, P. Biswas, P. Garg, and S. Kumar, "Combustion characteristics of biodiesel fuel in high recirculation conditions," *Fuel Process. Technol.*, vol. 118, pp. 310–317, 2014.

[66]   T. R. Cameretti M.C., Piazzesi, R., Reale F, "Combustion Simulation of an EGR Operated Micro-Gas Turbine," *ASME J. Eng. Gas Turbines Power*, vol. 131, pp. 051701–10, 2009.

[67]   2013 Cameretti M.C., Piazzesi R., Tuccillo R., "Study of an EGR Equipped Micro Gas Turbine Supplied with Bio-Fuels," *Appl. Therm. Eng.*, vol. 59, pp. 162–173, 2013.

[68]   T. R. Cameretti M.C., "Combustion Features of A Bio-Fuelled Micro-Gas Turbine," *Appl. Therm. Eng.*, vol. 89, pp. 280–290, 2015.

[69]   T. M. Bergthorson JM, "A review of the combustion and emissions properties of advanced transportation biofuels and their impact on existing and future engines," *Renew. Sustain. Energy*, vol. 42, pp. 1393–417, 2015.

[70]   Budzianowski WM, "A review of potential innovations for production, conditioning and utilization of biogas with multiple-criteria assessment.," *Renew. Sustain. Energy*, vol. 54, pp. 1148–71, 2016.

[71]   S. Y. Chiaramonti D, Oasmaa A, "Power generation using fast pyrolysis liquids from bio mass.," *Renew. Sustain. Energy*, vol. 11, pp. 1056–86, 2007.

[72]   J. A. Alfaro-Ayala, A. Gallegos-Muñoz, A. R. Uribe-Ramírez, and J. M. Belman-Flores, "Use of bioethanol in a gas turbine combustor," *Appl. Therm. Eng.*, vol. 61, no. 2, pp. 481–490, 2013.

[73]   M. A. Renouf, M. K. Wegener, and L. K. Nielsen, "An environmental life cycle assessment comparing Australian sugarcane with US corn and UK sugar beet as producers of sugars for fermentation," *Biomass and Bioenergy*, vol. 32, no. 12, pp. 1144–1155, 2008.

[74]   K. L. Kadam, "Environmental benefits on a life cycle basis of using bagasse derived ethanol as a gasoline oxygenate in India," *Energy*, pp. 371–384, 2002.

[75]   L. Luo, E. van der Voet, and G. Huppes, "Life cycle assessment and life cycle costing of bioethanol from sugarcane in Brazil," *Renew. Sustain. Energy Rev.*, vol. 13, no. 6–7, pp. 1613–1619, 2009.

[76]   M. V. P. M.A. Costagliola, L. De Simio, S. Iannaccone, "Combustion efficiency and engine out emissions of a SI engine fueled with alcohol/gasoline blends," *Appl. Energy Energy*, pp. 1162–1171, 2013.

[77]   T. H. L. W.D. Hsieh, R.H. Chen, T.L. Wu, "Engine performance and pollutant emission of an SI engine using ethanol-gasoline blended fuels," *Atmos. Environ.*, pp. 403–410, 2002.

[78]   M. V. P. M.A. Costagliola, L. De Simio, S. Iannaccone, "Combustion efficiency and engine out emissions of a SI engine fueled with alcohol/gasoline blends," *Renew. Sustain. Energy*, pp. 209–222, 2013.

[79]   A. Abdelhafez, S. S. Rashwan, M. A. Nemitallah, and M. A. Habib, "Stability map and shape of premixed CH4/O2/CO2 flames in a model gas-turbine combustor," *Appl. Energy*, vol. 215, no. December 2017, pp. 63–74, 2018.

[80]   H. K. Kim, Y. Kim, S. M. Lee, and K. Y. Ahn, "NO reduction in 0.03-0.2 MW oxy-fuel combustor using flue gas recirculation technology," *Proc. Combust. Inst.*, vol. 31 II, no. x, pp. 3377–3384, 2007.

[81]   M. A. Habib, S. S. Rashwan, M. A. Nemitallah, and A. Abdelhafez, "Stability maps of non-premixed methane flames in different oxidizing environments of a gas turbine model combustor," *Appl. Energy*, vol. 189, pp. 177–186, 2017.

[82]   M. M. Torkzadeh, F. Bolourchifard, and E. Amani, "An investigation of air-swirl design criteria for gas turbine combustors through a multi-objective CFD optimization," *Fuel*, vol. 186, pp. 734–749, Dec. 2016.

[83]   Y. Huang and V. Yang, "Dynamics and stability of lean-premixed swirl-stabilized combustion," *Prog. Energy Combust. Sci.*, vol. 35, pp. 293–364, 2009.

[84]   L. Y. M. Gicquel, G. Staffelbach, and T. Poinsot, "Large Eddy Simulations of gaseous flames in gas turbine combustion chambers," *Prog. Energy Combust. Sci.*, vol. 38, pp. 782–817, 2012.

[85]   Wu Y et al., "Effect of geometrical contraction on vortex breakdown of swirling turbulent flow in a model combustor," *Fuel*, vol. 170, pp. 210–225, 2016.

[86]   Y. _I. Ilbas M, Karyeyen S, "Effect of swirl number on combustion characteristics of hydrogen-containing fuels in a combustor," *Int. J. Hydrogen Energy*, 2016.

[87]   Zhang H et al, "Large eddy simulation/conditional moment closure modeling of swirl-stabilized non-premixed flames with local extinction," *Proc. Combust. Inst.*, vol. 35 (2), pp. 1167–74, 2015.

[88]   R. Q. Zhuren Zhu, Renfu Li, Dingggen Li, Peng Zhang, "Experimental study and RANS calculation on velocity and temperature of a kerosene-fueled swirl laboratory combustor with and without centerbody air injection," *Int. J. Heat Mass Transf.*, vol. 89, pp. 964–76, 2015.

[89]   M. G. Khelil A, Naji H, Loukarfi L, "Prediction of a high swirled natural gas diffusion flame using a PDF model," *Fuel 2009*, vol. 88, pp. 374–81, 2009.

[90]   K. I. Khidr, Y. A. Eldrainy, and M. M. EL-Kassaby, "Towards lower gas turbine emissions: Flameless distributed combustion," *Renewable and Sustainable Energy Reviews*, vol. 67. pp. 1237–1266, 2017.

[91]   Shehata M, "Emissions and wall temperatures for lean prevaporized premixed gas turbine combustor," *Fuel 2009*, vol. 88, pp. 446–55, 2009.

[92]   M. A. Habib, M. Elshafei, and M. Dajani, "Influence of combustion parameters on NOx production in an industrial boiler," *Comput. Fluids*, vol. 37, no. 1, pp. 12–23, 2008.

[93]   A. EP, "Standards of performance for stationary combustion turbines," 2006.

[94]   A. final rule. EP, "National emission standards for hazardous air pollutants for major sources: industrial, commercial, and institutional boilers and process heaters," *FederalRegister*, 2013.

[95]   B. Jp. Rao AG, Yin F, "Ahybrid engine concept for multi-fuel blended wing body," *Aircr. Eng. Aerosp. Technol.*, vol. 86, pp. 483–93, 2014.

[96]   AndrewsGE, "16 - Ultra-low nitrogen oxides (NOx) emissions combustion in gas turbine systems," *Modern Gas Turbine Systems*. pp. 715–90, 2013.

[97]   C. S. Bourgouin J-F, Moeck J, Durox D, Schuller T, "Sensitivity of swirling flows to small changes in the swirler geometry," *Comptes Rendus Mécanique*, vol. 341, pp. 211–19, 2013.

[98]   S. V Khandelwal B, Lili D, "Design and study on performance of axial swirler for annular combustor by changing different design parameters," *J. Energy Inst.*, vol. 87, pp. 372–82, 2014.

[99]   J. M. Eldrainy YA, Saqr KM, Aly HS, Lazim TM, "Large eddy simulation and preliminary modeling of the flow down stream a variable geometry swirler for gas turbine combustors," *Int. Commun. Heat Mass Transf.*, vol. 38, pp. 1104–9, 2011.

[100]   J. M. Eldrainy YA, Saqr KM, Aly HS, "CFD insight of the flow dynamics in a novel swirler for gas turbine combustors," *Int. Commun. Heat Mass Transf.*, vol. 36, pp. 936–41, 2009.

Chapter 3
Mathematical Modeling

3.1 Gas turbine combustor design equations

3.1.1. Diffuser

The main objective of the diffuser is to reduce velocity and distribute flow in the prescribed amount to all combustion zones. While maintaining uniform flow condition with no parasitic losses and flow recirculation of any kind.

3.1.1.1. Diffuser geometry

The straight-wall diffuser geometry is defined in terms of three geometric parameters which are area ratio AR, it is a major choice because the prescribed decrease in velocity is achieved by it. The second one is non-dimensional length by Sovran and Klomp [1], it may be wall or axial length. A third parameter is divergence angle θ which is the dependent parameter and related to other parameters. For 2-dimensional

$$AR = 1 + 2\frac{L}{W_1}\sin\theta \tag{3.1}$$

And for conical

$$AR = 1 + 2\frac{L}{R_1}\sin\theta + \left(\frac{L}{R_1}\sin\theta\right)^2 \tag{3.2}$$

Where L is the wall-length while N is the axial length and W is the height of the opening for two-dimensional diffusers. R is the radius of the opening of conical diffusers. Sovran and Klomp [1] recommend the use of L/ΔR for annular diffuser. This gives an expression similar to two-dimensional units when it approaches unity and similar to conical units when inlet radius ratios approach zero.
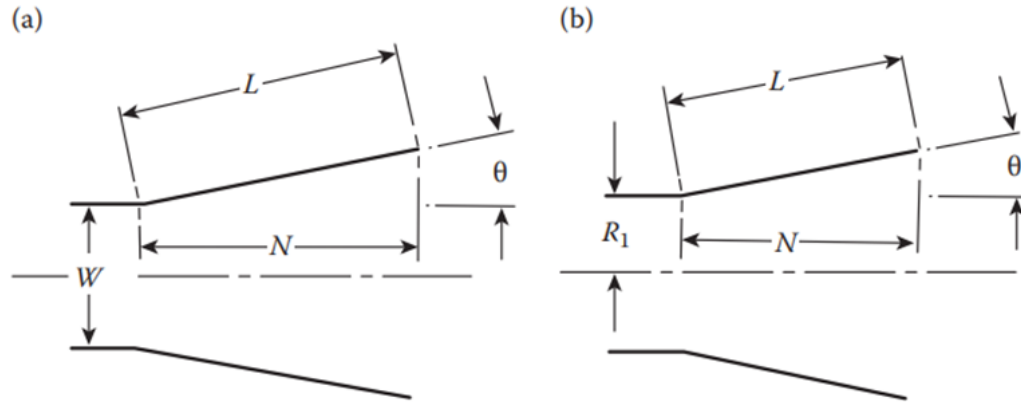
Figure 3-1. Diffuser geometry

3.1.1.2. Performance criteria

The function of the diffuser is to convert dynamic pressure 'q' to static pressure 'p' by velocity. By reducing velocity static pressure increases. For conversion efficiency, it is necessary to define the available mean velocity u, which is obtained directly from the continuity equation

$$u = \frac{\dot{m}}{\rho A}$$

(3.3)

And then dynamic pressure obtains by

$$q = \frac{\rho u^2}{2}$$

(3.4)

The pressure loss in the diffuser is

$$\Delta P_d = P_1 - P_2$$

(3.5)

From Continuity equation

$$\dot{m} = \rho A_1 u_1 = \rho A_2 u_2$$

(3.6)

Hence

$$AR = \frac{A_2}{A_1} = \frac{u_1}{u_2}$$

(3.7)

42

From Bernoulli equation

$$p_1 + q_1 = p_2 + q_2 + \Delta P_d \qquad (3.8)$$

3.1.1.2.1 Overall Effectiveness

It is the ratio of measured or real pressure recovery coefficient to ideal pressure recovery coefficient, and is denoted by η,

$$\eta = \frac{C_{p,measured}}{C_{p,ideal}} \qquad (3.9)$$

while

$$C_{p,ideal} = \frac{(p_2 - p_1)_{ideal}}{q_1} = 1 - \frac{1}{AR^2} \qquad (3.10)$$

And

$$C_{p,measured} = \frac{p_2 - p_1}{q_1} \qquad (3.11)$$

So

$$\eta = \frac{p_2 - p_1}{q_1\left(1 - \frac{1}{AR^2}\right)} \qquad (3.12)$$

η varies in the range of 0.5 to 0.9 [2] depending on the geometry and flow conditions.

3.1.1.2.2 Loss coefficient

It is defined as the ratio of diffuser pressure loss to the dynamic pressure at the inlet of the diffuser and denoted by λ

$$\lambda = \frac{P_1 - P_2}{q_1} \qquad (3.13)$$

The value of λ depends on the type of diffuser employed. For combustor diffuser of aerodynamically clean λ is usually 0.15 faired diffuser it is 0.45 for dump diffuser of

higher liner depth ratio in which there are support struts of normal complement and for vertex controlled diffuser in the range of 0.05 to 0.15 [3].

3.1.1.2.3 Kinetic-energy coefficient

For non-uniform flows, the kinetic energy flux is greater than uniform flow conditions while the flow rate is the same. For this velocity profile energy coefficient, 'α' is defined as

$$\alpha = \frac{\int \frac{u^2 \rho u dA}{2}}{\frac{\bar{u}^2 \dot{m}}{2}} \tag{3.14}$$

Its value is 1 for completely uniform flow and 1.05 for fully developed turbulent flow while around 2 at the point of flow separation for uniform flow [3]. Kinetic coefficient may be incorporated into the Bernoulli equation

$$p_1 + \alpha_1 q_1 = p_2 + \alpha_2 q_2 + \Delta P_d \tag{3.15}$$

And overall effectiveness become

$$\eta = \frac{p_2 - p_1}{q_1 \left(\alpha_1 - \frac{\alpha_2}{AR^2} \right)} \tag{3.16}$$

3.1.2. Aerodynamics

Aerodynamics processes play a vital rule in the design and performance of gas turbine combustion systems. Many types of combustors based on size, structure, concept, and method of fuel injection have been design, but many aerodynamic features are common to all systems. Within the combustor, liner attention is needed to focus on producing large scale recirculation for flame stabilization, effective dilution of the combustion products and efficient use of cooling air along the liner walls. Mixing processes are of paramount importance in combustion and mixing. In the primary zone, proper mixing is essential for a high burning rate and minimize soot and nitric formation and in the dilution zone for achieving specified uniform temperature. The primary objective of combustor design is

to produce satisfactory mixing with in the liner and a stable flow pattern throughout the combustion chamber with minimal length, flow losses, and pressure losses.

3.1.2.1. Reference quantities

$$A_{ref} = \frac{\dot{m}_3}{\rho_3 U_{ref}} \tag{3.17}$$

$$q_{ref} = \frac{\rho_3 U_{ref}^2}{2} \tag{3.18}$$

$$M_{ref} = \frac{U_{ref}}{\sqrt{\gamma R T_3}} \tag{3.19}$$

Where these reference parameters are among those which facilitate the analysis of combustor flow characteristics and to allow comparison of performance of different size and design combustors. U_{ref} is the mean velocity of flow across the casing of maximum cross-section area 'A_{ref}' without liner.

3.1.2.2. Pressure Loss Parameters

Two dimensionless pressure loss parameters are important in the combustor design. In which one is the overall pressure loss and the other is the pressure loss factor.

3.1.2.2.1 Overall pressure loss

It is the ratio of total pressure drop across the combustor to the combustor inlet total pressure. It depends on operating condition and is usually expressed in percentage

$$OPL = \frac{\Delta P_{3-4}}{P_3} \tag{3.20}$$

Its value ranges from 4% to 8% [4] while does not include the pressure losses due to combustion.

3.1.2.2.2 Pressure loss factor

It is the of total pressure drop across the combustor to reference dynamic pressure

$$PLF = \frac{\Delta P_{3-4}}{q_{ref}} \tag{3.21}$$

It is very important for combustor engineers because it denotes the flow resistance that is introduced between the compressor outlet and the turbine inlet. Aerodynamically it may be regarded as equivalent to a drag coefficient. The pressure loss factor is the fixed property of the combustion chamber and not depends on operating conditions. It is the sum of two separate pressure source losses such is pressure losses in a) diffuser b) across the liner.

$$PLF = \frac{\Delta P_d}{q_{ref}} + \frac{\Delta P_l}{q_{ref}} \tag{3.22}$$

It is important to minimize the pressure loss factor in the diffuser because it makes no contribution to combustion [5]. However, it is also important to minimize the pressure loss in the liner although the liner pressure loss in the liner is important for the combustion and dilution process. It gives high air velocities, steep penetration angle and high turbulence, which promotes good mixing and as a result combustion and shorter length of liner.

Pressure loss in liner can be calculated by equation

$$\Delta P_l = \frac{\rho_3 U_j^2}{2} \tag{3.23}$$

And maybe calculated by using hole effective area in the liner

$$\Delta P_l = P_3 \frac{R}{2} \left(\frac{\dot{m}_3 T_3^{0.5}}{A_{h.eff} P_3} \right)^2 \tag{3.24}$$

Where R is the universal gas constant

Overall Pressure Loss and Pressure Loss Factor can be compared by the equation

$$OPL = PLF \frac{R}{2} \left(\frac{\dot{m}_3 T_3^{0.5}}{A_{ref} P_3} \right)^2 \tag{3.25}$$

Thus, the total hole effective area is calculated by comparing equation (24) and (25)

46

$$\frac{\Delta P_l}{q_{ref}} = \left(\frac{A_{ref}}{A_{h.eff}}\right) \tag{3.26}$$

From equation (26) it is clear that the total effective hole area depends on the reference area of casing and pressure drop across liner

$$A_{h.eff} = \frac{A_{ref}}{\left(\frac{\Delta P_{3-4}}{q_{ref}} - \frac{\Delta P_d}{q_{ref}}\right)^{0.5}} \tag{3.27}$$

It may be calculated from equation

$$A_{h.eff} = \sum_{i=1}^{n} C_{d.i} A_{h.i} \tag{3.28}$$

The term $\frac{R}{2}\left(\frac{\dot{m}_3 T_3^{0.5}}{A_{ref} P_3}\right)^2$ in equation is reference velocity and can be written is $\frac{U_{ref}^2}{2RT_3}$. As the $\left(\frac{\dot{m}_3 T_3^{0.5}}{P_3}\right)^2$ is the fixed quantity and defined the compressor design so the only variable quantity is the A_{ref}.

Table 3-1: Pressure losses in combustion chamber

Type of combustor	OPL	PLF	$\dfrac{\dot{m}_3 T_3^{0.5}}{A_{ref} P_3}$
Can	0.07	37	0.0036
Can-annular	0.06	28	0.0039
Annular	0.06	20	0.0046

From table 1 [4]pressure loss factor varies in the range of 20 to 40. In actual the OPL is governed by various performance requirement, that dictates the pressure drop across the liner such as pattern factor, pollutant emissions, compressor outlet velocity and the type of diffuser used i.e. dump, faired or hybrid. In this, the pressure loss values are for cold pressure loss.

The pressure loss due to combustion is hot pressure loss and can be added to cold pressure losses. For uniform mixture which is flowing at low Mach number through a constant area may be calculated from momentum considerations as

$$\Delta P_{hot} = q_{ref}\left(\frac{\rho_3}{\rho_4} - 1\right) \tag{3.29}$$

Where ρ_3 and ρ_4 are the densities at the inlet and outlet of combustor respectively, where temperatures are T_3 and T_4. So the equation can be written is

$$\Delta P_{hot} \cong q_{ref}\left(\frac{T_4}{T_3} - 1\right) \tag{3.30}$$

For combustor in practical, the parameters effecting $\frac{\Delta P_{hot}}{q_{ref}}$ have the following relation

$$\Delta P_{hot} = q_{ref}K_1\left(\frac{T_4}{T_3} - K_2\right) \tag{3.31}$$

While K_1 and K_2 can be calculated experimentally and are given in [6]. For moderate temperature rise ΔP_{hot} usually lies in the range of 0.5% to 1% of P_3.

3.1.2.3. Relation between Size and Pressure Loss

For a straight-through combustor, the cross-sectional area can be calculated directly from overall pressure loss and combustion loading. But in the case of industrial and some aero gas turbine combustor, the casing area need to meet the gas turbine combustion requirements are so low as to give unacceptably high-pressure loss. Under these conditions, the overall pressure loss dictates the casing size

$$A_{ref} = \sqrt{\frac{R}{2}\left(\frac{\dot{m}_3 T_3^{0.5}}{P_3}\right)^2 \frac{\Delta P_{3-4}}{q_{ref}}\left(\frac{\Delta P_{3-4}}{P_3}\right)^{-1}} \tag{3.32}$$

It might be appearing that increasing the liner cross-sectional area is much as possible is advantageous to make velocities reduced and longer residence times within the liner which is beneficial for combustion efficiency, ignition, and stability. But for any given cross-section of casing increasing the liner cross-section area by the expense of annulus

area due to which the annulus velocities will be increased, and annular static pressure will lower and as a result liner holes static pressure drop reduced. This is undesirable because high static pressure drops required for high air penetrations and turbulence intensity to promote mixing and combustion. The optimum value of the ratio of liner cross-sectional area to casing cross-sectional area denoted by k_{opt} gives the highest value of $\Delta P_l/q_{pz}$ [7] and given by equation

$$k_{opt} = 1 - \left[\frac{(1 - \dot{m}_{sn})^2 - \lambda}{\Delta P_{3-4}/q_{ref} - \lambda r^2}\right]^{\frac{1}{3}} \quad (3.33)$$

$$A_l = K_{opt}A_{ref} \quad (3.34)$$

These two equations are valid for straight-through Annular, Tubular or Can and Tub-annular.

3.1.3. Flow in the annulus

Flow conditions in the annulus have a substantial effect on the airflow pattern within the liner and influence the liner wall temperature. The mean velocity is governed by the reference velocity and the ratio of liner and casing cross-section area. In practice, appreciable variation occurs because of changes in the inlet velocity profile and air entering the liner through dilution holes and cooling slots. However high velocity enhances convective cooling of the liner, but low annulus velocity has the following benefits and thus preferred

1. It ensures that all the liner holes in the same row pass the same airflow
2. Higher hole discharge coefficient
3. Steeper angles of jet penetration
4. Lower skin-friction loss
5. Lower sudden expansion means lower losses downstream of liner holes and cooling slots

In most combustors, the critical areas are at the upstream end of the liner and the vicinity of dilution holes.

3.1.3.1. Flow through Liner Holes

The flow-through liner holes not only depend on the size but also the geometry and the pressure drop across it and flow conditions in the vicinity of the holes, which defined its effective flow area.

3.1.3.1.1 Discharge coefficient

It depends on the geometry of the system; the approach velocity and the pressure drop across the liner. The equation is

$$C_d = \frac{\dot{m}_h}{A_{h.geom}\left[2\rho_3(P_1 - p_j)\right]^{1/2}} \tag{3.35}$$

Where P_1 is the total pressure upstream of the hole and p_j is the static pressure downstream of the hole. In practical, the coefficient of discharge [4] is affected by

1. Type (i.e. plain or plunged)
2. Shape (i.e. circular or rectangular)
3. Ratio of hole spacing to annulus height
4. Liner pressure drop
5. Distribution of static pressure around the hole in the liner
6. Presence of swirl in the flow
7. Local annulus air velocity

For incompressible, non-swirling flow the coefficient discharge by Kaddah [8] for Plain circular, oval and rectangular holes is

$$C_d = \frac{1.25(K - 1)}{[4K^2 - K(2 - \alpha)^2]^{1/2}} \tag{3.36}$$

Where α is the ratio of hole mass flow rate to annulus mass flow rate $\dot{m}_h/\dot{m}_{an}$ and K is the ratio of jet dynamic pressure to the annulus dynamic pressure upstream of the holes. Thus for plunged circular, oval and rectangular holes, Freeman [9] modified Kaddah equation by raising constantly from 1.25 to 1.65

$$C_d = \frac{1.65(K - 1)}{[4K^2 - K(2 - \alpha)^2]^{1/2}} \tag{3.37}$$

Local values of K around the liner annuli depend on a number of factors.

1. Circumferential variations in combustor inlet velocity profile
2. Manufacturing tolerances
3. Small changes in airflow distribution during combustor development

The values of K upstream of primary holes should be greater than 6, corresponding to U_h/U_{an} of 2. At higher K would give higher and stable C_d, but the increase in the diffuser area ratio. Higher values of K and C_d are assured for holes downstream required a satisfactory value of K at the primary holes, that are assured by the annular feed passages.

3.1.3.1.2 Initial jet angle

The reduction in the initial jet angle 'θ' shown in Figure 3-2 must reduce the effective hole area. Thus, the initial jet angle related to C_d and such a relation has been established by Fletcher, R. S., and Bastress, E.K [10]

$$\sin^2 \theta = \frac{C_d}{C_{d\infty}} \tag{3.38}$$

Where $C_{d\infty}$ is the asymptotic value of C_d where K tends to infinity. This relation is by Kaddah's experimental data.

3.1.3.1.3 Jet mixing

Jet mixing plays an important role in combustion performance. In the primary zone, proper mixing promotes efficient combustion and minimum pollutant formation. In the secondary zone, the rapid mixing of air and hot gases from the primary zone promotes unburned carbon and soot oxidation to produce normal products. While in the dilution zone rapid mixing provides proper composition and temperature of the products. The mixing rate of the air and hot gases is influenced by the following factors [4]

1. The size and to some extent the size of the holes
2. The initial angle of jet penetration
3. The momentum flux ratio, J
4. The presence of other jets, both opposed and penetration
5. The length of the jet penetration path
6. The proximity of walls

7. The inlet velocity and temperature profiles of jet and hot gases

In practice, the key factors governing mixing rates are momentum flux ratio, length of mixing path and the number, size and the initial angle of the jets.
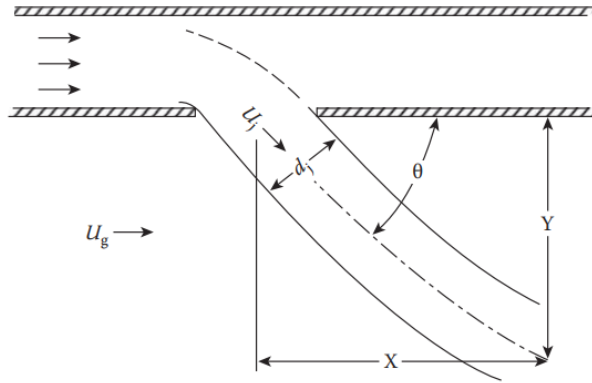

Figure 3-2. Air entry through-hole

3.1.4. Dilution Zone design

It is the lost zone in the combustor where mostly air and hot gases mix to produce diluted mixture at the exit. The principal parameters of dilution zone design are the length of the zone and the number and size of air admission holes. If the dilution holes area is covered by a large number of holes of small sizes, then the penetration will be inadequate and the core will be formed in the dilution zone. And if the dilution hole size is large and small number then the cold-core will be formed due to over-penetration and unsatisfactory mixing. So that's why the first step in the design process is to determine the optimum number and size of the dilution holes.

Here two methods for calculation of dilution hole size and numbers

3.1.4.1. Cranfield Design Method

If the liner wall contains a row of n dilution holes and diameter is d_j, then the mass flow rate will be

$$\dot{m}_j = \left(\frac{\pi}{4}\right) n d_j^2 \rho_3 U_j \qquad (3.39)$$

Hence

$$U_j = \left(\frac{2\Delta P_l}{\rho_3}\right)^{\frac{1}{2}}$$

(3.40)

Then

$$\dot{m}_j = \left(\frac{\pi}{4}\right) n d_j^2 \rho_3 \left(\frac{2\Delta P_l}{\rho_3}\right)^{\frac{1}{2}}$$

(3.41)

And

$$n d_j^2 = 15.25 \dot{m}_j \left(\frac{P_3 \Delta P_l}{T_3}\right)^{-\frac{1}{2}}$$

(3.42)

$$y_{max} = \frac{1.25 d_j J^{0.5} \dot{m}_g}{\left(\dot{m}_g + \dot{m}_j\right)}$$

(3.43)

While y_{max} for tubular combustor is $0.33 D_l$ and for annular combustor is $0.4 D_l$ and then the comparison of these 2 equations gives the value of the diameter of the jet d_j, and then gives the number of dilution holes. $C_d = 0.6$ from NACA technical note. The actual diameter of holes is given by

$$d_h = \frac{d_j}{C_d^{0.5}}$$

(3.44)

For both Annular and Tubular combustor the dilution length is $1.5 D_l$. Shorter length results in inadequate mixing while longer length does not improve pattern factor significantly. Because the additional wall cooling air required reduces the amount available for dilution.

3.1.4.2. NASA Design Method

Holdeman et al analyze experimental and CFD data from a number of NASA- Lewis-sponsored studies and then obtained the expression for the optimum number of holes and is given by

$$n_{opt} = \frac{\pi(2J)^{\frac{1}{2}}}{C} \qquad \text{(3.45)}$$

Where C is experimentally derived constant. According to Holdeman, the optimum value of C is 2.5 for single-sided air injection through cylindrical and rectangular ducts. For rectangular ducts, of inline and opposing rows of jets is 1.25 while for staggered and opposing rows of jets is 5.

The main differences in both approaches (Cranfield and NASA) are that one stresses the size of the hole and the other stresses on the spacing of the holes. Thus, for any given value of J and downstream distance, the Cranfield method leads to an optimum hole size and the hole size is then chosen to provide the design value of $\dot{m}_j/\dot{m}_g$. On the other hand, NASA technique first identify the optimum hole spacing and the hole size is then estimated to give $\dot{m}_j/\dot{m}_g$.

3.1.4.3. Comparison of Cranfield and NASA Design Methods

Unfortunately, both methods do not always give the same results. For example, when J is increased by increasing U_j then both methods give the same result in terms of hole spacing, numbers, and size. However, if J is increased by reducing U_g then both approaches give different results. An interesting feature of Cranfield is that it takes account in a very direct manner the adverse effects on jet penetration and mixing arise from the aerodynamic blockage created by the presence of adjacent air jets. This could be useful when $\dot{m}_j/\dot{m}_g$ is exceptionally high.

3.1.5. Swirler

One of the most effective ways of inducing flow recirculation in the primary zone is to fit a swirler in the dome around the fuel injector. The recirculation in swirling flow is caused by vortex breakdown when the amount of rotation imparted to the flow is high. Swirl components produce strong shear regions, high turbulence, and rapid mixing rates. These characteristics of swirling flow has been used in the control of combustion stability and intensity, and the shape of flame regions. Air swirlers are widely used in annular and tubular combustor. It may be axial or radial.

3.1.5.1. Axial Swirler

An important design requirement is that the swirler should pass the desired airflow rate for a given pressure drop ΔP_{sw}, which is usually assumed to be equal to the liner pressure drop ΔP_l.

$$\dot{m}_{sw} = \left\{ \frac{2\rho_3 \Delta P_{sw}}{K_{sw}[(\sec \beta / A_{sw})^2 - 1/A_l^2]} \right\}^{\frac{1}{2}} \tag{3.46}$$

Where A_{sw} is the swirler frontal area and θ is the vane angle. A_{sw} is simply the swirler area minus the area occupied by the vanes and hub.

$$A_{sw} = \frac{\pi}{4}(D_{sw}^2 - D_{hub}^2) - 0.5 t_v n_v (D_{sw} - D_{hub}) \tag{3.47}$$

n_v is the number of vanes in the swirler and t_v is the vane thickness. From [11], [12] θ is in the range of 40° to 50°, t_v is in the range of 0.7 to 1.5 mm, n_v is in the range of 8 to 16 and ΔP_{sw} is from 3% to 4% of combustor inlet pressure. While K_{sw} is 1.3 for flat vanes and 1.15 for curved vanes.

For flat vane, the β is constant, while for curved vanes β is 0° at the inlet and at outlet vane angle is β.

3.1.5.1.1 Swirl Number

Expressions for the swirl number of various swirler has been derived by Beer and Chigier [13]. Expression for axial swirler with constant vane angle is [5]

$$S_N = \frac{2}{3} \left[\frac{1 - (D_{hub}/D_{sw})^3}{1 - (D_{hub}/D_{sw})^2} \right] \tan \beta \tag{3.48}$$

If S_N is less than 0.4 then no flow recirculation and the swirl is week, while for strong swirl the S_N should be greater than 0.6 which is of practical interest. It is of interest that under a very strong swirl and vane angle of 65° the reverse flow actually exceeds the swirl flow, Mathur and Maccalum's [14].

3.1.5.1.2 Size of recirculation zone

Experimental data from Kilik [15] shows that the recirculation zone increased by

1. An increase in vane angle

2. An increase in the number of vanes
3. A decrease in the Aspect ratio
4. Change from flat to curved vanes

3.1.5.2. Radial Swirler

It is now widely used in dry low emissions and conventional combustor. The design rules for the radial provide useful guidance for the axial swirler. Flow area of the swirler is calculated by relation

$$A_{sw} = n_v s_v w_v C_d \tag{3.49}$$

s_v is the vane gap, w_v is the vane width and C_d is the vane discharge coefficient. According to Dodds and Bahr [11] C_d for preliminary design purposes, an appropriate value is 0.7.

3.1.6. Temperature traverse quality

One of the most important and at the same time most difficult problems in the design and development of Gas Turbine Combustor is the satisfactory and consistent distribution of temperature of the gases into the Turbine. In the past experience and hit and trial played a major role in the determination of temperature traverse quality of satisfactory individual combustor design.

As for overall engine performance is concerned, the most important temperature is the turbine inlet temperature T_4 which is the mass flow weighted of the mean of all the exit temperatures recorded for one standard of liner. Since the nozzle guide vane is fixed relative to the combustor they must be designed to withstand maximum temperature found in the traverse. Thus the parameter most relevance to the design of nozzle guide vanes is the overall distribution temperature pattern factor [4], that highlights the maximum temperature

$$Pattern\ Factor = \frac{T_{max} - T_4}{T_4 - T_3} \tag{3.50}$$

T_4 is the mean exit temperature, T_3 is the combustor inlet temperature and T_{max} is the maximum recorded exit temperature.

The expression used to describe the radial distribution factor is called a profile factor.

$$Profile\ Factor = \frac{T_{mr} - T_4}{T_4 - T_3} \qquad (3.51)$$

T_{mr} is the maximum circumferential mean temperature. The temperature of most significance to the turbine blades are those that constitute the average radial profile. They are obtained by measuring the radial temperature along the liner at different positions and then divide by the number of locations at each radius.

A parameter that takes the design profile into account is the turbine profile factor and defined as

$$Turbine\ Profile\ Factor = \frac{(T_{4.r} - T_{4.des})_{max}}{T_4 - T_3} \qquad (3.52)$$

$(T_{4.r} - T_{4.des})_{max}$ is the maximum temperature difference between the average temperature at any given radius around the circumference and the design temperature for the same radius.

3.1.7. Combustion performance

A combustion chamber is required to burn fuel stable over a wide range of operating conditions with a level of combustion efficiency close to 100%. The important parameter in the gas turbine combustor is combustion efficiency, stability, and ignition.

3.1.7.1. Combustion efficiency

High levels of combustion of efficiency are only acceptable because combustion inefficiency consider as waste of fuel, but mainly it is manifested in the form of pollutant emissions such as unburned hydrocarbon and carbon monoxide. When the engine control system compensates inefficiency of combustor then more fuel will be supplied and then extra fuel may cause the rich extinction of the flame. Thus important consideration required for the design of the gas turbine combustion chamber.

The primary purpose of combustion is to raise the temperature of the airflow by burning fuel efficiently. From a design point of view, an important requirement is a means of relating combustion efficiency to the operating variables of air pressure, temperature, mass flow rate and to the combustor dimensions. But the various processes taking place in the combustion zone is highly complex. Combustion efficiency is defined by [16] which is

$$\eta_c = \frac{\rho_g A_f S_T c_p \Delta T}{q \dot{m}_A H} \tag{3.53}$$

Where $qH = c_p \Delta T$, A_f is the flame area and assume to be proportional to the combustor reference area A_{ref}. Thus $\dot{m}_A$ in terms of U_{ref} so equation is

$$\eta_c \propto \frac{S_T}{U_{ref}} \tag{3.54}$$

If U_{ref} consider in terms of $\dot{m}_A$, P_3, and A_{ref} and describes S_T in terms of laminar burning velocity and turbulent intensity, then equation is

$$\eta_c = \left[\frac{P_3 A_{ref} \left(P_3 D_{ref} \right)^m \exp(T_3/b)}{\dot{m}_A} \right] \left[\frac{\Delta P_l}{q_{ref}} \right]^{0.5m} \tag{3.55}$$

By considering the pressure loss factor is negligible, so equation become

$$\eta_\theta = f(\theta) = f \left[\frac{P_3 A_{ref} \left(P_3 D_{ref} \right)^m \exp(T_3/b)}{\dot{m}_A} \right] \tag{3.56}$$

And from emissions of combustor the combustion efficiency [17], [18] is

$$\eta_c = \frac{CO_2 + 0.645CO}{CO_2 + CO + UHC} \tag{3.57}$$

3.2 Summary

This chapter is about the mathematical study of the code which I generated for the combustor design given in the appendix. I used different equations got from different

papers and books, which is presented and explained in this chapter. Here I convey that what is the importance of these equations in the design of the combustion chamber for MGT.

References

[1]   E. D. Sovran, G., and Klomp, "Experimentally Determined Optimum Geometries for Rectilinear Diffusers with Rectangular, Conical or Annular Cross Section," *Fluid Mech. Intern. Flow*, pp. 270– 319, 1967.

[2]   A. L. Cockrell, D. J., and King, "A Review of the Literature on Subsonic Fluid Flow through Diffusers," *Br. Hydromechanics Res. Assoc.*, p. 902, 1967.

[3]   A. H. Lefebvre, And, and D. R. Ballal, *GAS Turbine Combustion Alternative Fuels and Emissions*, 3rd ed. Boca Raton: CRC Press, LLC, 2010.

[4]   A. H. Lefebvre, And, and D. R. Ballal, *GAS Turbine Combustion Alternative Fuels and Emissions*. Boca Raton: Taylor and Francis Group, LLC, 2010.

[5]   F. X. Tan *et al.*, "Design of combustor for micro gas turbine test rig and its performance prediction," *J. Teknol.*, vol. 77, no. 8, pp. 113–117, 2015.

[6]   W. R. Scull, W. E., and Mickelsen, "Flow and Mixing Processes in Combustion Processes," *Chap. II,NACA Rep. 1300,* 1957.

[7]   Lefebvre, A. H., and Norster, E. R., "The Design of Tubular Combustion Chambers for Optimum Mixing Performance," *Proc. Inst. Mech. Eng. Inst. Mech. Eng. London*, 1969.

[8]   K. S. Kaddah, "Discharge Coefficients and Jet Deflection Angles for Combustor Liner Air Entry Holes," *Coll. Aeronaut. MSc thesis, Cranfield, UK*, 1964.

[9]   Freeman, B. C., "Discharge Coefficients of Combustion Chamber Dilution Holes," *Coll. Aeronaut. MSc thesis, Cranfield, UK*, 1965.

[10]   Fletcher, R. S., and Bastress, E.K., "The Design and Performance of Gas Turbine Combustion Chambers," *North. Res. Eng. Corp. NREC Rep. 1082*, 1964.

[11]   Dodds, W. J., and Bahr, D. W., "Combustion System Design," in A. M. Mellor, ed., Design of Modern Gas Turbine Combustors," *Acad. Press. San Diego, CA,* 1990.

[12]   R. B. Knight, M. A., and Walker, "The Component Pressure Losses in Combustion Chambers," *Aeronaut. Res. Counc. R M 2987, UK,* 1957.

[13]   Beer, J. M., and Chigier, N. A., "Combustion Aerodynamics," *Appl. Sci. London,* 1972.

[14]   N. R. L. Mathur, M. L., and Maccallum, "Swirling Air Jets Issuing from Vane Swirlers, part I, Free Jets," *J. Inst. Fuel,* vol. 40, pp. 214–225, 1967.

[15]   Kilik, E., "The Influence of Swirler Design Parameters on the Aerodynamics of the Downstream Recirculation Region," *PhD thesis, Sch. Mech. Eng. Cranf. Inst. Technol. UK,* 1976.

[16]   A. H. Lefebvre and D. R. Ballal, *Gas Turbine Combustion: Alternative Fuels and Emissions*, vol. 1. Boca Raton: Taylor and Francis Group, LLC, 2010.

[17]   R. C. Zhang, W. J. Fan, Q. Shi, and W. L. Tan, "Combustion and emissions characteristics of dual-channel double-vortex combustion for gas turbine engines," *Appl. Energy*, vol. 130, pp. 314–325, 2014.

[18]   R. C. Zhang, F. Hao, and W. J. Fan, "Combustion and stability characteristics of ultra-compact combustor using cavity for gas turbines," *Appl. Energy*, vol. 225, no. May, pp. 940–954, 2018.

Chapter 4

Modeling and Simulation

4.1 Modeling and Simulation

A combustion chamber has modeled based on the code generated from the data available in the book [1]. Schematic of the combustion chamber for Case 1 and 2 are shown in Figure 4-1. The dilution holes are at a position of 10.2 mm, and 9.1 mm from the entry of liner in Case 1 and 2 respectively, while the swirler vane angle is 42° for both cases. In Case 3 the angle of the swirler blade is changed to 45°, while the position of dilution holes is the same as case 1.

4.1.1. SolidWorks Model

The combustion chamber along with the swirler shown in Figure 4-2 has modeled in SolidWorks. The combustor has twenty swirlers comprised of eight vanes with twenty fuel injectors passing through their hub. The length and depth of the liner are 14.1 mm and 6.4 mm respectively, while the depth of the outlet is 5 mm. The liner different zones such as primary, secondary and dilution zones have the number of holes arranged in equal spacings around the liner. Primary holes numbers are forty, while each secondary and dilution holes are eighty. The remaining parameters are listed in Table 4-1.

Table 4-1. Dimensions of MGTC

Parameter	Value
Radius of the outer liner	38
Radius of inner liner	31.6
Diameter of primary holes	1.2
Diameter of dilution holes	1.6
Diameter of swirler	3.6
Diameter of the hub	1.4
Numbers of swirler blade	8

All parameters in Table I. are in mm
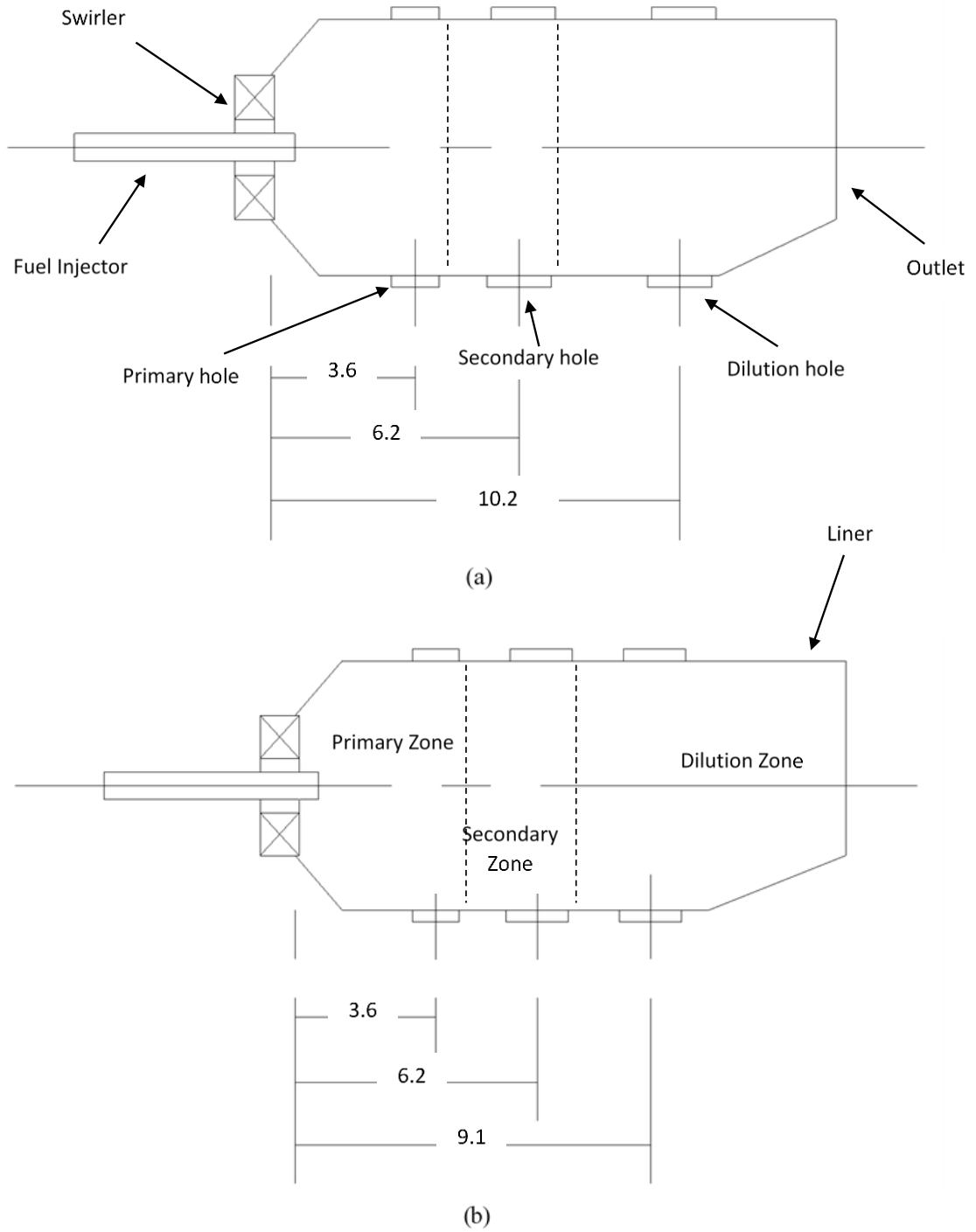
Figure 4-1. Schematic of Gas Turbine Combustion chamber (a) Case 1 (b) Case 2
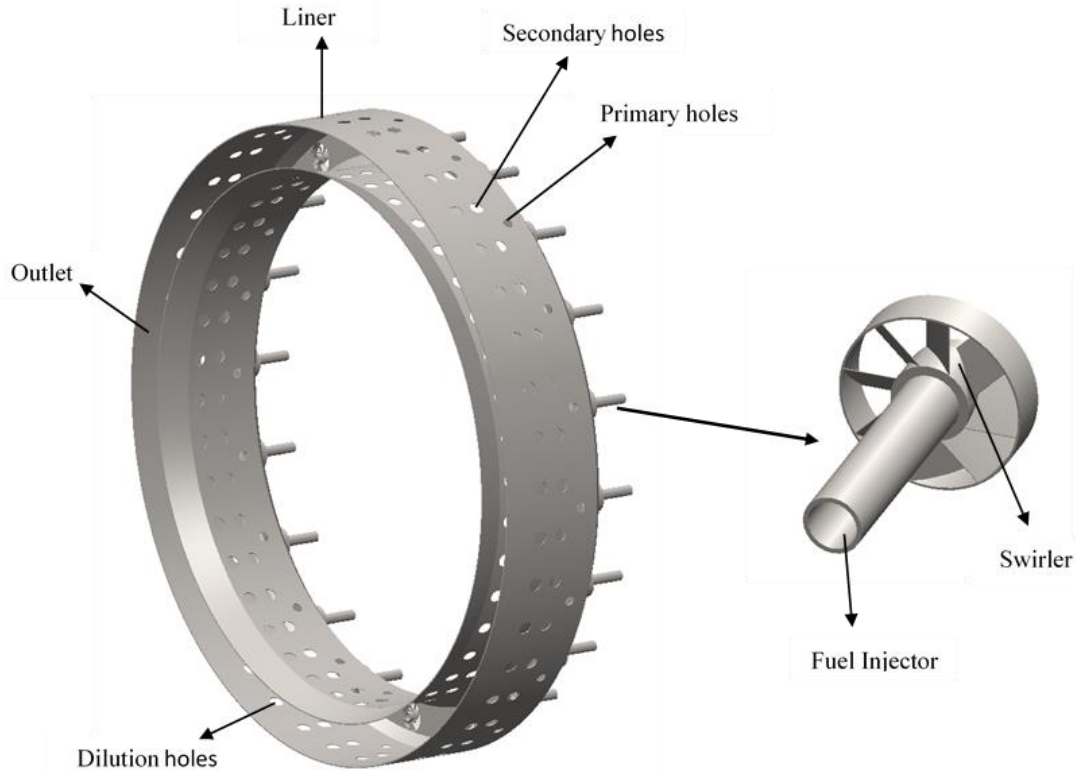
Figure 4-2. SolidWorks model of Annular combustion chamber

4.1.2. Mesh

Mesh of $1/20^{th}$ part of the combustor part has generated in a fluent Mesher with an element size of 0.1 mm. The mesh of the whole part and some magnified portion of the part is shown in Figure 4-3. Total nodes and elements in the part are 977864 and 5278275 respectively.

4.1.3. Ansys Simulations

After meshing, the setup was prepared for simulation. The model of a non-premixed combustion along with equilibrium probability density function, P1 radiation, and turbulence flow k-epsilon model were applied. And simulation has done for the given part of the combustion chamber. Using three different fuels, the simulations have performed for all the above combustion chambers in ANSYS fluent.
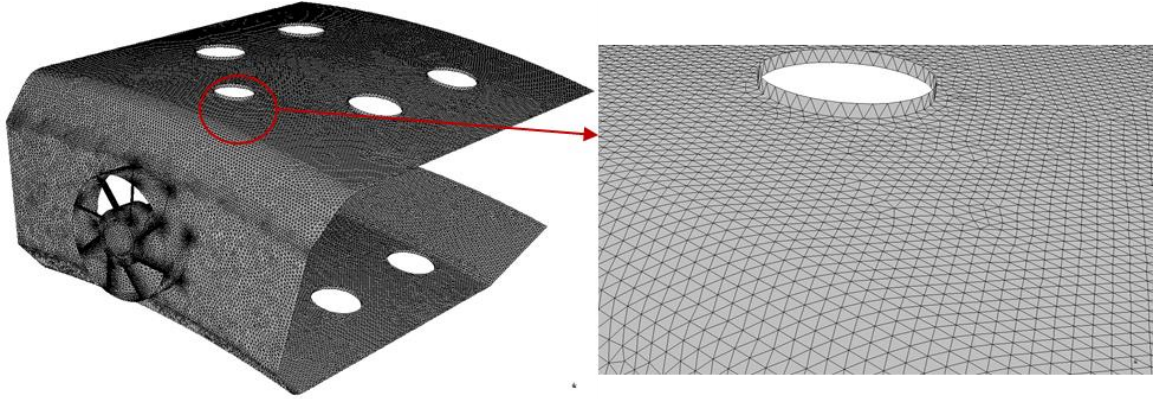
Figure 4-3. Meshed combustor liner with swirler

4.1.3.1. Non-Premixed combustion model

The non-premixed combustion was applied for achieving stable combustion. The non-premixed combustion model predicts the diffusion flame by employing a fast chemistry assumption. For methane, 100% CH_4 is introduced. Natural gas composition given in Table 2 was used, while for ethanol 100 % C_2H_5OH injected and the probability density function and PDF table for all three fuels are developed. The radiation P1 model, while convection heat loss is assumed to be zero has used.

4.1.3.2. k-epsilon model

Usually, researchers prefer k-ε for turbulent flow and has been validated by academic and industrial applications [2]. Comparing to the LES model, k-ε gives acceptable results within a short time [3]. This model is used to simulate flow characteristics for turbulent flow conditions. It is a model of two-equation described turbulence by two transport equations. The first variable k is for the turbulence kinetic energy, while the last variable ε is for the dissipation of turbulence energy. In this simulation work, the k-epsilon (k-ε) turbulence flow model with standard wall functions was applied.

The equation for turbulence kinetic energy is

$$\frac{\partial(\rho k)}{\partial t} + \frac{\partial(\rho k u_i)}{\partial x_i} = \frac{\partial}{\partial x_j}\left[\frac{\mu_t}{\sigma_k}\frac{\partial k}{\partial x_j}\right] + 2\mu_t E_{ij}E_{ij} - \rho\varepsilon \tag{4.1}$$

The equation for dissipation of turbulence energy is

$$\frac{\partial(\rho\varepsilon)}{\partial t} + \frac{\partial(\rho\varepsilon u_i)}{\partial x_i} = \frac{\partial}{\partial x_j}\left[\frac{\mu_t}{\sigma_\varepsilon}\frac{\partial\varepsilon}{\partial x_j}\right] + C_{1\varepsilon}\frac{\varepsilon}{k}2\mu_t E_{ij}E_{ij} - C_{2\varepsilon}\rho\frac{\varepsilon^2}{k} \qquad (4.2)$$

4.1.3.3. Boundary conditions

In fluent boundary conditions, fuel was injected through the injector into the combustion chamber. 19.374% of total air was introduced through the swirler parallel to the injector, while 10% of air was introduced through the primary holes into the primary zone and 35.313% into intermediate or secondary zone through secondary holes. The remaining air entered the liner through the dilution holes. The boundary conditions parameters are given in Table 4-2.

Table 4-2. Boundary conditions

Parameter	Value
Mass of air through swirler	0.0013 kg/s
Mass of air through primary hole	0.000665 kg/s
Mass of air through dilution holes	0.004745 kg/s
Mass of fuel	0.00011 kg/s
Pressure of air	500000 Pa
Pressure of fuel	600000 Pa
Ain inlet temperature	500 K
Fuel inlet temperature	500 K
Emissivity	1
Outlet pressure	382000 Pa

4.1.4. Combustion operations

The fuel properties are necessary for combustion operations. Some of which are given in Table 4-3. Stoichiometric air-fuel ratio for methane is 17.255, 16.66 for natural gas and 9.0026 for ethanol and their stoichiometric combustion reactions are presented in equations (4.3), (4.4) and (4.5) respectively. In this research work, the authors used a

constant air-fuel ratio of 60, gives moles of air 6.95 for methane, 7.38 for natural gas and 19.99 for ethanol presented in chemical equations (4.6), (4.7) and (4.8) respectively. As a result of the air-fuel ratio of 60, the excess air is 247.5% for methane, 260% for natural gas and 566% for ethanol chemical reactions.
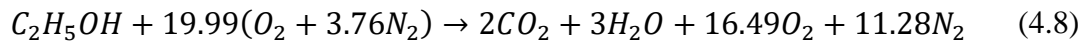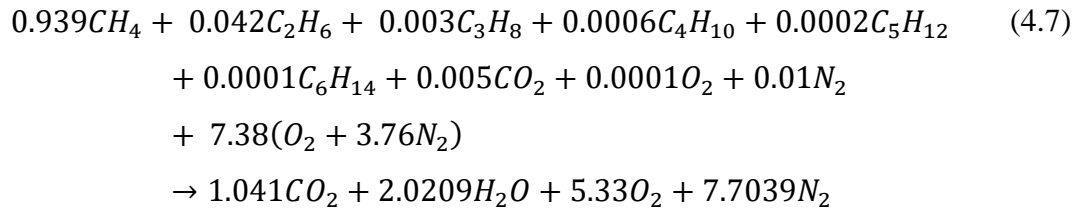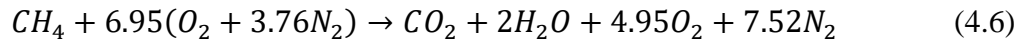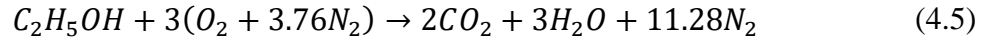
$$CH_4 + 2(O_2 + 3.76N_2) \rightarrow CO_2 + 2H_2O + 7.52N_2 \qquad (4.3)$$

$$0.939CH_4 + 0.042C_2H_6 + 0.003C_3H_8 + 0.0006C_4H_{10} + 0.0002C_5H_{12} \qquad (4.4)$$
$$+ 0.0001C_6H_{14} + 0.005CO_2 + 0.0001O_2 + 0.01N_2$$
$$+ 2.0489(O_2 + 3.76N_2)$$
$$\rightarrow 1.041CO_2 + 2.0209H_2O + 7.7039N_2$$

$$C_2H_5OH + 3(O_2 + 3.76N_2) \rightarrow 2CO_2 + 3H_2O + 11.28N_2 \qquad (4.5)$$

$$CH_4 + 6.95(O_2 + 3.76N_2) \rightarrow CO_2 + 2H_2O + 4.95O_2 + 7.52N_2 \qquad (4.6)$$

$$0.939CH_4 + 0.042C_2H_6 + 0.003C_3H_8 + 0.0006C_4H_{10} + 0.0002C_5H_{12} \qquad (4.7)$$
$$+ 0.0001C_6H_{14} + 0.005CO_2 + 0.0001O_2 + 0.01N_2$$
$$+ 7.38(O_2 + 3.76N_2)$$
$$\rightarrow 1.041CO_2 + 2.0209H_2O + 5.33O_2 + 7.7039N_2$$

$$C_2H_5OH + 19.99(O_2 + 3.76N_2) \rightarrow 2CO_2 + 3H_2O + 16.49O_2 + 11.28N_2 \qquad (4.8)$$
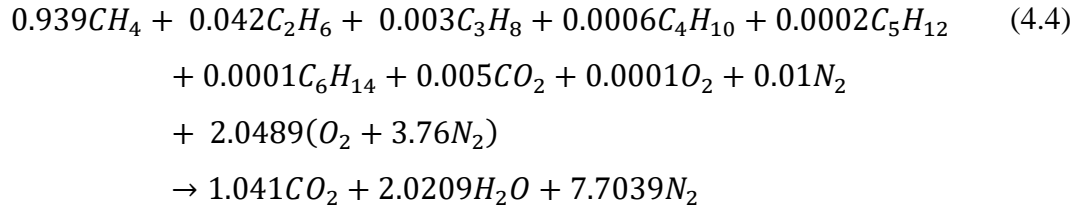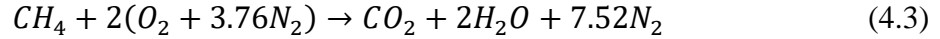
Table 4-3. Fuel composition and properties

Fuel composition and properties	Pure Methane	Natural Gas	Ethanol
CH_4	100	93.9	0
C_2H_6	0	4.2	0
C3H8	0	0.3	0
C4H10	0	0.06	0
C5H12	0	0.02	0
C6H14	0	0.01	0
C2H5OH	0	0	100
CO2	0	0.5	0
N2	0	1	0
O2	0	0.01	0
Mol weight (g/Mol)	16.04206	17.01995	46.06744
LHV (MJ/kg)	50	47.182	26.7
Octane Number	120	130	113
Autoignition (K)	810.15	853.15	638.15
Flash Point (K)	85.15	494.15	289.73

4.2 Summary

This chapter is about the methodology of the research. While using the previous related papers, all the techniques used in this study is presented by detail. This includes the SolidWorks model, Mesh generation and its cell size, combustion operation and Ansys simulations while using non-premixed combustion.

References

[1]   A. H. Lefebvre, And, and D. R. Ballal, *GAS Turbine Combustion Alternative Fuels and Emissions*, 3rd ed. Boca Raton: CRC Press, LLC, 2010.

[2]   P. Ghose, J. Patra, A. Datta, and A. Mukhopadhyay, "Effect of air flow distribution on soot formation and radiative heat transfer in a model liquid fuel spray combustor firing kerosene," *Int. J. Heat Mass Transf.*, vol. 74, pp. 143–155, Jul. 2014.

[3]   F. Fantozzi, P. Laranci, M. Bianchi, A. De Pascale, M. Pinelli, and M. Cadorin, "CFD Simulation of a Microturbine Annular Combustion Chamber Fuelled With Methane and Biomass Pyrolysis Syngas: Preliminary Results." pp. 811–822, 08-Jun-2009.

Chapter 5

Results and Discussion

5.1 Results and Discussions

After the generation of mesh, the part is simulated with non-premixed combustion, k-ε viscous and radiation of the P1 model. All the cases were computed with the given boundary conditions. Different cases are discussed and compared:

5.1.1. Case 1

The combustion of pure methane gives a total average temperature of 1129 K at the combustion chamber outlet. However, the mole fractions of carbon monoxides at the outlet are 1448 ppm and unburned fuels are 129 ppm. It is the consequence of incomplete combustion, due to which the temperature of the product at the outlet is low. Changing fuel to natural gas of composition given in Table 3 results in the total average temperature at the outlet of the combustion chamber 1120 K. The mole fractions of carbon monoxides and unburned hydrocarbons liberates at the outlet are 487 ppm and 30 ppm respectively and is the indication of good combustion. The ethanol gives 850 K of temperature, while mole fractions of carbon monoxides are 24 ppm and unburned fuels 19 ppm at the outlet of the combustion chamber. Moreover, NO_x at the outlet of the combustion chamber is determined negligible, which is also justifying from their temperatures.

5.1.2. Case 2

In the case of pure methane, the total average temperature of 1120 K is obtained at the outlet of the combustion chamber. However, the mole fractions of unburned fuel are 583 ppm and carbon monoxides are 725 ppm, while the emissions of NOx at the outlet are insignificant. When the fuel natural gas was injected to the combustion chamber, the total average temperature of the product at the outlet dropped to 1110 K. The mole fractions of unburned fuels and carbon monoxides emitted at the combustion chamber outlet are 182

ppm and 1174 ppm respectively, while emissions of NO_x are approximately zero. By using ethanol as a fuel, the temperature at the outlet of the combustion chamber decreased to 820 K. The mole fractions of unburned fuels are 42 ppm and carbon monoxides are 31 ppm at the exit of the combustion chamber. Likely case 1, the emission of NO_x is negligible at the outlet.

5.1.3. Case 3

The total average temperature of 1165 is resulted in the outlet of the combustion chamber for pure methane in Case 3, whereas the mole fractions of unburned fuels are negligible and carbon monoxides are 207 ppm. NO_x at the outlet is negligible and approximately equal to zero. When natural gas is injected and combust, the temperature at the outlet drops to 1146 K. The mole fractions of unburned fuels are negligible; however, carbon monoxides are 84 ppm. While NO_x emissions are approximately zero at the outlet of the combustion chamber. The temperature drops to 857 K by using ethanol as a fuel. At the exit, the mole fractions of unburned fuels are 2 ppm, but carbon monoxides are 10 ppm at the exit of the combustor. While mole fractions of NO_x are zero at the outlet as in Case 1 and 2.

5.1.4. Comparison

To investigate the combustion performance, results of all three cases for the respective fuels such as pure methane, natural gas, and pure ethanol are compared in terms of temperatures value and its homogeneity, unburned fuel, CO and NO emissions in the combustion chamber and at the exit. The effects of the hole positions and swirler vane angles on the temperature distribution in the combustion chamber are shown in Figure 5-1 and Figure 5-2. As in Case 2 secondary and dilution holes are close to each other and mass flow rate of air through these holes combined before taking part in combustion while not giving space to the fuels and leave the combustion chamber without combustion. It results lower temperatures and homogeneity at the outlet of the combustion chamber. In Case 1, most fuel burned, and almost complete combustion was achieved, while in Case 3 swirler vanes angle increases due to which mixing of air-fuel increases and causes

further enhancement of combustion compared to Case 1. It validates results [1], that maximum combustion efficiency has resulted in the swirler vane angle 45°. Figure 5-2 presenting the contours of outlet combustion chamber temperature and the purpose is to see the homogeneity of different cases. It presents the temperature is more homogenous in Case 1 compared to Case 2. It is also found that case 3 contours homogeneity is better than Case 1. Furthermore, the values of total average temperatures at the outlet of the combustion chamber are graphically presented in Figure 5-3 for all cases. It is determined that Case 3 gives higher temperatures than the remaining two cases for the respective fuels because of trends toward complete combustion.
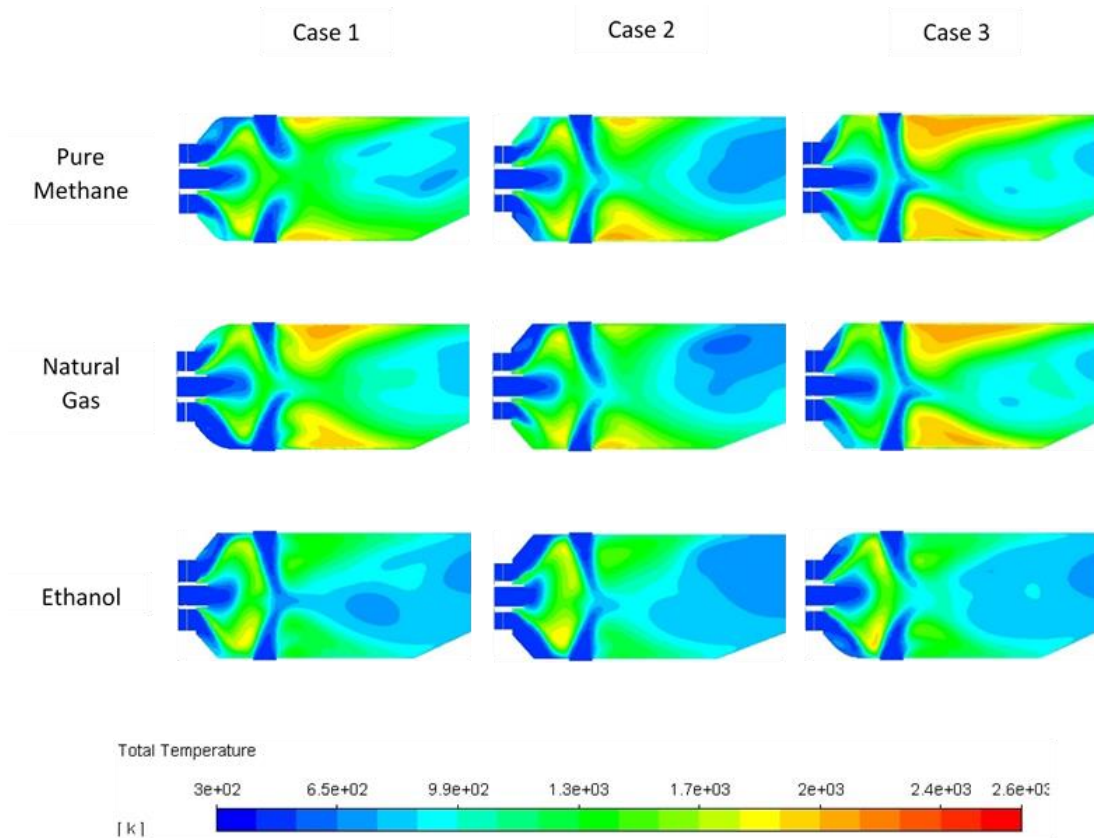
Figure 5-1. Temperature distribution in the combustion chamber
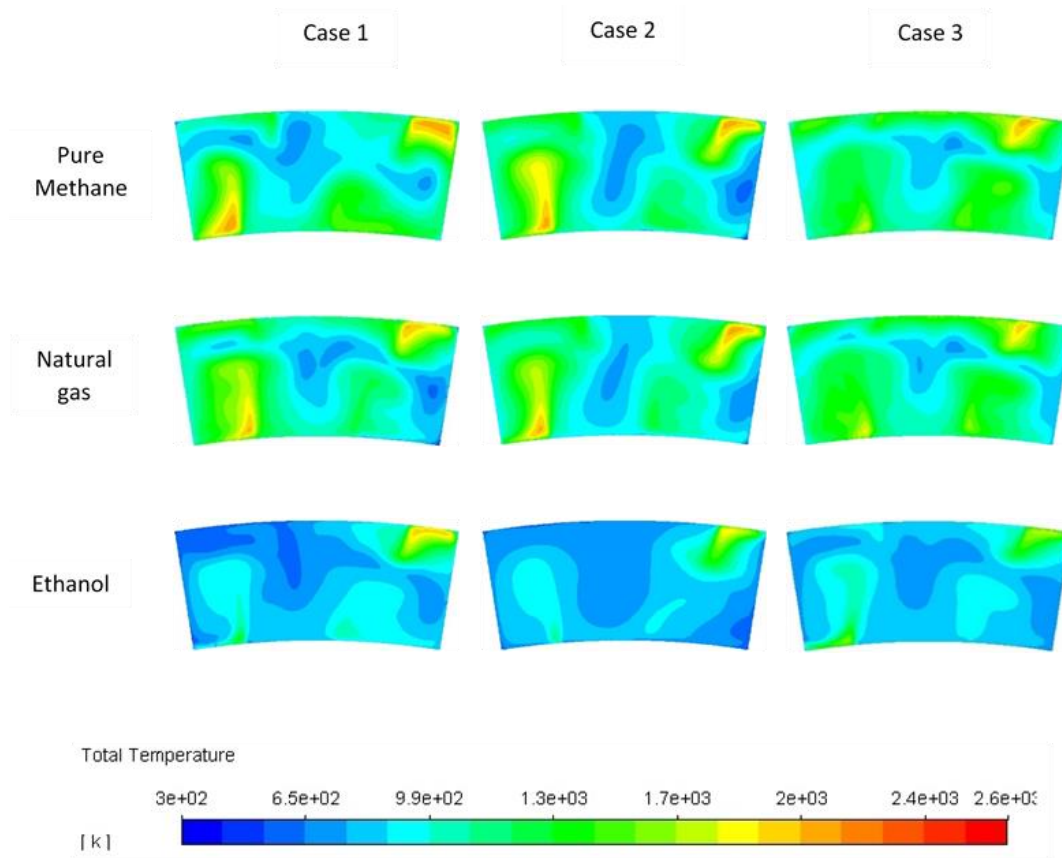
Figure 5-2. Distribution of the outlet total average temperature
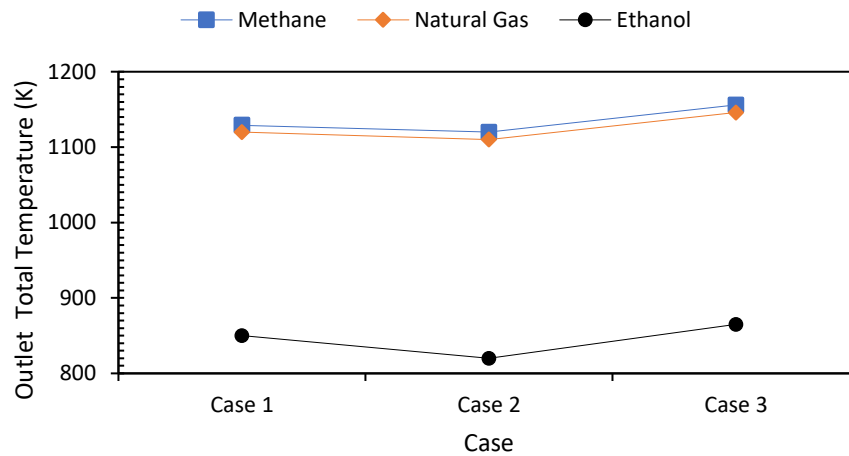
Figure 5-3. Comparison of total average temperature at outlet

Figure 5-4 illustrates the distribution of fuels and the development of combustion in the combustion chamber and shows that combustion uniformly reaches the lean zone except for Case 2. While Figure 5-5 comparing contours of mole fractions of the fuels that remain unburned and released at the outlet of the combustion chamber. From this figure contours, it has observed that there is little amount of unburned fuel in case 1, while in Case 2 contours a substantial amount of the unburned fuels exists. In Case 3 the unburned fuels at the outlet are negligible. The mole fractions of the unburned fuels at the outlet of the combustion chamber are graphically presented in Figure 5-6 and determined, that in Case 3 the emissions of unburned fuels are lowest from the other two cases for respective fuels. From CO presented in the above cases, it is determined that their emissions are lower in Case 3 compared to all other cases.
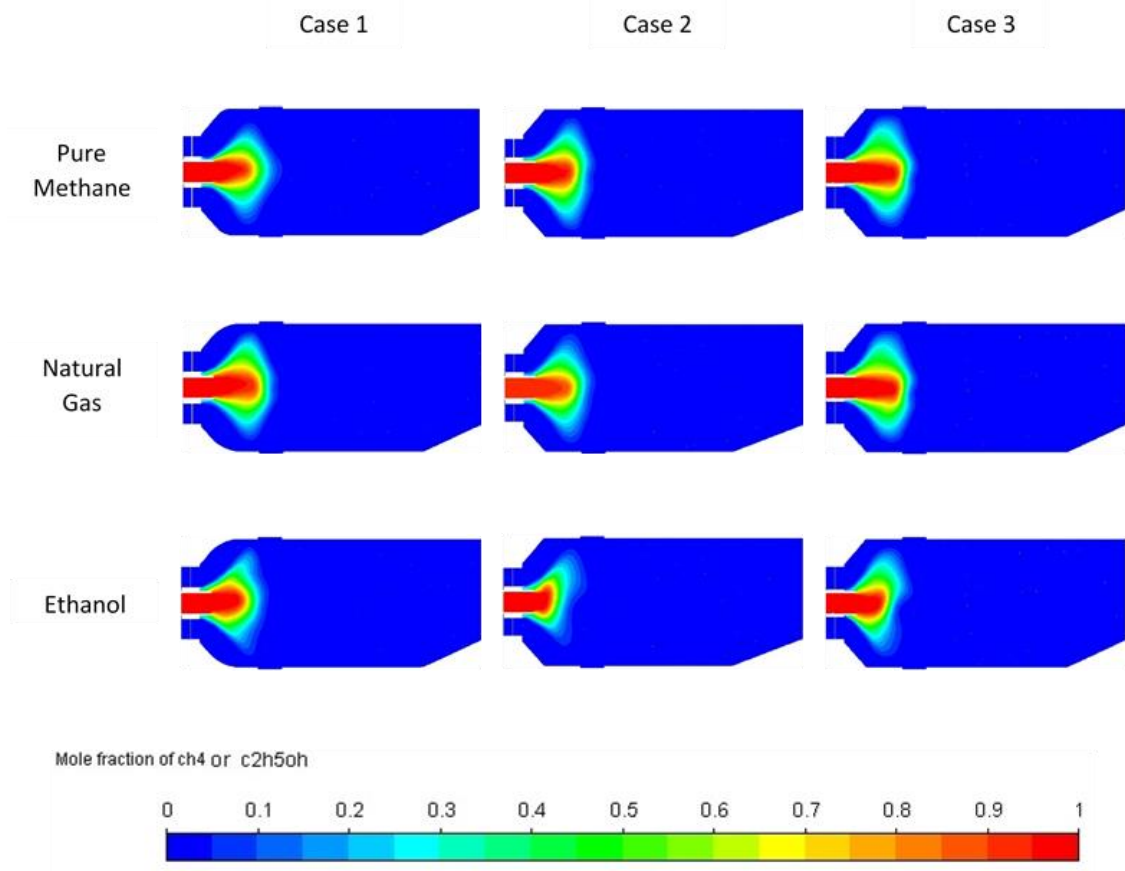
Figure 5-4. Distribution of mole fraction of fuel

Figure 5-7 illustrates the production of NO and it has been observed that all cases and fuels have very little or negligible mole fractions of NO emissions and comparatively case 3 emits no NO and perform well is compared to other cases because of high swirl number [2]. For ethanol it is lower because of low resulted temperature [3]. As in Case 3, unburned fuels and CO emissions are nearly negligible and the temperature is the highest, which explains that the design of Case 3 combustor is most satisfactory.

Moreover, it has been observed, that in all cases the ethanol combustion is good and the pollutant emissions to the environment are lower, but their energy density is lower compared to the other two fuels, resulting in lower temperature at the combustion chamber outlet and require less air-fuel ratio to achieve compatible temperature of other fuels, but it will ultimately result incomplete combustion.
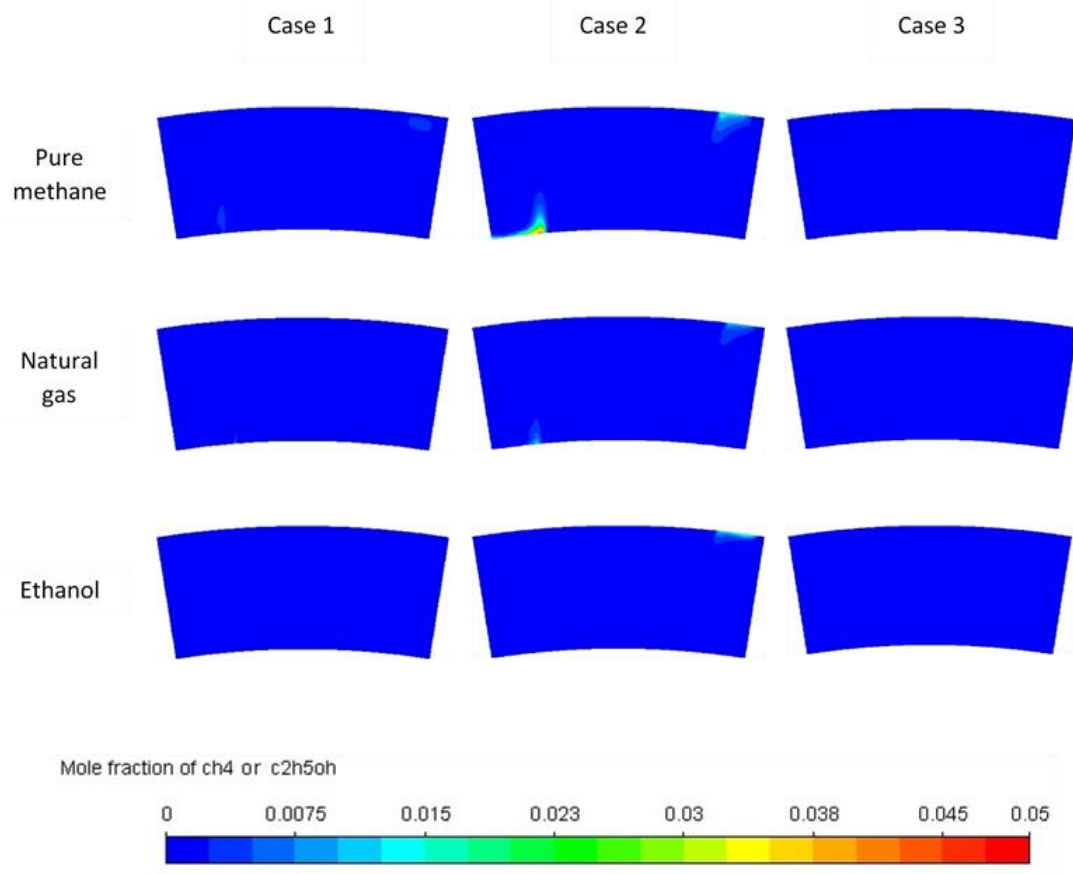
Figure 5-5. Unburned fuel at the outlet of the combustion chamber
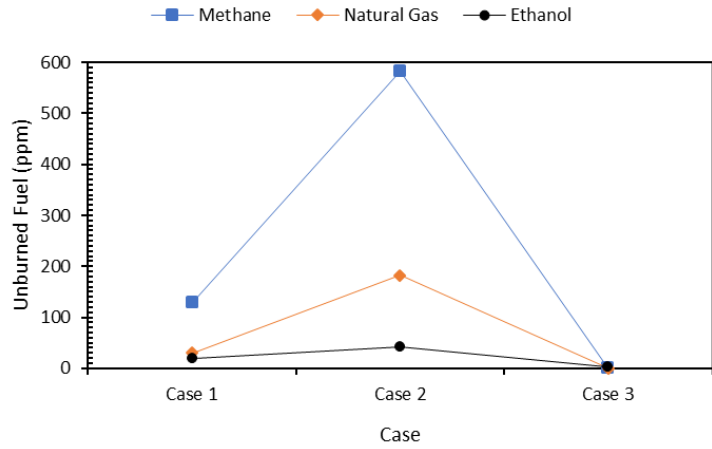
Figure 5-6. Comparison of unburned fuel at the outlet
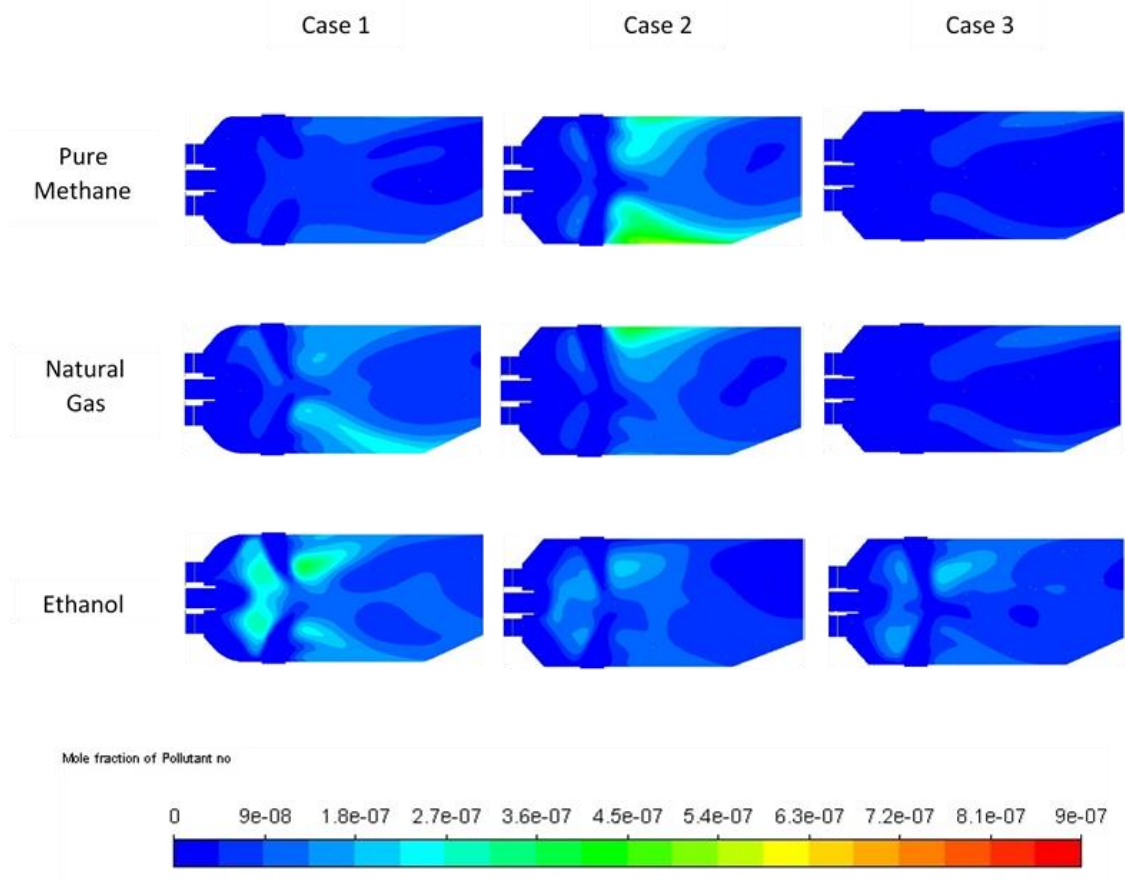
Figure 5-7. Nitric oxides production in the combustion chamber

5.1.5. Combustion performance

The combustion efficiency is determined by using equation (7) [4], [5].

$$\eta_c = \frac{CO_2 + 0.645CO}{CO_2 + CO + UHC} \tag{7}$$

From the graph given in Figure 5-8 the efficiency of the combustion chamber for Case 3 is higher than the remaining cases, ethanol gives maximum efficiency of 99.97% and follows trends of complete combustion. In all cases, ethanol combustion is almost complete. Pure methane and natural gas, combustion efficiency is fluctuating due to incomplete combustion, while in Case 3 combustion efficiency of 99.77% and 99.83% respectively is achieved. It is verified that combustion is good in Case 3 for all fuels (pure methane, natural gas, and ethanol). As the excess air ratio is high due to which combustion efficiency is high and validate the results [6].
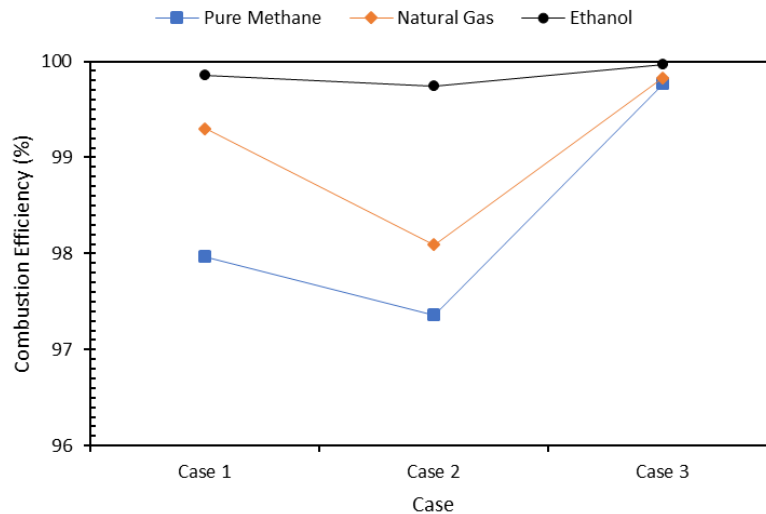
Figure 5-8. Comparison of combustion efficiency

5.1.6. Theoretical Comparison

Theoretically, we can determine temperature by using an energy balancing equation or the law of conservation of energy applied to combustion reaction in which the total energy

of reactants is equal to the total energy of products and the combustion is considered as complete combustion. The combustion reaction is given in equation

$$aCH_4 + b(O_2 + 3.76N_2) \rightarrow cCO_2 + dH_2O + eO_2 + fN_2 \qquad (5.2)$$
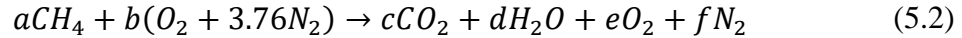
And the energy balance equation is

$$\sum(H_f^o + \bar{H}_T - \bar{H}_{298})_R = \sum\left(H_f^o + \bar{H}_T - \bar{H}_{298}\right)_P \qquad (5.3)$$

5.1.6.1. Comparison of theoretical and simulation temperature of methane

As theoretically we determined temperature by using an energy balancing equation or the law of conservation of energy applied to combustion reaction in which total energy of reactants is equal to the total energy of products. The mole fraction of different components in reaction is determined while using methane is fuel. By using the energy equation, we calculate the theoretical temperature for the given combustion. The theoretical value of temperature is 1203 K, and in Figure 5-9 shows that theoretical temperature and simulation temperature for all 3 cases which is different for all cases. But theoretical temperature is higher compared to simulation because of ideal and complete combustion but for simulation, some fuels remain unburned and carbon monoxides also produced.
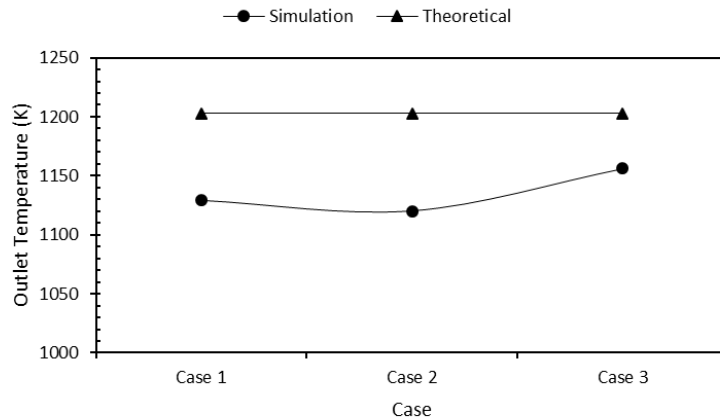

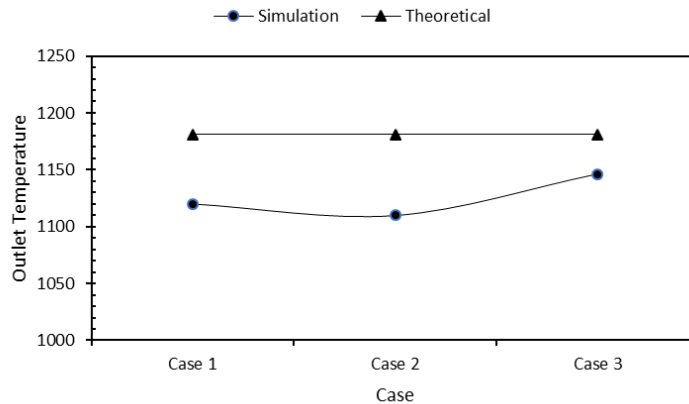Figure 5-9. Comparison of Simulation and Theoretical Outlet Temperature

5.1.6.2. Comparison of theoretical and simulation temperature of natural gas

As theoretically we determined temperature by using the energy balancing equation or the law of conservation of energy applied to the combustion reaction. The mole fraction of different components in reaction is determined while using natural gas is fuel. By using the energy equation, we calculate the theoretical temperature for the given combustion. The theoretical value of temperature is 1181 K, and in Figure 5-10 shows that theoretical temperature is higher than simulation temperature for all 3 cases but simulation temperature varying for all cases. Theoretical temperature is higher compared to simulation and the reason is assumed ideal and complete combustion but for simulation, some fuels remain unburned and carbon monoxides also produced.
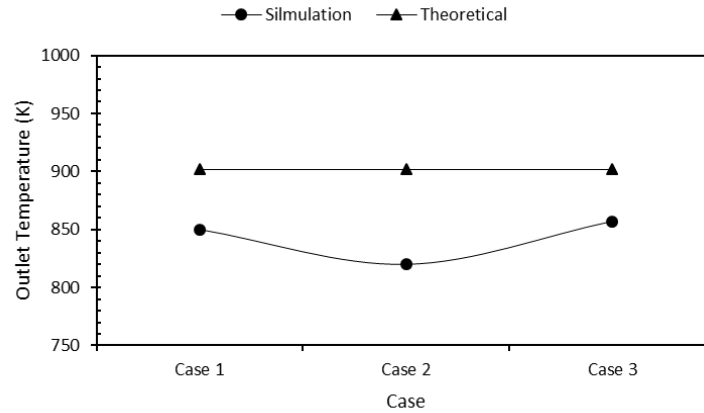

Figure 5-10. Comparison of Simulation and Theoretical Outlet Temperature

5.1.6.3. Comparison of theoretical and simulation temperature of ethanol

As theoretically we determined temperature by using energy balancing equations and chemical reactions. The mole fraction of different components in reaction is determined while using pure ethanol is fuel. By using the energy equation, we calculate the theoretical temperature for the given combustion. The theoretical value of temperature is 901.7 K, and in Figure 5-11 shows that theoretical temperature is higher than simulation temperature for all 3 cases but simulation temperature varying for all cases. Theoretical temperature is higher compared to simulation and the reason is assumed ideal and complete combustion but for simulation, some fuels remain unburned and carbon monoxides also produced.

Figure 5-11. Comparison of Simulation and Theoretical Outlet Temperature

5.2 Summary

In this chapter, the results of the simulation of the combustion in the annular combustion chamber is presented both graphically and theoretically. The considered parameters include temperature, NO, CO, and unburned fuel. The results are explained with references and disclose critically. The results of the simulation are compared for different fuels and different designs of the combustion chamber. In the end, these results are compared with theoretical data for the purpose of validation.

References

[1]   S. H. Pourhoseini, S. Fakhri, E. Taheri, R. Asadi, and M. Moghiman, "An Investigation on the Effect of Air Swirler Vane Angle on Liquid Fuel Combustion Characteristics," *Heat Transf. Res.*, vol. 46, no. 7, pp. 750–760, Nov. 2017.

[2]   R. Jarpala, N. V. S. Aditya Burle, M. Voleti, and R. Sadanandan, "Effect of Swirl on the Flame Dynamics and Pollutant Emissions in an Ultra-Lean Non-Premixed Model Gas Turbine Burner," *Combust. Sci. Technol.*, vol. 189, no. 10, pp. 1832–1848, Oct. 2017.

[3]   J. A. Alfaro-Ayala, A. Gallegos-Muñoz, A. R. Uribe-Ramírez, and J. M. Belman-Flores, "Use of bioethanol in a gas turbine combustor," *Appl. Therm. Eng.*, vol. 61, no. 2, pp. 481–490, 2013.

[4]   R. C. Zhang, W. J. Fan, Q. Shi, and W. L. Tan, "Combustion and emissions characteristics of dual-channel double-vortex combustion for gas turbine engines," *Appl. Energy*, vol. 130, pp. 314–325, 2014.

[5]   R. C. Zhang, F. Hao, and W. J. Fan, "Combustion and stability characteristics of ultra-compact combustor using cavity for gas turbines," *Appl. Energy*, vol. 225, no. May, pp. 940–954, 2018.

[6]   N. Kahraman, S. Tangöz, and S. O. Akansu, "Numerical analysis of a gas turbine combustor fueled by hydrogen in comparison with jet-A fuel," *Fuel*, vol. 217, no. August 2017, pp. 66–77, 2018.

Chapter 6

Conclusions and Recommendations

Fuels are reviewed to present their combustion characteristics, availability, price, environmental impacts, energy density, its compatibility to the existing infrastructure and easy excess to everyone. Based on combustion characteristics, price, availability it is estimated that Petroleum fuels have a good energy density, while on the other side they have a bad impact on environmental and facing depletion problems and price fluctuation. Biofuels complete their consumption and production cycle because they produced from biomatter and after burning emit products to the environment and then absorbed by plants, this shows environment-friendly behavior, but they have some issues like energy density is lower as compared to fossil fuel, Production and synthesis of biofuels are still problems and they have competition with edible biomatter. Based on their use and region of their use appropriate fuel can select. Natural fuel such as petroleum fuels is appropriate in those regions in which they are easily and cheaply available for a long time and their environmental impacts are not so much critical. It is concluded that for combustion the fuel should be environment-friendly and economic or maintain the balance between these two factors.

In order to understand the potential application of micro gas turbine annular combustor using multifuel comprising pure methane, ethanol, and natural gas, 3-D CFD simulations were performed using ANSYS fluent. The constant mass flow rate of air and fuel was injected with an air-fuel ratio of 60. The variable parameters were dilution hole positions and swirler blade angles. The results are compared for all the cases in terms of total average temperature, unburned fuel, CO and NO emissions at the combustion chamber outlet. The main findings of this work could be summarized as follows:

- Methane fuel combustion results in the highest temperature, while the lowest temperature was achieved for ethanol because of less energy density. Moreover,

Case 3 in which the swirler vane angle is 45º gives the highest temperature for their respective fuel.

- In the first two cases, the combustion of pure methane and natural gas emits substantial CO and unburned fuel emissions, whereas Case 3 liberates the lowest mole fraction of unburned fuel and CO. When the ethanol was injected, pollutant emissions further decreased. However, NO emissions were negligible in all cases for the methane, natural gas, and ethanol.

- In Case 2 combustion efficiency was approximately 98% for both methane and natural gas. Case 1 displayed higher efficiency than 98% and for Case 3 it was slightly 100%. A combustion efficiency of 99.97% was recorded for ethanol in all three cases.

- The outlet temperature distribution was homogeneous in Case 3 compared to the other two cases because of the swirler vane angle of 45º.

The above findings indicate that swirler vane angle 45º widely improved combustion performance. Moreover, this design outcomes are useful and can provide a baseline for micro gas turbine application. However, in order to provide further evidence, this design requires quantitative experimental analysis, since simulations usually overpredict the performance.

Appendix

MATLAB Code

1. % Given Reference Quantities
2. R = 287; % J/kg/K
3. T_3 = 800; % K
4. P_3 = 30*10^5; % Pa
5. %m_dot_3 = 132; % kg
6. %OPL = 0.06;
7. % PLF = 20;
8. u_1 = 170; % m/s
9. U_ref = 20; % m/s
10. r = 1.4;
11. W_1ia = 0.4;   % W_1ia mean assume value
12. cp_gas_1800 = 1590.988; %J/kg/K
13. cp_gas_1000 = 1459.673;
14. cp_air_800 = 1402.511; %J/kg/K
15. cp_air_300 = 1245.285;
16. % Assumption
17. Q_dot = 250000; %Watt
18. T_4 = 1800; %K
19. T_2 = 300; %K
20. T_5 = 1000; %K
21. m_dot_3 = Q_dot/ ((cp_gas_1800*T_4 - cp_gas_1000*T_5)-(cp_air_800*T_3 - cp_air_300*T_2));
22. % Reference Quantities
23. rho_3 = P_3/(T_3*R);
24. A_ref = m_dot_3/(rho_3*U_ref);
25. q_ref = rho_3*U_ref^2/2;
26. M_ref = U_ref/((r*R*T_3)^0.5);

27. % % for diffuser

28. eff = 0.8;

29. %AR = (1/(1-eff))^0.5;   % eff is effectiveness in the range of 0.5 to 0.9

30. % % LC is loss coefficient LC is 0.15 for aerodynamically clean

31. % % 0.45 for dump diffusers of high liner/depth ratio (D_L/h_1)

32. % % for vertex-controlled diffusers 0.05 to 0.15

33. A_1 = m_dot_3/(rho_3*u_1);

34. W_1oa = (A_1/3.14 + (W_1ia^2))^0.5; % m

35. W_1 = W_1oa - W_1ia;

36. %W_2 = (A_2*4/3.14)^0.5;

37. u_2 = u_1*0.50;

38. Q = 9;

39. %L = 0.122;

40. A_2 = m_dot_3/(rho_3*u_2);

41. AR = A_2/A_1;

42. L = (AR - 1)*W_1/(2*sind(Q));

43. L_d = L*cosd(Q);

44. h = L*sind(Q);   % Q is the divergence angle in the range of 6 to 12 degree

45. q_1 = rho_3*u_1^2/2;

46. q_2 = rho_3*u_2^2/2;

47. LC = 0.15;

48. P_1 = P_3;

49. p_1 = P_1 - q_1;

50. p_2 = eff*q_1 + p_1;

51. %P_2 = (P_1- LC*q_1);

52. P_2 = p_2 + q_2;

53. deltaP_diff = P_1 - P_2;

54. %A_2 = pi*(W_2o^2-W_2i^2)/4;

55. % % After Diffuser

56. % %Pressure-Loss Parameter

57. % % Cold losses

58. OPL = 0.06;

59. deltaP_34 = OPL*P_3;

60. %OPL = deltaP_34/P_3;   % Overall pressure loss 4% to 8%

61. P_4 = P_3 - deltaP_34;

62. % Pressure loss factor PLF

63. PLF = OPL*2/(R*((m_dot_3*T_3^0.5)/(A_ref*P_3))^2) ;

64. % %Assumption Pressure loss factor is equal to pressure drop across the liner

65. % %and no loss in diffuser

66. deltaP_L = deltaP_34- deltaP_diff ;

67. U_j = (deltaP_L*2/rho_3)^0.5;

68. A_heff = A_ref/(deltaP_L/q_ref)^0.5;

69. n = 150;

70. d_h = (A_heff*4/(pi*n))^0.5;

71. % % Hot losses

72. % rho_4 = P_4/(R*T_4);

73. % deltaP_hot = ((rho_3/rho_4)-1)*q_ref;

74. % % Cranfield Design Method

75. % d_j = d_h*C_d^0.5;

76. % % m_j = n*d_j^2*rho_3*U_j*3.14;

77. % % For fully developed flow a is 1.05

78. a = 1.05;

79. % K = U_j^2/U_an^2;

80. %D_sw = 0.05;

81. n_v = 12;

82. t_v = 0.0011;

83. x = 50;

84. K_sw = 1.3;

85. deltaP_sw = 0.03*P_3;

86. m_lh = 0.2*m_dot_3;

87. m_dot_sw = m_lh/30;

88. A_L = A_ref*(1 - (((1 - (m_lh/m_dot_3)^2) - LC)/(deltaP_34/q_ref - LC*(A_ref/A_1)^2))^0.3333));

89. A_an = A_ref-A_L;

90. A_sw = (((secd(x))^2)/(2*rho_3*deltaP_sw/(K_sw*(m_dot_sw)^2) + 1/(A_L^2)))^0.5;

91. %A_sw = (3.14/4)*(D_sw^2 - D_hub^2) - (0.5*n_v*t_v*(D_sw - D_hub));

92. %m_dot_sw = (2*rho_3*deltaP_sw/(K_sw*(((secd(x)/A_sw)^2)-(1/(A_L^2)))))^0.5;

93. D_sw = (0.5*n_v*t_v + ((0.5*n_v*t_v)^2 + (0.75*pi*A_sw))^0.5)/(2*0.75*pi/4); %Quadratic Equation

94. D_hub = D_sw*0.5;

95. R_ci = 0.28;

96. R_co = (A_ref/pi + (R_ci^2))^0.5;

97. D_c = R_co - R_ci;

98. D_ref = 2*D_c;

99. R_c = R_ci + (D_c/2);

100.   W_1i = R_c - W_1/2;

101.   W_1o = R_c + W_1/2;

102.   W_2o = W_1o + h;

103.   W_2i = W_1i - h;

104.   W_2 = W_2o - W_2i;

105.   z = A_sw*30;

106.   % % n_v = 8 - 16 number of vanes

107.   % % t_v = 0.7 - 1.5mm Vane thickness

108.   % % x = 30 - 60 Vane angle

109.   % % deltaP_sw = 3% - 4% of P_3

110.   % % K_sw = 1.3 for flat vanes and 1.15 for curved vanes

111.   m_dot_an = m_dot_3-m_lh;

112.   U_an = m_dot_an/(rho_3*A_an);

113.   %R_Lo = (R_co^2 - (A_an/pi))^0.5;

114.   %R_Li = (R_Lo^2 - (A_L/pi))^0.5;

115.   A = A_L/A_ref;

116.   m_offset = 0.1*m_dot_3;

117.   m_dot_foran = m_dot_an - m_offset;

118.   m_dot_ao = m_dot_foran/2;

119.   m_dot_ai = m_dot_foran/2 + m_offset;

120.   A_an_o = m_dot_ao/(rho_3*U_an);

121.   A_an_i = m_dot_ai/(rho_3*U_an);

122.   R_Lo = (R_co^2 - (A_an_o/pi))^0.5;

123.   R_Li = (R_ci^2 + (A_an_i/pi))^0.5;

124.   %R_Li = (R_Lo^2 - (A_L/pi))^0.5;

125.   y_o = R_co - R_Lo;

126.   y_i = R_Li - R_ci;

127.   D_L = R_Lo - R_Li;

128.   L_D = 1.45*D_L;

129.   Y_max = 0.4*D_L;

130.   m_dot_j = m_dot_foran;

131.   d_j = (4*m_dot_j/(pi*n*rho_3*U_j))^0.5;

132.   C_d = (d_j/d_h)^2;

133.   % C_d = 1.25*(K-1)/(4*K^2-K*(2-a)^2)^0.5;

134.   L_L = 2*D_L; % from shakariyants thesis

135.   L_g = 1.02*W_2; % d_g is the gap length between dome and diffuser

136.   % swirler

137.   r_s = (D_sw-D_hub)/2;

138.   b_s = r_s/(tand(x));

139.   h_L = D_L/2;

140.   h_Li = h_L - r_s;

141.   b_Li = h_Li/(tand(x));

142.   L_pz = h_L/(tand(x)) + d_h;

143.   %L_c = 2*D_c;

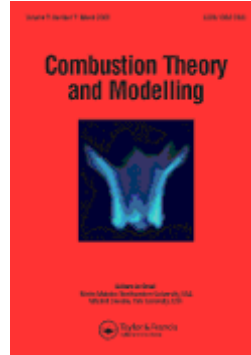144.   S_N = 2/3*((1 - (D_hub/D_sw)^3)/(1 - (D_hub/D_sw)^2))*tand(x);

145. x1 = 45;

146. B = (R_co - W_2o)/tand(x1);

147. L_c = L_L + L + B;

148. L_s = B - L_g; % L_s is the length of dome space

Computational Analysis of a Multi-Fuel Annular Combustion Chamber for Micro Gas Turbine Application with Focus on Swirler and Dilution Hole Design

SCHOLARONE™
Manuscripts

Combustion of multi-fuel in combustion chamber

Computational Analysis of a Multi-Fuel Annular Combustion Chamber for Micro Gas Turbine Application with Focus on Swirler and Dilution Hole Design

Anis Ahmad Sher[a], Adeel Javed[a*], Patrick Phelan[b]

[a]*Thermal Energy Engineering, U.S-Pakistan Center for Advanced Studies in Energy (USPCAS-E), National University of Sciences & Technology (NUST), Islamabad, Pakistan*

[b]*Mechanical and Aerospace Engineering, Ira A. Fulton Schools of Engineering, Arizona State University (ASU), Arizona, USA*

Corresponding Author's email: [*]adeeljaved@uspcase.nust.edu.pk

1

Computational Analysis of a Multi-Fuel Annular Combustion Chamber for Micro Gas Turbine Application with Focus on Swirler and Dilution Hole Design

Abstract: In this research, an annular combustion chamber with swirlers is introduced in a micro gas turbine engine for power production. The impact of the dilution holes position and swirler vane angles on the performance of the combustion chamber is investigated. In addition, the combustion chamber is optimized for a multi-fuel comprised of pure methane, natural gas, and ethanol. The combustor is designed in SolidWorks, and simulations are performed in Ansys Fluent for two positions of dilution holes in the liner and swirler blade angles. The model used is non-premixed with a compressible k-ε turbulent flow model and an equilibrium probability density function for the chemical reaction. In order to measure the performance of the combustion chamber, pollutant emissions, combustion efficiency, and outlet temperature are examined. Pollutant emissions as carbon monoxides (CO) and unburned fuels exist in a small amount, however nitric oxides (NO) are negligible. The combustion efficiency found is above 98% for methane and natural gas, and almost 100% for ethanol. Furthermore, simulation results reveal that the swirler vane angle of 45o widely improves combustor performance.

Keywords: Annular Combustion Chamber; Micro Gas Turbine; emissions, fuel flexibility, Swirler

Introduction:

A Micro Gas Turbine (MGT) is a typical gas turbine (GT) with power in the range of 1 kW – 300 kW [1] or even up to 500 kW [2]. Their specifications are the same as a typical Large Gas Turbine (LGT), but due to scaling down both turbine and combustion efficiency decrease [3]. In the last 10 years, MGT have gained a lot of interest for both industrial applications and electricity generation. They are advantageous in terms of line losses and can easily be installed with a low initial cost. In general, MGT have a low weight per unit power and have the capability of adapting to a variety of fuels which is

2

Combustion of multi-fuel in combustion chamber

the main reason for the high level of research interest [2]. MGT are usually used for combined heat and power. Their electrical efficiency is approximately 15% – 25%. Their thermal efficiency may reach 70% for combined heat and power by MGT while the overall efficiency is in the range of 75% - 85% [3]. MGT are generally light weight, of simple geometry and their maintenance can be performed easily. Their pollutant emissions are low, and overall efficiency is high, but thermal efficiency is lower than for large gas turbine engines. The combustor in a micro gas turbine is usually of a simple geometry with lower combustion efficiency relative to those in larger engines. They can be replaced by an annular combustor, but this is complex and consists of multiple injectors and swirlers, located in a single liner and casing. However, since annular combustors are small and compact, engineers are introducing them in MGT, but their high cost is still a limitation [4].

Annular combustors are either reverse flow or straight-through flow type. Various components include the liner, casing, and fuel injectors, while some combustors also contain a swirler for swirling air. The liner has different zones: the primary zone where air and fuel are initially mixed and combust and the secondary zone in which more air is introduced through holes for completing combustion. The last zone is an intermediate or dilution zone in which the temperature of the hot combustion gases are reduced by mixing extra air, making it compatible with the turbine blade material. These zones are usually present in every type of combustor, while some combustors may have no secondary zone which affects combustion. Combustion may be diffusion combustion or dry low NO_x or dry low emission combustion [5]. In diffusion combustion, the combustor usually has a single injector, while in dry low NO_x the combustor has multiple fuel injectors. Moreover, in a diffusion-type combustor, steam or water is injected for limiting and controlling NOx production.

3

Combustion of multi-fuel in combustion chamber

In the last few years, a great deal of experimental and computational research on gas turbine combustors has been performed including flame stability over a range of air-fuel ratios with low weight-to-unit power [6]. Computational Fluid Dynamics (CFD) is applied by a number of researchers for the design, emissions and performance analysis of the combustor [7–10]. In [11] a turbulent non-premixed hydrogen and hydrogen carbon flame were investigated numerically using Fluent. The k-ε model is usually used for swirling and turbulence modeling [12,13]. In [14], the researchers determined that a high swirl number reduces NOx pollutant emissions despite the operating conditions, and maximum efficiency is possible at a swirler vane angle of 45º [15].

The use of GT has been dominant both in power production and propulsion for many decades while using natural hydrocarbon fuel. However, the issue is natural hydrocarbon fuel depletion and pollutant emissions and requires switching to alternative fuels having less pollutant emissions. In [7,16–20] the authors analysed combustion operations for MGT combustors in which they focused on renewable fuels and optimized pollutant emissions. [21] compared the stability domain and pollutant emissions of combustion, using either kerosene without hydrogen and a kerosene-hydrogen blend as a fuel and achieved improvements in combustion performance by hydrogen blending. [22–28] focused especially on biofuel, and showed improvements in thermal efficiency, and in reduction of pollutant emissions with the desired power production. Among biofuels, bioethanol blended with gasoline was studied [29] where the sole purpose was to find the effect of fuel change on the environment. Renewable fuels such as ethanol produced from biomass may have net-zero carbon emissions and can easily be produced with both economic and environmental benefits [30][31]. Research on issues with the life cycle assessment of bioethanol is discussed in [32–35], and they show lower greenhouse gas

4

Combustion of multi-fuel in combustion chamber

emissions relative to conventional hydrocarbons. Technological development can help in lowering both the environmental impact and the costs of ethanol fuels.

The MGT are or can be installed in undeveloped areas that are out of reach of the electricity grid. But the combustion chambers usually applied in the MGT are less efficient and the fuel they are conventional fuel, which is expensive and causes environmental pollution. The main purpose of this research is to provide an efficient combustion chamber for the MGT that can be able to operate on multi-fuel especially renewable fuel.

In this work, an annular straight flow combustion chamber is introduced in an MGT for power production and three-dimensional CFD simulations are performed for multi fuels such as pure methane, natural gas, and ethanol. Moreover, the impact of the dilution holes position and swirler blade angles on the performance of the combustion chamber is determined. The pollutant emissions and outlet combustion temperatures are presented and discussed.

Methodology:

A combustion chamber was modeled based on the code generated from the data available in [36]. A schematic of the combustion chamber for Case 1 and 2 is shown in Figure 1. The dilution holes are at a position of 10.2 mm and 9.1 mm from the entry of the liner in Case 1 and 2 respectively, while the swirler vane angle is 42° for both cases. In Case 3 the angle of the swirler blade is changed to 45°, while the position of the dilution holes is the same as for case 1.

SolidWorks Model:

The combustion chamber along with the swirler shown in Figure 2 was modeled in SolidWorks. The combustor has twenty swirlers comprised of eight vanes with twenty

5

Combustion of multi-fuel in combustion chamber

fuel injectors passing through their hub. The length and depth of the liner are 14.1 mm

and 6.4 mm respectively, while the depth of the outlet is 5 mm. The liner zones--primary,

secondary and dilution--have the holes arranged in equal spacings around the liner. There

are 40 primary holes, and 80 secondary and 80 dilution holes. The remaining parameters
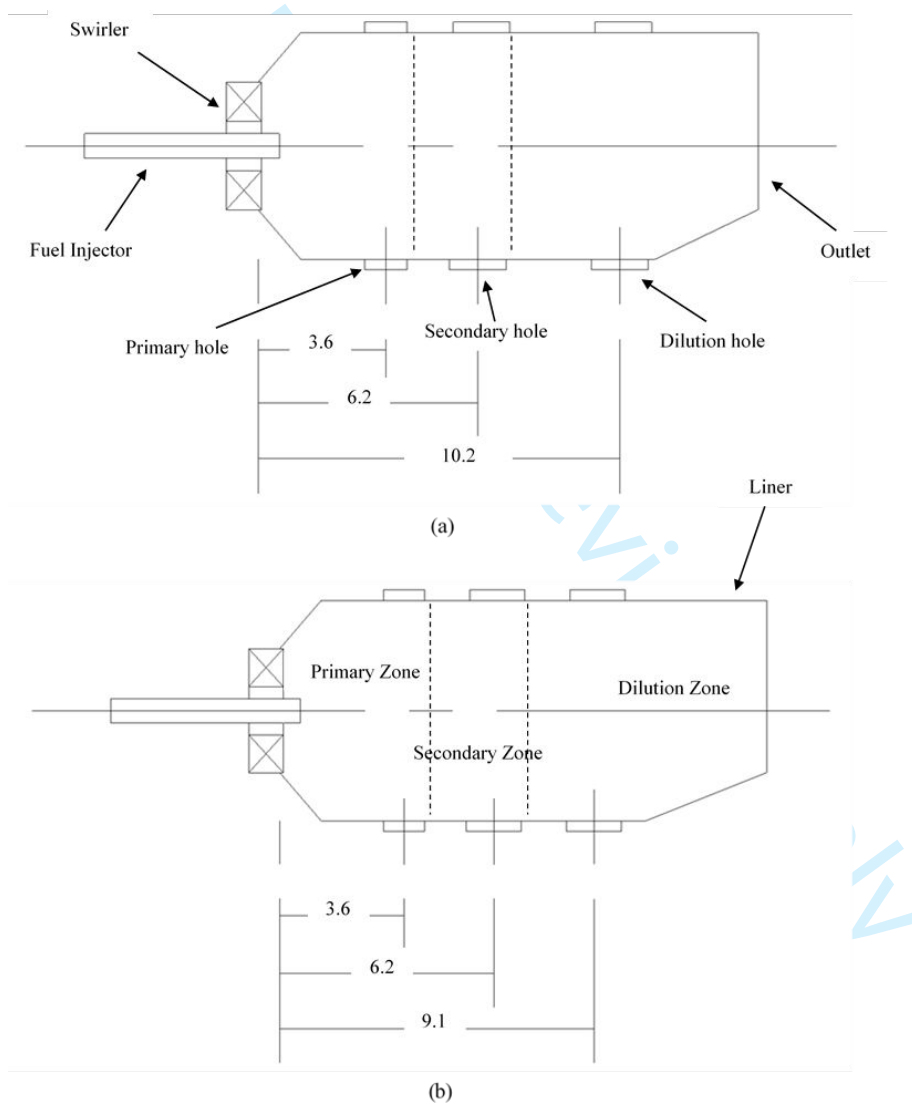
are listed in Table 1.

Figure 1. Schematic of the gas turbine combustion chamber (a) Case 1 (b) Case 2

6

Combustion Theory and Modelling
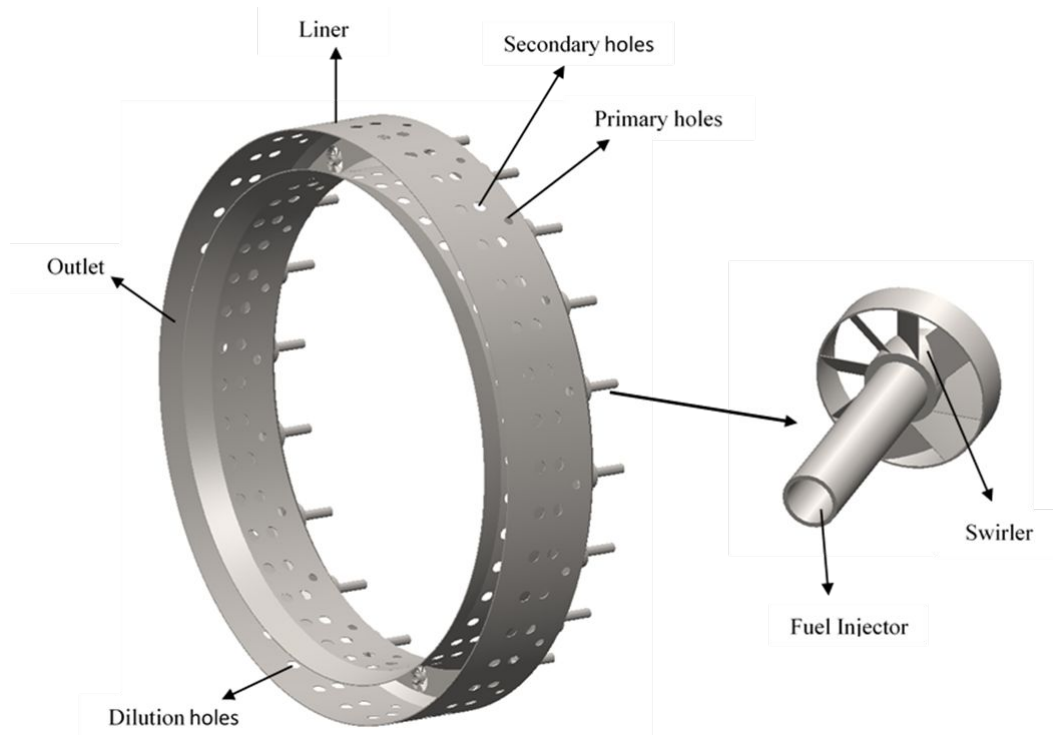
Combustion of multi-fuel in combustion chamber

Figure 2. SolidWorks model of the annular combustion chamber

Table 1. Dimensions of the micro gas turbine combustion chamber

Parameter	Value
Radius of outer liner	38
Radius of inner liner	31.6
Diameter of primary holes	1.2
Diameter of dilution holes	1.6
Diameter of swirler	3.6
Diameter of hub	1.4
Numbers of swirler blade	8

All parameters in Table 1. are in mm

7

Combustion of multi-fuel in combustion chamber

Mesh:

The mesh of 1/20th part of the combustor was generated in Fluent with an element size of 0.1 mm. The mesh of the whole part and some magnified portion of the part is shown in Figure 3. The total number of nodes and elements are 977864 and 5278275, respectively.
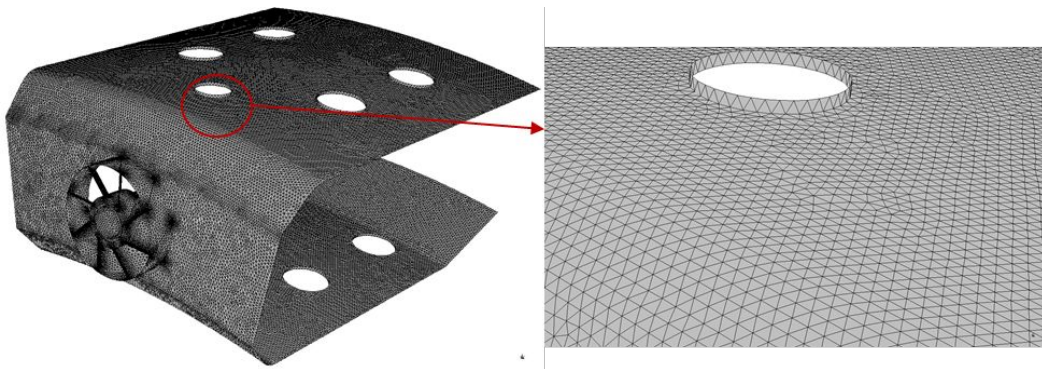

Figure 3. Meshed combustor liner with swirler

Ansys Simulations:

After meshing, the setup was prepared for simulation. Models for non-premixed combustion along with equilibrium probability density function, P1 radiation, and turbulence flow k-epsilon model were applied. The simulation has performed for the given part of the combustion chamber. Using three different fuels, the simulations were performed for all the above cases in ANSYS Fluent.

Non-Premixed Combustion Model:

Non-premixed combustion was applied for achieving stable combustion. The non-premixed combustion model predicts the diffusion flame by employing a fast chemistry assumption. For methane, 100% CH_4 is introduced. The natural gas composition given in Table 2 was used, while for ethanol 100% C_2H_5OH was injected, and the probability density function (PDF) for all three fuels was developed. The radiation P1 model, with zero assumed convection heat loss, is applied.

8

Combustion of multi-fuel in combustion chamber

k-epsilon (k-ε) Model:

Usually, researchers prefer the k-ε model for turbulent flow, as it has been validated by academic and industrial applications [13]. Compared to the large eddy simulation (LES) model, k-ε gives acceptable results within a short time [37]. This model is used to simulate flow characteristics for turbulent flow conditions and describes turbulence by two transport equations. The first variable k is for the turbulent kinetic energy, while the last variable ε is for the dissipation of turbulent energy. Here, the k-ε turbulent flow model with standard wall functions was applied.

Boundary Conditions:

For the Fluent boundary conditions, fuel was injected through the injector into the combustion chamber. 19.374% of total air was introduced through the swirler parallel to the injector, while 10% of air was introduced through the primary holes into the primary zone and 35.313% into the intermediate or secondary zones through secondary holes. The remaining air entered the liner through the dilution holes. The boundary condition parameters are given in Table 2.
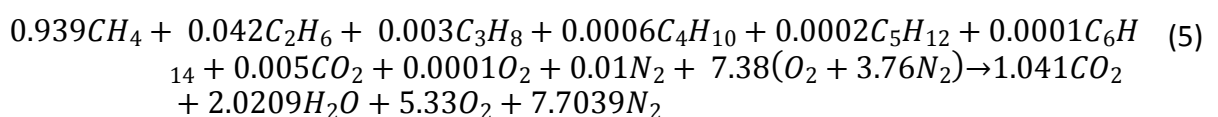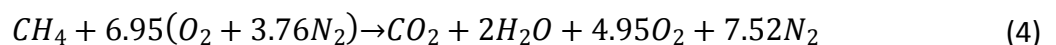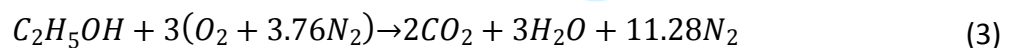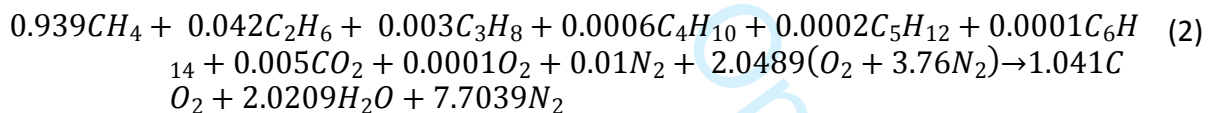
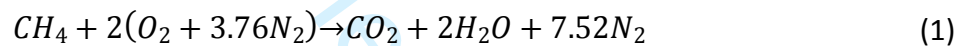Table 2. Boundary conditions

Parameter	Value
Mass of air through swirler	0.0013 kg/s
Mass of air through primary hole	0.000665 kg/s
Mass of air through dilution holes	0.0023725 kg/s
Mass of air through dilution holes	0.0023725 kg/s
Mass of fuel	0.00011 kg/s
Pressure of air	500000 Pa
Pressure of fuel	600000 Pa

9

Combustion of multi-fuel in combustion chamber

Ain inlet temperature	500 K
Fuel inlet temperature	500 K
Outlet pressure	382000 Pa

Combustion operations:

The fuel properties are necessary for combustion operations, and some of these are given in Table 3. The stoichiometric air-fuel ratio is 17.255 for methane, 16.66 for natural gas and 9.0026 for ethanol, and their stoichiometric combustion reactions are presented in equations (1), (2) and (3) respectively. Here authors use a constant air-fuel ratio of 60, which gives 6.95 moles of air for methane, 7.38 for natural gas and 19.99 for ethanol presented in chemical equations (4), (5) and (6) respectively. As a result of the fixed air-fuel ratio of 60, the excess air is 247.5% for methane, 260% for natural gas and 566% for ethanol chemical reactions.

$$CH_4 + 2(O_2 + 3.76N_2) \rightarrow CO_2 + 2H_2O + 7.52N_2 \tag{1}$$

$$0.939CH_4 + 0.042C_2H_6 + 0.003C_3H_8 + 0.0006C_4H_{10} + 0.0002C_5H_{12} + 0.0001C_6H_{14} + 0.005CO_2 + 0.0001O_2 + 0.01N_2 + 2.0489(O_2 + 3.76N_2) \rightarrow 1.041CO_2 + 2.0209H_2O + 7.7039N_2 \tag{2}$$

$$C_2H_5OH + 3(O_2 + 3.76N_2) \rightarrow 2CO_2 + 3H_2O + 11.28N_2 \tag{3}$$

$$CH_4 + 6.95(O_2 + 3.76N_2) \rightarrow CO_2 + 2H_2O + 4.95O_2 + 7.52N_2 \tag{4}$$

$$0.939CH_4 + 0.042C_2H_6 + 0.003C_3H_8 + 0.0006C_4H_{10} + 0.0002C_5H_{12} + 0.0001C_6H_{14} + 0.005CO_2 + 0.0001O_2 + 0.01N_2 + 7.38(O_2 + 3.76N_2) \rightarrow 1.041CO_2 + 2.0209H_2O + 5.33O_2 + 7.7039N_2 \tag{5}$$

10

Combustion of multi-fuel in combustion chamber

$$C_2H_5OH + 19.99(O_2 + 3.76N_2) \rightarrow 2CO_2 + 3H_2O + 16.49O_2 + 11.28N_2 \qquad (6)$$

Table 3. Fuel composition and properties

Fuel composition and properties	Pure Methane	Natural Gas	Ethanol
CH_4	100	93.9	0
C_2H_6	0	4.2	0
C_3H_8	0	0.3	0
C_4H_{10}	0	0.06	0
C_5H_{12}	0	0.02	0
C_6H_{14}	0	0.01	0
C_2H_5OH	0	0	100
CO_2	0	0.5	0
N_2	0	1	0
O_2	0	0.01	0
Mol weight (g/Mol)	16.04206	17.01995	46.06744
LHV (MJ/kg)	50	47.182	26.7
Octane Number	120	130	113
Autoignition (K)	810.15	853.15	638.15
Flash Point (K)	85.15	494.15	289.73

Properties of natural gas from the Ortech Report No. 26392, combustion property calculations for a typical Union Gas Composition, 2017, while for methane and ethanol from Engineering Toolbox.

11

Combustion of multi-fuel in combustion chamber

Results and Discussion:

After the mesh generation, the part was simulated with non-premixed combustion, k-ε turbulence, and P1 radiation models. All the cases were computed with the given boundary conditions. The following cases are discussed and compared:

Case 1:

The combustion of pure methane gives a total average temperature (average of total temperature) of 1129 K (849.85 °C) at the combustion chamber outlet. However, the mole fractions of carbon monoxides at the outlet are 1448 ppm and unburned fuels are 129 ppm. This is a consequence of incomplete combustion, due to which the temperature of the product at the outlet is low. Changing the fuel to natural gas of the composition given in Table 3 results in the total average temperature at the outlet of the combustion chamber changing slightly to 1120 K (855.85 °C). The mole fractions of carbon monoxides and unburned hydrocarbons liberated at the outlet become 487 ppm and 30 ppm respectively, and are an indication of good combustion. The ethanol fuel yields an outlet temperature of 850 K (576.85 °C), and mole fractions of 24 ppm and 19 ppm for carbon monoxides and unburned fuels, respectively, at the outlet of the combustion chamber. Moreover, NO at the outlet is negligible, which is also justified from these temperatures.

Case 2:

In the case of pure methane, the total average temperature of 1120 K (846.85 °C) is obtained at the outlet of the combustion chamber. However, the mole fractions of unburned fuel are 583 ppm and carbon monoxides are 725 ppm, while the emissions of NO at the outlet are insignificant. When the natural gas fuel was injected into the combustion chamber, the total average temperature of the product at the outlet dropped to 1110 K (836.85 °C). The mole fractions of unburned fuels and carbon monoxides at

Combustion of multi-fuel in combustion chamber

the combustion chamber outlet became 182 ppm and 1174 ppm respectively, while NO

emissions were approximately zero. By using ethanol as a fuel, the outlet temperature

decreased to 820 K (546.85 °C), and the mole fractions of unburned fuels and carbon

monoxides were 42 ppm and 31 ppm, respectively. Like in case 1, the emission of NO

was negligible.

Case 3:

For Case 3, pure methane resulted in a total average temperature of 1165 K (891.85 °C),

whereas the mole fractions of unburned fuels were negligible and that for carbon

monoxides was 207 ppm. The NO at the outlet was negligible and was approximately

equal to zero. When natural gas was injected and combusted, the outlet temperature

dropped to 1146 K (872.85 °C). The mole fractions of unburned fuels were negligible;

however, carbon monoxides were 84 ppm, and the NO emissions remained approximately

zero. The temperature dropped to 857 K (583.85 °C) by using ethanol as a fuel. At the

exit, the mole fractions of unburned fuels were 2 ppm, but carbon monoxides were 10

ppm, while the mole fraction of NO remained zero as in Case 1 and 2.

The average of total temperature at the outlet of the combustion chamber for each case

and fuel are presented in Table 4.

Table 4. Total average temperature at outlet for each case and fuel

Case and Fuel	Total average temperature (K) at outlet
Case 1 and Pure Methane	1129
Case 1 and Natural gas	1120

Combustion of multi-fuel in combustion chamber

Case 1 and Ethanol	850
Case 2 and Pure Methane	1120
Case 2 and Natural gas	1110
Case 2 and Ethanol	820
Case 3 and Pure Methane	1165
Case 3 and Natural gas	1146
Case 3 and Ethanol	857

Comparison:

To investigate the combustion performance, the results for all three cases for the respective fuels (methane, natural gas, and pure ethanol) are compared in terms of temperatures and their homogeneity, unburned fuel, CO and NO emissions in the combustion chamber and at the exit. The effects of the hole positions and swirler vane angles on the temperature distribution in the combustion chamber are shown in Figures 4 and 5. In Case 2 the secondary and dilution holes are close to each other and therefore the mass flow rate of air through these holes combines before taking part in combustion. Meanwhile, insufficient volume is given to the fuels, which end up leaving the combustion chamber without complete combustion. This results in lower temperatures and homogeneity at the outlet of the combustion chamber. In Case 1, most of the fuel burned, and almost complete combustion was achieved, while in Case 3 the increase in the swirler vanes angle caused increased mixing of the air and fuel and thus further combustion enhancement compared to Case 1. Figure 5 presents the contours of outlet combustion chamber temperature and the purpose is to see the homogeneity for the different cases. The temperature for Case 1 is more homogenous compared to that for Case 2, and Case 3 is more homogeneous than Case 1. Furthermore, the values of total

14

Combustion of multi-fuel in combustion chamber

average temperatures at the outlet of the combustion chamber are graphically presented in Figure 6 for all cases. It is determined that Case 3 gives higher temperatures than the remaining two cases for the respective fuels because of the trend towards complete combustion.
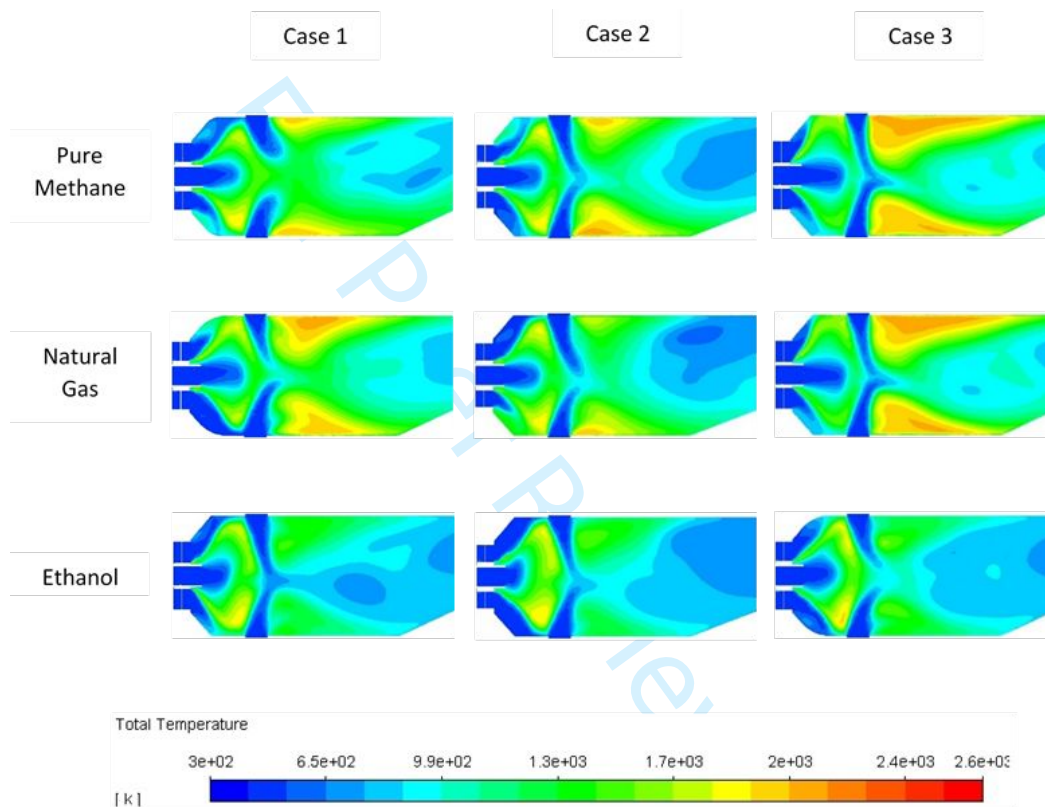

Figure 4. Temperature distribution in the combustion chamber

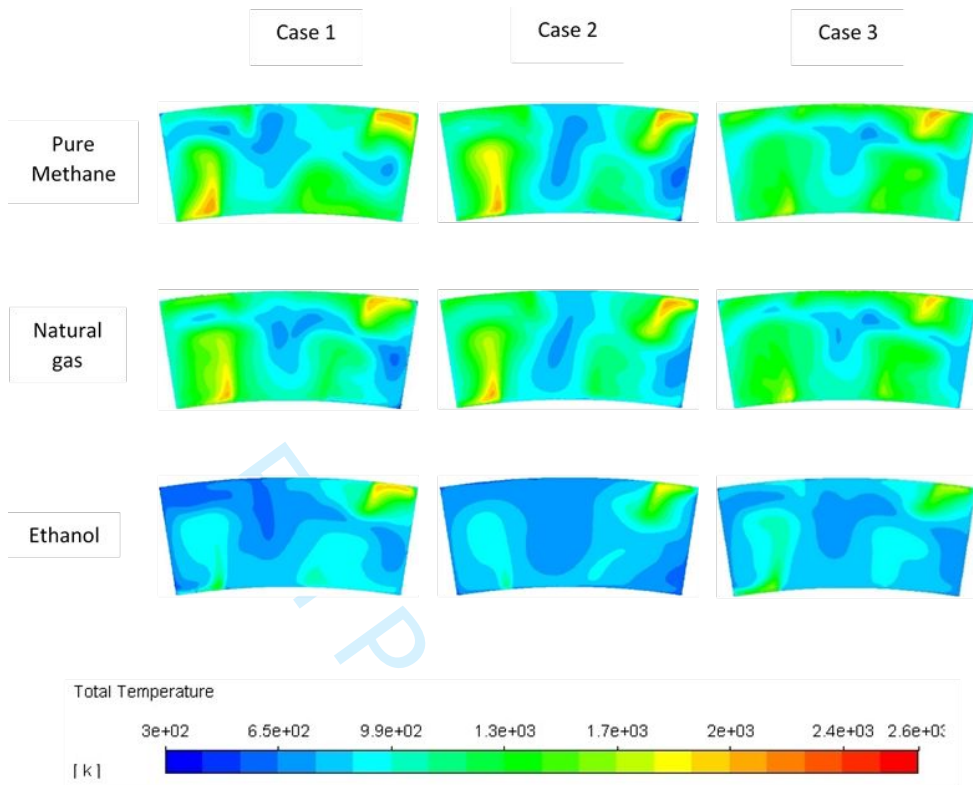Combustion of multi-fuel in combustion chamber

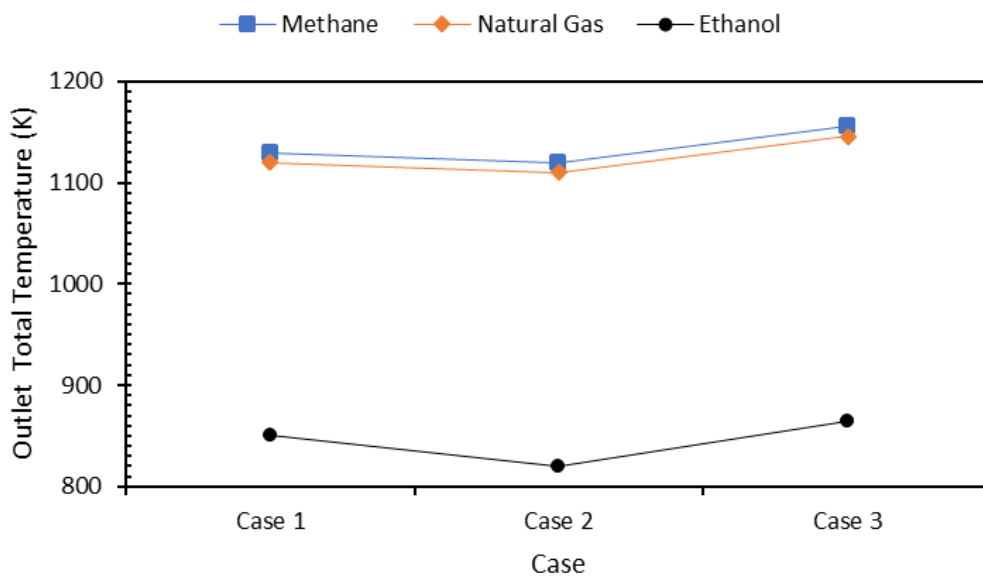Figure 5. Distribution of the outlet total average temperatures

Figure 6. Comparison of total average temperatures at the outlet of the combustion chamber

Combustion of multi-fuel in combustion chamber

Figure 7 illustrates the distribution of fuels and the development of combustion in the combustion chamber and shows that combustion uniformly reaches the lean zone except for Case 2. Figure 8, on the other hand, compares unburned fuel mole fraction contours that are released at the combustion chamber outlet. From Figure 8 we can observe that there is only a small amount of unburned fuel in Case 1, while in Case 2 a substantial amount of the unburned fuels remains. In Case 3 the unburned fuels at the outlet are negligible. The mole fractions of the unburned fuels at the outlet of the combustion chamber are graphically presented in Figure 9, where it is determined that in Case 3 the emissions of unburned fuels are the lowest compared to the other two cases for each fuel. From the CO contours presented in the above cases, it is determined that those emissions are lower in Case 3 compared to the other two cases. Figure 10 illustrates the production of NO and it is observed that for all cases and fuels there are little or negligible NO emissions.
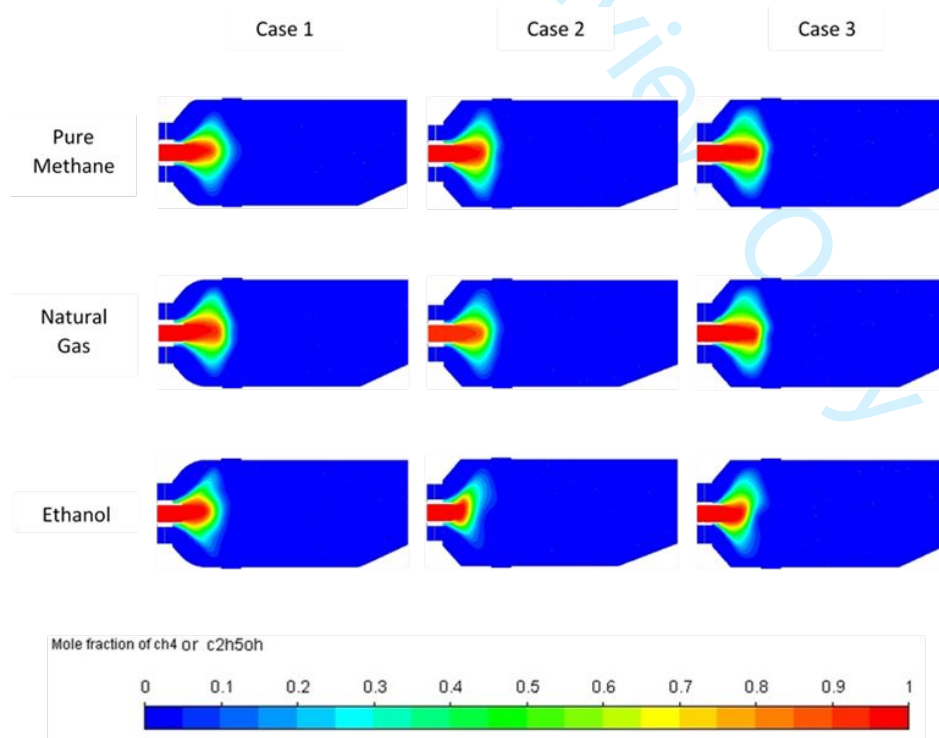

Figure 7. Distribution of fuel in the combustion chamber

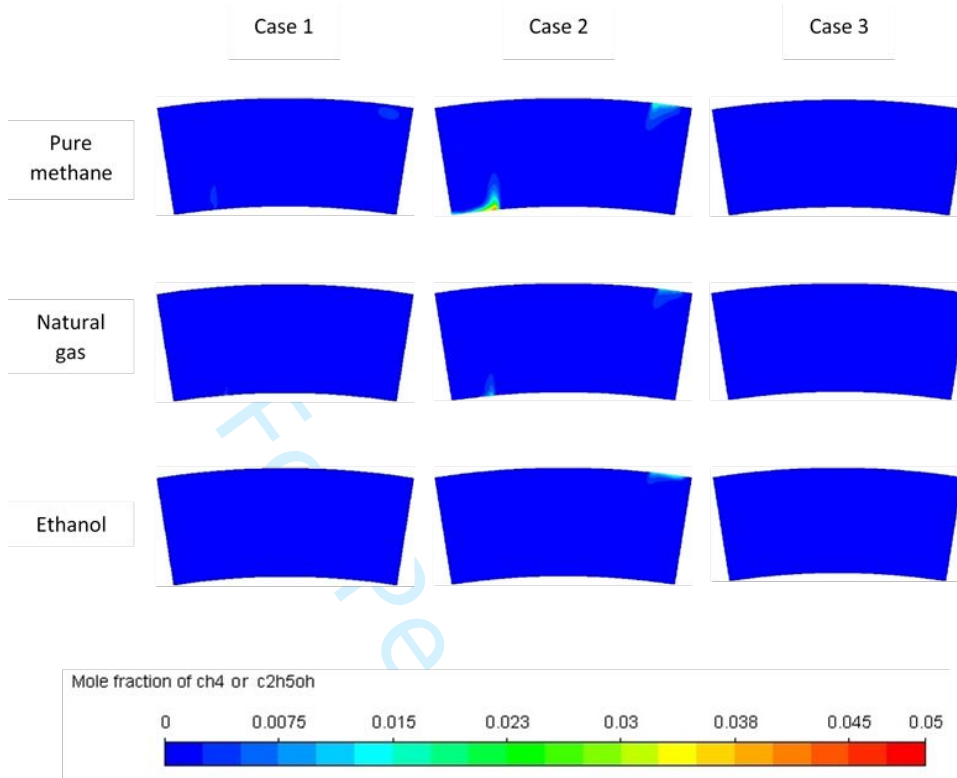Combustion of multi-fuel in combustion chamber

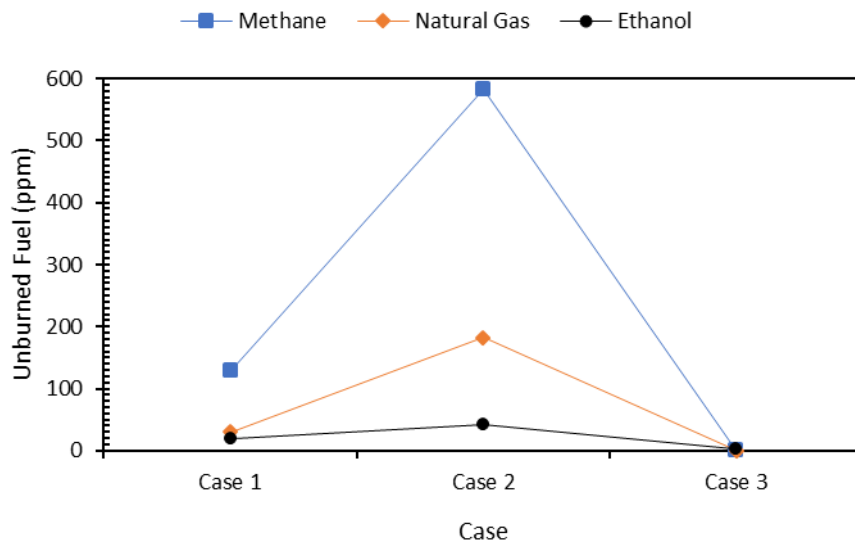Figure 8. Distribution of unburned fuel at the outlet of the combustion chamber

Figure 9. Comparison of unburned fuel at the outlet of the combustion chamber

18

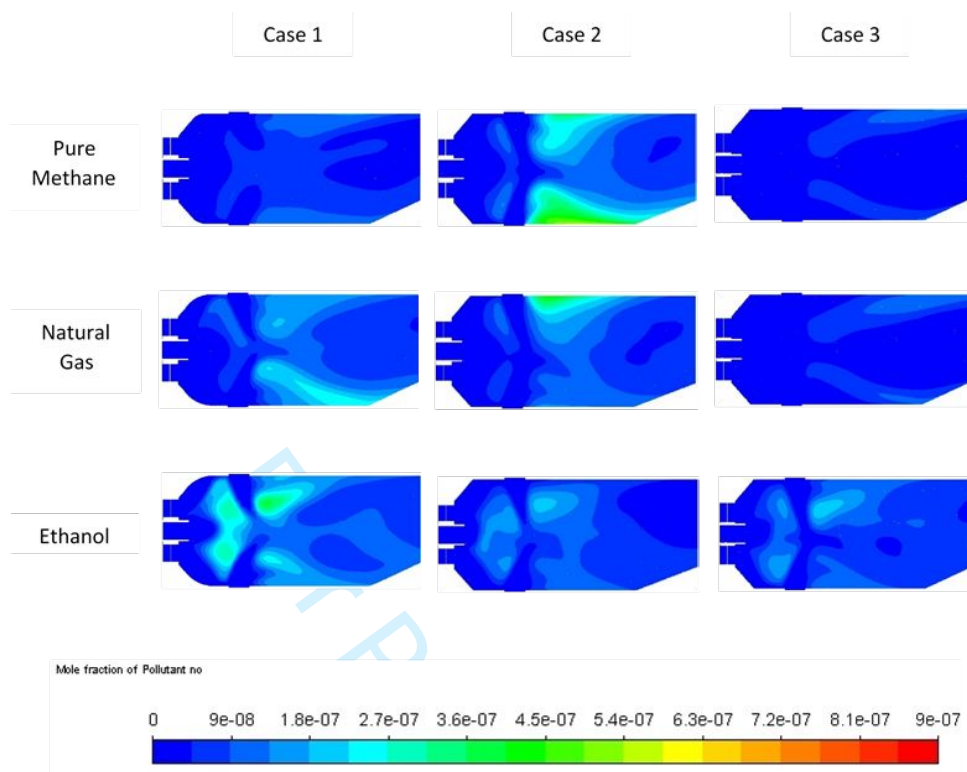Combustion of multi-fuel in combustion chamber

Figure 10. Nitric oxides production in the combustion chamber

Combustion efficiency:

The combustion efficiency is determined by using equation (7) [38,39].

$$\eta_c = \frac{CO_2 + 0.645CO}{CO_2 + CO + UHC} \qquad (7)$$

From Figure 11 the efficiency of the combustion chamber for Case 3 is higher than the other cases. In all cases, ethanol combustion is almost complete, but is slightly higher (99.97%) for Case 3 and almost complete combustion. In Case 3 combustion efficiencies of 99.77% and 99.83% respectively are achieved for pure methane and natural gas, while in the other two cases the combustion efficiency is relatively low due to incomplete combustion. It is verified that combustion is best for Case 3 for all fuels (pure methane,

19

Combustion of multi-fuel in combustion chamber

natural gas, and ethanol) and these outcome validates the results in [15], in which the

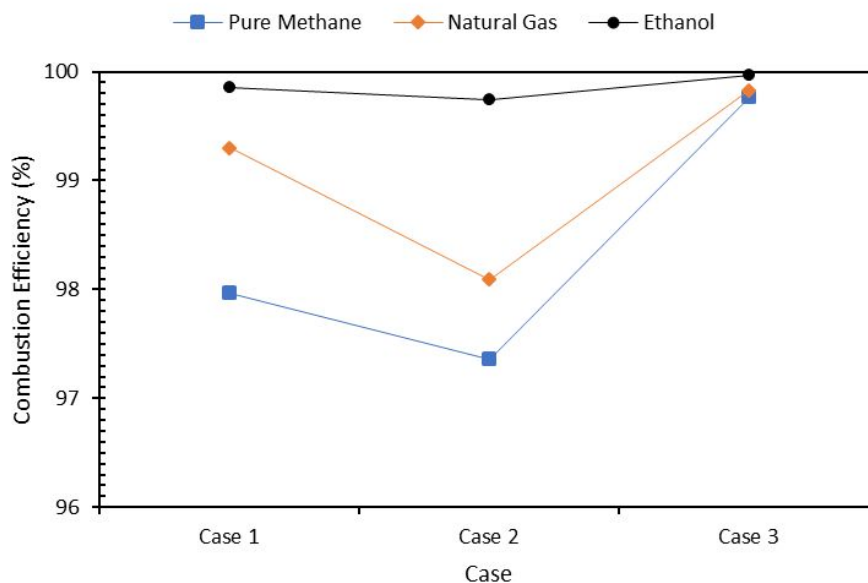maximum combustion efficiency resulted at a swirler vane angle of 45°.

Figure 11. Comparison of the combustion efficiency

Conclusion:

In order to understand the potential application of a micro gas turbine annular combustion

chamber using multi-fuels comprised of pure methane, ethanol, or natural gas, 3-D CFD

simulations were performed using ANSYS Fluent. A constant mass flow rate of air and

fuel was injected with a fixed air-fuel ratio of 60. The variable parameters were dilution

hole positions and swirler blade angles. The results are compared for all the cases in terms

of total average temperature, unburned fuel, CO and NO emissions at the combustion

chamber outlet. The main findings of this work are summarized as follows:

- Methane fuel combustion results in the highest temperature, while the lowest
  temperature was achieved for ethanol because of its relatively smaller energy
  density. Moreover, the Case 3 geometry in which the swirler vane angle is 45°
  yields the highest temperature for each fuel.

20

Combustion of multi-fuel in combustion chamber

- In the first two cases, the combustion of pure methane and natural gas emits substantial CO and unburned fuel, whereas Case 3 produces the lowest mole fraction of unburned fuel and CO. When ethanol was injected as fuel, pollutant emissions further decreased. Furthermore, NO emissions were negligible in all cases for methane, natural gas, and ethanol.

- In Case 2 the combustion efficiency was approximately 98% for both methane and natural gas. Case 1 led to efficiencies greater than 98%, and for Case 3 it was slightly below 100%. A combustion efficiency of 99.97% was recorded for ethanol in all three cases.

- The outlet temperature distribution was more homogeneous in Case 3 compared to the other two cases because of the swirler vane angle of 45°.

The above findings indicate that a swirler vane angle of 45° widely improved combustion performance. Moreover, these design outcomes are useful and can provide a baseline for micro gas turbine applications. These results, however, require quantitative experimental validation, since simulations often overpredict the performance.

Acknowledgment:

References:

[1]   Gutirrez Velsques EI, Batista Gomes EE, de L, dos Santos EC, Goulart FL, Alexis Miranda R, et al. Micro Gas Turbine Engine: A Review. Prog Gas Turbine Perform 2013. doi:10.5772/54444.

[2]   Enagi II, Al-attab KA, Zainal ZA. Combustion chamber design and performance for micro gas turbine application. Fuel Process Technol 2017;166:258–68. doi:10.1016/j.fuproc.2017.05.037.

Combustion of multi-fuel in combustion chamber

[3]   Boukhanouf R. Small combined heat and power (CHP) systems for commercial buildings and institutions. Small Micro Comb Heat Power Syst 2011:365–94. doi:10.1533/9780857092755.3.365.

[4]   Li C, Yang D, Li S, Zhu M. An analytical study of the effect of flame response to simultaneous axial and transverse perturbations on azimuthal thermoacoustic modes in annular combustors. Proc Combust Inst 2019;37:5279–87. doi:10.1016/J.PROCI.2018.05.121.

[5]   Boyce MP. Advanced industrial gas turbines for power generation. Comb Cycle Syst Near-Zero Emiss Power Gener 2012:44–102. doi:10.1016/B978-0-85709-013-3.50002-X.

[6]   Ayon AA, Waitz IA, Schmidt MA, Xin Zhang, Spadaccini CM, Mehra A. A six-wafer combustion system for a silicon micro gas turbine engine. J Microelectromechanical Syst 2002;9:517–27. doi:10.1109/84.896774.

[7]   Shih HY, Liu CR. A computational study on the combustion of hydrogen/methane blended fuels for a micro gas turbines. Int J Hydrogen Energy 2014;39:15103–15. doi:10.1016/j.ijhydene.2014.07.046.

[8]   Asgari B, Amani E. A multi-objective CFD optimization of liquid fuel spray injection in dry-low-emission gas-turbine combustors. Appl Energy 2017;203:696–710. doi:10.1016/j.apenergy.2017.06.080.

[9]   Abagnale C, Cameretti MC, De Robbio R, Tuccillo R. CFD Study of a MGT Combustor Supplied with Syngas. Energy Procedia, vol. 101, Elsevier; 2016, p. 933–40. doi:10.1016/j.egypro.2016.11.118.

[10]   Farokhipour A, Hamidpour E, Amani E. A numerical study of NOx reduction by water spray injection in gas turbine combustion chambers. Fuel 2018;212:173–86. doi:10.1016/j.fuel.2017.10.033.

[11]   Ilbas M, Yılmaz İ, Veziroglu TN, Kaplan Y. Hydrogen as burner fuel: modelling of hydrogen–hydrocarbon composite fuel combustion and NOx formation in a small burner. Int J Energy Res 2005;29:973–90. doi:10.1002/er.1104.

[12]   Jeong D, Huh KY. Numerical Simulation of Non-Reacting and Reacting Flows in a 5MW Commercial Gas Turbine Combustor 2009:739–48. doi:10.1115/GT2009-59987.

[13]   Ghose P, Patra J, Datta A, Mukhopadhyay A. Effect of air flow distribution on soot formation and radiative heat transfer in a model liquid fuel spray combustor

Combustion of multi-fuel in combustion chamber

firing kerosene. Int J Heat Mass Transf 2014;74:143–55. doi:10.1016/J.IJHEATMASSTRANSFER.2014.03.001.

[14]   Jarpala R, Aditya Burle NVS, Voleti M, Sadanandan R. Effect of Swirl on the Flame Dynamics and Pollutant Emissions in an Ultra-Lean Non-Premixed Model Gas Turbine Burner. Combust Sci Technol 2017;189:1832–48. doi:10.1080/00102202.2017.1333500.

[15]   Pourhoseini SH, Fakhri S, Taheri E, Asadi R, Moghiman M. An Investigation on the Effect of Air Swirler Vane Angle on Liquid Fuel Combustion Characteristics. Heat Transf Res 2017;46:750–60. doi:10.1002/htj.21241.

[16]   Cameretti MC, Reale F, Tuccillo R. Cycle Optimization and Combustion Analysis in a Low-NOx Micro-Gas Turbine. J Eng Gas Turbines Power 2006;129:994–1003. doi:10.1115/1.2718232.

[17]   Cameretti MC, Tuccillo R, Piazzesi R. Study of an exhaust gas recirculation equipped micro gas turbine supplied with bio-fuels. Appl Therm Eng 2013;59:162–73. doi:10.1016/J.APPLTHERMALENG.2013.04.029.

[18]   Cameretti MC, Tuccillo R, Piazzesi R. Fuelling an EGR Equipped Micro Gas Turbine With Bio-Fuels 2012:629–40. doi:10.1115/GT2012-68720.

[19]   Cameretti MC, Piazzesi R, Reale F, Tuccillo R. Comparison of External and Internal EGR Concepts for Low Emission Micro Gas Turbines 2010:581–93. doi:10.1115/GT2010-22413.

[20]   Cameretti MC, Piazzesi R, Reale F, Tuccillo R. Combustion Simulation of an Exhaust Gas Recirculation Operated Micro-gas Turbine. J Eng Gas Turbines Power 2009;131. doi:10.1115/1.3078193.

[21]   Frenillot JP, Cabot G, Cazalens M, Renou B, Boukhalfa MA. Impact of H2 addition on flame stability and pollutant emissions for an atmospheric kerosene/air swirled flame of laboratory scaled gas turbine. Int J Hydrogen Energy 2009;34:3930–44. doi:10.1016/J.IJHYDENE.2009.02.059.

[22]   Danon B, De Jong W, Roekaerts DJEM. Experimental and numerical investigation of a FLOX combustor firing low calorific value gases. Combust Sci Technol 2010;182:1261–78. doi:10.1080/00102201003639284.

[23]   H. Zehra, P. Ramkumar G-S. Performance and emission characteristics of biofuel in a small-scale gas turbine engine. Appl Energy 2010;87:1701–9. doi:10.1016/j.apenergy.2009.10.024.

23

Combustion of multi-fuel in combustion chamber

[24]   E.E. Ahmed, K. Vaibhav, Arghode, Ashwani K. Gupta SCL. Low calorific value fuelled distributed combustion with swirl for gas turbine applications. Appl Energy 2012;89:69–78. doi:apenergy.2012.02.074 (Elsevier).

[25]   Escudero M, Jimenez A, Gonzalez C, Nieto R, Lopez I. Analysis of the behaviour of biofuel-fired gas turbine power plants. Therm Sci 2012;16:849–64. doi:10.2298/TSCI120216131E.

[26]   De Pascale A, Fussi M, Peretto A. Numerical Simulation of Biomass Derived Syngas Combustion in a Swirl Flame Combustor 2010:571–82. doi:10.1115/GT2010-22791.

[27]   Cadorin M, Pinelli M, Vaccari A, Calabria R, Chiariello F, Massoli P, et al. Analysis of a Micro Gas Turbine Fed by Natural Gas and Synthesis Gas: MGT Test Bench and Combustor CFD Analysis. J Eng Gas Turbines Power 2012;134. doi:10.1115/1.4005977.

[28]   Glaude PA, Fournet R, Bounaceur R, Molière M. Adiabatic flame temperature from biofuels and fossil fuels and derived effect on NOx emissions. Fuel Process Technol 2010;91:229–35. doi:10.1016/j.fuproc.2009.10.002.

[29]   Tibaquirá EJ, Huertas IJ, Ospina S, Quirama FL, Niño EJ. The Effect of Using Ethanol-Gasoline Blends on the Mechanical, Energy and Environmental Performance of In-Use Vehicles. Energies 2018;11. doi:10.3390/en11010221.

[30]   Ayad SMME, Belchior CRP, da Silva GLR, Lucena RS, Carreira ES, de Miranda PE V. Analysis of performance parameters of an ethanol fueled spark ignition engine operating with hydrogen enrichment. Int J Hydrogen Energy 2019.

[31]   Cooney CP, Worm JJ, Naber JD. Combustion characterization in an internal combustion engine with ethanol− gasoline blended fuels varying compression ratios and ignition timing. Energy & Fuels 2009;23:2319–24.

[32]   Luo L, van der Voet E, Huppes G. Life cycle assessment and life cycle costing of bioethanol from sugarcane in Brazil. Renew Sustain Energy Rev 2009;13:1613–9. doi:10.1016/j.rser.2008.09.024.

[33]   Renouf MA, Wegener MK, Nielsen LK. An environmental life cycle assessment comparing Australian sugarcane with US corn and UK sugar beet as producers of sugars for fermentation. Biomass and Bioenergy 2008;32:1144–55. doi:10.1016/j.biombioe.2008.02.012.

Combustion of multi-fuel in combustion chamber

[34]   García CA, Fuentes A, Hennecke A, Riegelhaupt E, Manzini F, Masera O. Life-cycle greenhouse gas emissions and energy balances of sugarcane ethanol production in Mexico. Appl Energy 2011;88:2088–97. doi:10.1016/j.apenergy.2010.12.072.

[35]   Kadam KL. Environmental benefits on a life cycle basis of using bagasse-derived ethanol as a gasoline oxygenate in India. Energy Policy 2002;30:371–84. doi:10.1016/S0301-4215(01)00104-5.

[36]   Lefebvre AH, Ballal DR. Gas Turbine Combustion: Alternative Fuels and Emissions. vol. 1. Boca Raton: Taylor and Francis Group, LLC; 2010. doi:10.1017/CBO9781107415324.004.

[37]   Fantozzi F, Laranci P, Bianchi M, De Pascale A, Pinelli M, Cadorin M. CFD Simulation of a Microturbine Annular Combustion Chamber Fuelled With Methane and Biomass Pyrolysis Syngas: Preliminary Results 2009:811–22. doi:10.1115/GT2009-60030.

[38]   Zhang RC, Fan WJ, Shi Q, Tan WL. Combustion and emissions characteristics of dual-channel double-vortex combustion for gas turbine engines. Appl Energy 2014;130:314–25. doi:10.1016/j.apenergy.2014.05.059.

[39]   Zhang RC, Hao F, Fan WJ. Combustion and stability characteristics of ultra-compact combustor using cavity for gas turbines. Appl Energy 2018;225:940–54. doi:10.1016/j.apenergy.2018.05.084.